

Development of Transaminases for the Synthesis of Enantiomerically Pure Chiral Amines

A thesis submitted to the University of Manchester for the degree of
Doctor of Philosophy
in the Faculty of Engineering and Physical Sciences.

2012

Jennifer Hopwood

School of Chemistry

Table of contents

Table of contents	4
Abstract	9
Declaration	10
Copyright statement	10
Acknowledgements	11
Abbreviations	12
1. Introduction	14
1.1 Biocatalysis	14
1.2 Enzymatic synthesis of chiral amines	18
1.2.1 Chiral amines	18
1.2.2 Biocatalytic synthesis of chiral amines	19
1.2.3 Kinetic resolution	19
1.2.4 Dynamic kinetic resolution	22
1.2.5 Deracemisation.....	26
1.2.6 Asymmetric synthesis	28
1.3 Transaminases	30
1.3.1 Pyridoxal 5'-phosphate and the transaminase active site.....	30
1.3.2 Transaminase mechanism	32
1.3.3 Methods to overcome transaminase challenges	32
1.3.4 Screening of transaminase enzymes.....	36
1.3.5 Transaminases for chiral amine synthesis.....	38
1.4 Aims of the project	42
2. Results and discussion- Colourimetric assay	43
2.1 Path length determination.....	44
2.2 Determination of extinction coefficient of pyrogallol red.....	45
2.3 Background activity of Pyrogallol red	46

2.4	Screening of amine substrates	47
2.5	Varying ATA-117 concentration.....	48
2.6	Effect of adding external pyridoxal-5'-phosphate.....	51
2.7	Comparison of forward and reverse transamination reaction.....	52
2.8	Determination of enantioselectivity	54
2.9	pH Stability.....	55
2.10	Screening of whole cell transaminases	56
2.11	Transaminase activity with purified enzyme	57
2.12	Conclusion	59
3.	Results and discussion- Cloning identification and characterisation of two transaminase enzymes	61
3.1	Initiation of screen.....	62
3.2	Solid phase screen	66
3.3	Identification of unknown microorganisms.....	67
3.4	Protein identification	67
3.5	Cloning and expression of <i>Ochrobactrum anthropi</i>	69
3.6	Cloning and expression of <i>C. violaceum</i> (CMCC 104818).....	72
3.7	Homology modelling of the <i>Chromobacterium violaceum</i> transaminases	76
3.8	Conclusion.....	78
4.	Results and discussion- Biotransformations using transaminases	80
4.1	4-Bromoacetophenone.....	81
4.2	Cascade reactions	85
4.2.1	Galactose oxidase/transaminase cascade	85
4.2.2	Monoamine oxidase and transaminase cascade	87
4.3	3 Methyl-3,4-dihydroisoquinoline.....	95
4.4	Conclusion.....	97
5.	Summary, conclusion and future work.....	100
5.1	Summary and conclusion	100

5.2	Future work	101
6.	Experimental	102
6.1	Materials	102
6.1.1	Chemicals, reagents and kits.....	102
6.1.2	Enzymes	102
6.1.3	Strains.....	102
6.1.4	Plasmids	103
6.1.5	Buffer solutions.....	103
6.1.6	Growth media.....	104
6.1.7	Antibiotics.....	106
6.1.8	IPTG.....	106
6.1.9	Enzyme stocks for solution phase assay	106
6.1.10	Sample preparation for colony PCR	107
6.1.11	DNA and protein gel markers	107
6.2	Methods	108
6.2.1	Colourimetric transaminase assay with PGR.....	108
6.2.2	Colourimetric transaminase assay with TBHBA 4-AAP.....	109
6.2.3	Path length determination	109
6.2.4	Extinction coefficient of pyrogallol red	110
6.2.5	Genomic DNA purification.....	110
6.2.6	16S rRNA sequencing PCR recipe	111
6.2.7	Plasmid DNA purification.....	111
6.2.8	PCR of <i>C. violaceum</i>	112
6.2.9	PCR of <i>Ochrobactrum sp</i> genomic DNA.	113
6.2.10	Gel extraction	113
6.2.11	DNA quantification.....	113
6.2.12	Cloning (Zero blunt TOPO).....	114
6.2.13	Restriction Enzyme digests.....	114

6.2.14	Transformation of <i>E. coli</i>	115
6.2.15	Expression of PJH2 in BL21 (DE3).....	115
6.2.16	Expression of PJH3 in BL21 (DE3).....	115
6.2.17	MAO-N transformation and expression.....	115
6.2.18	GOase expression.....	115
6.2.19	Purification of proteins on anion exchange column.....	116
6.2.20	Purification of His-tagged proteins	116
6.2.21	Chemistry and biotransformations	117
6.2.22	Biotransformation's for the synthesis of chiral amines.....	117
6.2.23	MAO-N stereoselective conversion general procedure	123
7.	References	124
8.	Appendix	133
8.1	Solution phase assay.....	133
8.1.2	PGR colour spectrum	133
8.1.3	PGR Absorption spectrum	134
8.1.4	Pyrogallol red standard curve.....	134
8.2	pH and temperature profile of Cv TA2	135
8.3	Plasmids.....	136
8.3.1	PJH1 Vector map	136
8.3.2	Vector map of PJH2.....	136
8.3.3	Vector map of PJH3.....	137
8.3.4	pET16b Vector map	138
8.3.5	Zero blunt topopCR vector map.....	139
8.4	DNA sequences	140
8.4.1	<i>Chromobacterium violaceum</i> Cv TA2.....	140
8.4.2	<i>Ochrobactrum antropi</i> Oa TA1	140
8.5	Analytical traces	141
8.5.1	(2 <i>S</i> ,5 <i>R</i>)-2-Methyl-5-phenylpyrrolidine.	141

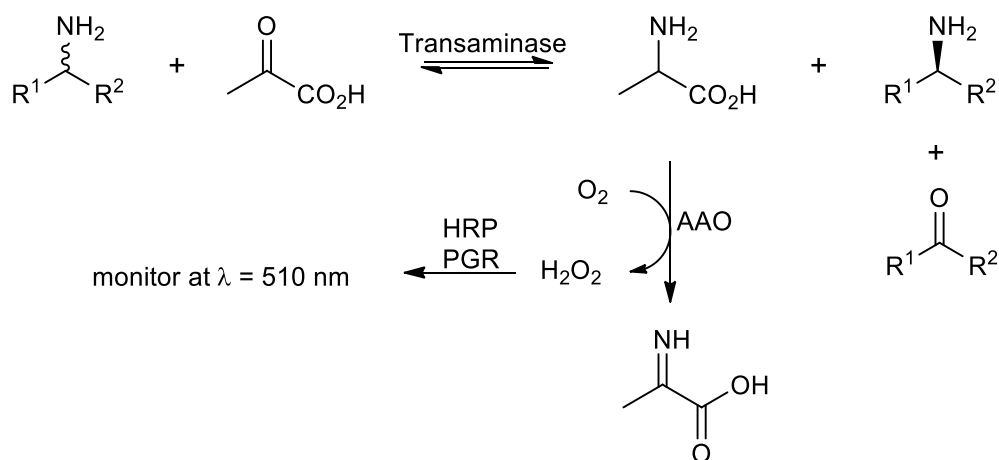
8.5.2	(2 <i>R</i> ,5 <i>R</i>)-2-Methyl-5-phenylpyrrolidine.....	142
8.5.3	(2 <i>S</i> ,5 <i>R</i>)-2-Methyl-5-benzylpyrrolidine.....	143
8.5.4	(2 <i>R</i> ,5 <i>R</i>)-2-Methyl-5-benzylpyrrolidine.....	143
8.5.5	(2 <i>S</i> ,5 <i>R</i>)-2-Ethyl-5-phenylpyrrolidine.....	144
8.5.6	(<i>S</i>)-1-Phenylethylamine.....	145
8.5.7	(<i>S</i>)-4-Bromo-1-phenylethylamine.....	145
8.5.10	(<i>S</i>)-4-Bromo-1-phenylethylamine.....	147
8.6	NMR data.....	149
8.6.2	2,5-Dimethyl-3,4-dihydro-2 <i>H</i> -pyrrole.....	150
8.6.3	4-Bromo-1-phenylethylamine.....	151
8.6.4	3-Methyl-1,2,3,4-tetrahydroisoquinoline.....	152
8.6.5	3-Methyl-3,4-dihydroisoquinoline.....	155
8.6.6	2-Methylindene oxide.....	156
8.6.7	2-(2-Oxo-propyl)benzaldehyde.....	157
8.6.8	2-Methyl-5-phenyl-3,4-dihydro-2 <i>H</i> -pyrrole.....	158
8.6.9	5-Phenyl-2-ethyl-3,4-dihydro-2 <i>H</i> -pyrrole.....	159
8.7	Publications.....	160

Abstract

Enantiomerically pure amines have a variety of industrial applications. They are valuable components within the pharmaceutical and agrochemical industry, resolving agents for separation of racemic mixtures by dimeric salt formation and ligands for transition metal catalysts and chemocatalysts. Biocatalysis is increasingly seen as the method of choice for the synthesis of chiral amines. New commercial enzymes being readily available and new screening/evolution technologies allow for enzyme optimisation towards a set of required conditions for chiral amine synthesis.

Transaminases are a class of pyridoxal 5'-phosphate (PLP) dependant enzymes that catalyse the reversible transfer of ammonia from an amine donor (e.g. alanine) to a keto acceptor (e.g. acetophenone), allowing the potential for asymmetric methodologies. Transaminases are already well established for the industrial production of α -amino acids and now that research scientists have dealt with some of the problems with equilibrium and substrate/product inhibition, they are being investigated for the industrial application of chiral amines.

A multi-enzyme kinetic assay has been utilised for characterisation of newly identified transaminase enzymes in solution phase. Identified transaminases that showed desirable characteristics were cloned and expressed and utilised in the synthesis of amines of interest to industry. Dual enzyme cascade reactions utilising transaminases and either galactose oxidase from *Fusarium* sp. or monoamine oxidase from *Aspergillus niger* were used to produce a number of primary and secondary amines in high *e.e.* and conversion.



Overview of the colourimetric assay.

Declaration

I declare that no portion of the work referred to in the thesis has been submitted in support of an application for another degree or qualification of this or any other university or other institute of learning.

Copyright statement

i. The author of this thesis (including any appendices and/or schedules to this thesis) owns certain copyright or related rights in it (the “Copyright”) and she has given The University of Manchester certain rights to use such Copyright, including for administrative purposes.

ii. Copies of this thesis, either in full or in extracts and whether in hard or electronic copy, may be made only in accordance with the Copyright, Designs and Patents Act 1988 (as amended) and regulations issued under it or, where appropriate, in accordance with licensing agreements which the University has from time to time. This page must form part of any such copies made.

iii. The ownership of certain Copyright, patents, designs, trademarks and other intellectual property (the “Intellectual Property”) and any reproductions of copyright works in the thesis, for example graphs and tables (“Reproductions”), which may be described in this thesis, may not be owned by the author and may be owned by third parties. Such Intellectual Property and Reproductions can not and must not be made available for use without the prior written permission of the owner(s) of the relevant Intellectual Property and/or Reproductions.

iv. Further information on the conditions under which disclosure, publication and commercialisation of this thesis, the Copyright and any Intellectual Property and/or Reproductions described in it may take place is available in the University IP Policy (see <http://documents.manchester.ac.uk/DocuInfo.aspx?DocID=487>), in any relevant Thesis restriction declarations deposited in the University Library, The University Library’s regulations (<http://www.manchester.ac.uk/library/aboutus/regulations>) and in The University’s policy on Presentation of Thesis.

Acknowledgements

I would like to thank my supervisor Prof. Nicholas Turner for his guidance, support, and the opportunity to work on this project. I would also like to thank Dr. Richard Lloyd for his ideas throughout my Ph.D and also for reading through the final draft of this report.

I wish to thank members of the Turner/Flitsch group, particularly Dr. Ian Rowles, Dr. Maeve O'Neill, Dr. Valeria Barattini, Lucy Campbell and Dr. Kirk Malone for their constant support and making my time so far at the Manchester Interdisciplinary Biocentre thoroughly enjoyable. The past four years at the MIB have been some of the best years of my life! I have been given the most horrendous animal nickname (which I refuse to place in my thesis) and I am sure my liver is in a far worst condition to what it was when I started; however, I would not change a thing. I consider some of the friends I made during my Ph.D to be my best mates and even though in the near future I will be leaving the MIB, they will not get rid of me in their lives!

To everyone based down in Cambridge at the Dr. Reddy's site, thank you, for making me feel really welcome, I had some of the best nights out, and finally thank you for the 'few' extra pounds I gained from the irresistible cakes and the Friday lunch outing at the Red Lion. I would like to pay particular thanks to Dr. Ian Taylor, Dr Toni Fleming and Dr Matt Bycroft for the help with my molecular biology problems and a good laugh within the lab. Dr. Ania Fryszkowska, Dr. Richard Lloyd and Dr. Justine Taylor, thank you for your friendship, bike rides and your help to carry out my mission to try every pub in Cambridge before I left.

Finally to my family and close friends, in particular my parents, Sarah Hollingdrake, Dr. Valeria Barattini, Dr. Kirk Malone, Lisa Tuckley and Dr. Ania Fryszkowska, a massive thank you for putting up with my mood swings and the constant support throughout the four years.

I would like to show my gratitude to Dr Reddy's and the BBSRC for funding my CASE studentship.

Abbreviations

AAO	Amino acid oxidase
4-AAP	4-Aminoantipyrine
CO ₂	Carbon dioxide
CMCC	Chirotech microbial culture collection
dH ₂ O	Distilled water
DKR	Dynamic kinetic resolution
<i>e.e.</i>	Enantiomeric excess
<i>E. coli</i>	<i>Escherichia coli</i>
EDTA	Ethylenediaminetetraacetic acid
GC	Gas chromatography
GDH	Glucose dehydrogenase
FAD	Flavin adenine dinucleotide
FDA	Food and Drug Administration
FDH	Formate dehydrogenase
HPLC	High performance liquid chromatography
HRP	Horseradish peroxidase
H ₂ O ₂	Hydrogen peroxide
LDH	Lactate dehydrogenase
In	Indium
IPA	Isopropylamine
IPTG	Isopropyl-β-D-thiogalactopyranoside
MS	Mass spectra
MTP	Microtitre plate
MAO	Monoamine oxidase
NADH	Nicotinamide adenine dinucleotide
NMR	Nuclear magnetic resonance
OD	Optical density
PLP	Pyridoxal 5'-phosphate
PMP	Pyridoxamine 5'-phosphate
PGR	Pyrogallol Red
PDO	Pyruvate decarboxylase
TBHBA	2,4,6-Tribromo-3-hydroxybenzoic acid
TFA	Trifluoroacetic acid

TFP	1,3,5-Triphenylformazan
TTC	2,3,5-Triphenyltetrazolium chloride
TAE	Tris-acetate EDTA
TGS	Tris-glycine SDS
UCL	University College London
<i>wt</i>	Wild-type

1. Introduction

1.1 Biocatalysis

Biocatalysis is the general term for the use of natural catalysts, enzymes, to undertake chemical transformations on organic substrates. Straathof *et al.*, defined the process as the use of enzymes and/or whole cells to convert a pre-formed precursor molecule to a desired chemical, rather than a fermentation process with *de novo* production from a carbon and energy source.¹ Biocatalysis has become much more commonplace in recent times, and it is now accepted as an important strategy in synthetic organic chemistry. Biocatalysts can be applied to a chemical reaction in various different forms. They can be utilised as partially purified or purified cell free extract, whole cell microorganisms and employed as a catalyst either in solution or immobilised onto a support. The cost of commercial enzymes has started to decrease over the years² and chemists are now utilising enzymes more often in their research, either to replace existing chemical synthetic steps or to develop new paths to chiral compounds which would have previously been dismissed due to high enzyme costs.

The chirality of a pharmaceutical is very important with respect to the metabolism of the drug, due to the known fact that whilst one enantiomer can have desirable effect(s), the other enantiomer can be potentially harmful.

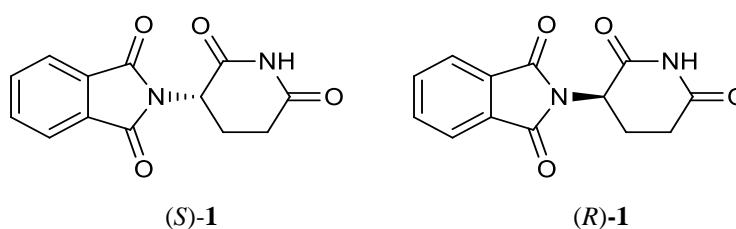
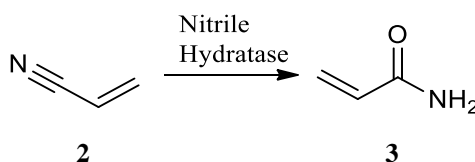


Figure 1: The two enantiomers of Thalidomide, (S)-1 was found to cause malformations in embryos and (R)-1 relieved the symptoms of morning sickness.

A classic example of this is Thalidomide **1** (Figure 1), the racemic drug prescribed to pregnant women between 1957-61 to relieve the symptoms of morning sickness.³ The effect of both administering the racemate and inadequate *in vivo* testing resulted in severe birth defects.

In 1992 the Food and Drug Administration (FDA), followed by the European committee for proprietary medicinal products in 1993, required that both enantiomers be tested for their pharmacological properties if administering a racemic drug.^{4,5} In 1997 the FDA introduced a fast track program which allowed faster approval of a single enantiomer. Synthesising single enantiomer drugs therefore became a more attractive approach to the pharmaceutical industry due to the lower dosage required for administration to achieve the desirable effects, fewer drug interactions and better pharmacological profiles in comparison to administering the racemate.⁶

The application of enzymes as catalysts has gained momentum and is now a key component in a process chemist's toolbox due to biocatalysts' high regioselectivity and stereoselectivity.⁷ The replacement of conventional chemical steps with biological methods is in demand, not only to produce single enantiomers in optically pure form (*e.e.* > 99%), but also because of the economical advantage the biological process may have to the pharmaceutical industry. The cost of a synthesis may be reduced in many ways by employing a biocatalyst: the number of protection/deprotection steps may be reduced, therefore freeing up valuable reactor time and increasing the atom efficiency of the process; no requirement for high temperatures and pressures; reduction in the amount of organic solvents used on a large scale and also enzymatic steps often produce cleaner waste streams.⁸ Scheme 1 shows a biological process for the production of acrylamide **3** from acrylonitrile **2**.⁹ The use of a microbial nitrile hydratase from *Pseudomonas chlororaphis* replaces the hydration of nitrile **2** using copper salts, palladium complexes or concentrated sulphuric acid. High concentrations (400 g/L) of acrylamide **3** were produced in high yield (99%) after 7.5 hours using low reaction temperatures (10-20 °C).

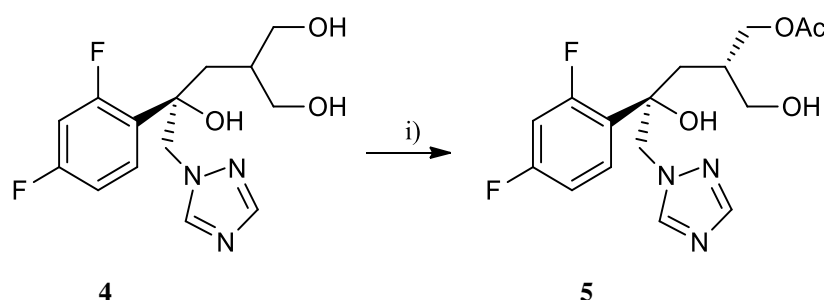


Scheme 1: Production of acrylamide **3** in high yield employing a nitrile hydratase as the biocatalyst.

Generally, for an enzymatic reaction to be industrially viable, product concentrations of ≥ 50 g/L must be employed, along with high chiral purity ($> 98\%$ *e.e.*)¹⁰ This can be difficult to achieve as enzymes often work in the millimolar range in their natural environment, therefore high concentrations can inhibit or denature the biocatalyst.

Large substrate loadings are necessary for the higher product concentrations required for an industrial process, however this often renders the substrate insoluble in aqueous media, an enzyme's natural environment. The addition of a co-solvent helps overcome this problem but often reduces the activity of the biocatalyst. These challenges that have limited the use of enzymes within industry¹¹ can now be overcome by employing directed evolution techniques to improve enzyme stability.^{12,13} The cost of making the biocatalyst and its reusability are two important factors that need to be considered when developing a biocatalytic process. Large scale fermentations can now be carried out and also enzyme immobilisation techniques can be utilised to recover and reuse the enzyme.

There are two enzymatic routes to enantiopure compounds: asymmetric synthesis and kinetic resolutions. Asymmetric synthesis converts a prochiral or *meso* substrate (desymmetrisation) into an optical isomer allowing yields of up to 100%. Scheme 2 shows an example of a lipase-catalysed diastereoselective acetylation of prochiral diol **4** to yield mono-acetate **5** in high yield (95%) and *d.e.* (97%).¹⁴



Reagents and conditions: i) Immobilised CAL-B, vinyl acetate and acetonitrile.

Scheme 2: Lipase catalysed desymmetrisation of diol **4**.

Kinetic resolutions produce an enantiopure compound from a racemic mixture based on the difference in reaction rates of the two enantiomers.¹⁵ Kinetic resolutions can only achieve a maximum yield of 50%, however, this can be overcome by an *in-situ* racemisation of the slowest enantiomer resulting in a theoretical yield of 100% (Figure 2).¹⁶

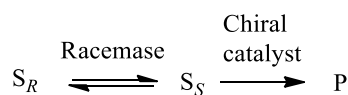


Figure 2: Dynamic kinetic resolution of a racemic mixture (S) for the synthesis of product (P).

Current industrial applications of enzymes mainly include lipases, esterases and proteases, which are largely involved in the kinetic resolutions of racemic starting materials. However they have numerous other important applications. Lipases have

been applied in the food processing industry for the modification of fats and oils, used in the detergent and textile industries to aid dyeing and the removal of lubricants.¹⁷ Likewise proteases are a major part in the detergent industry, new Subtilisins are being improved to create better detergent proteases for the future.¹⁸ Esterases are important enzymes for the degradation of industrial pollutants such as cereal wastes, toxic chemicals and plastics.¹⁹ Technology is expanding to include other enzymes such as transaminases and nitrilases for asymmetric synthesis to allow access to products in 100% yield.

1.2 Enzymatic synthesis of chiral amines

1.2.1 Chiral amines

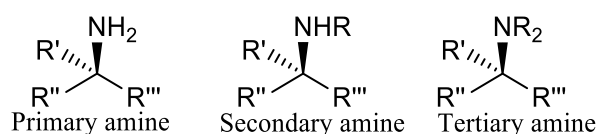


Figure 3: General structure of chiral amines.

Enantiomerically pure amines (Figure 3) have a variety of industrial applications. They are valuable components within the pharmaceutical and agrochemical industry, as resolving agents for separation of racemic mixtures by dimeric salt formation and ligands for transition metal catalysts and chemocatalysts.²⁰ Figure 4 shows an example of a pharmaceutical compound which contains a chiral amine moiety. Rivastigmine tartrate **6** is sold by the pharmaceutical company Dr Reddy's for the treatment of Alzheimer's disease, and is also sold under the name EXELON® which is licenced by Novartis Pharmaceuticals Corporation. Rivastigmine tartrate had US sales of approx. \$93 million dollars for the year ending June 2011.²¹

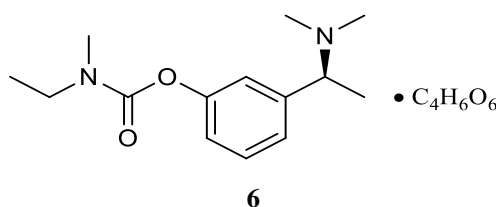


Figure 4: Structure of Rivastigmine tartrate **6** sold by Dr Reddy's for the treatment of Alzheimer's.

There are numerous methods for the synthesis of chiral amines, for example the asymmetric hydrogenation of an imine.²² However, the use of expensive metal catalysts is undesirable, and the removal of auxiliary groups to give the free amine can be problematic.²³ The most recognised method is still using classic resolution techniques *viadiastereomeric* salt formation, but the use of enzymes for chiral amine synthesis provides a much more attractive approach. Standard conditions in which biocatalysts work tend to be lower in temperature and pressure than traditional chemical methods and most reactions are carried out in water, making them more desirable processes compared to current synthetic chemistry techniques.

1.2.2 Biocatalytic synthesis of chiral amines

Biocatalysis is being increasingly seen as the method of choice for the synthesis of chiral amines. This is due to new commercial enzymes being readily available and new screening/evolution technologies that allow for enzyme optimisation towards a set of required conditions. There are various different routes to enantiomerically pure chiral amines using biocatalysts that are demonstrated in Figure 5. Existing technologies include the use of hydrolases and oxidases (e.g. lipases), but one of the most attractive approaches is the use of transaminases from a prochiral or *meso* ketone to give access to the enantiomerically pure amine in 100% yield.²⁴

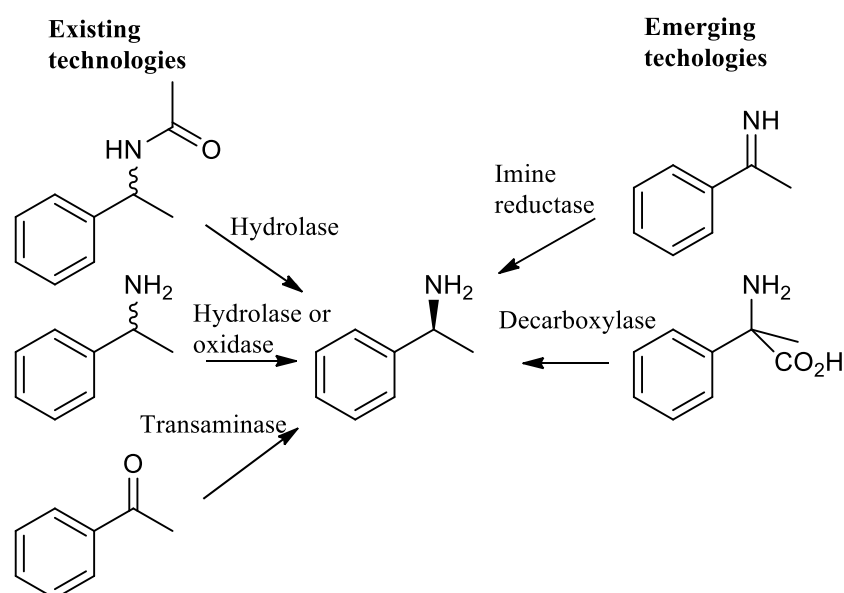


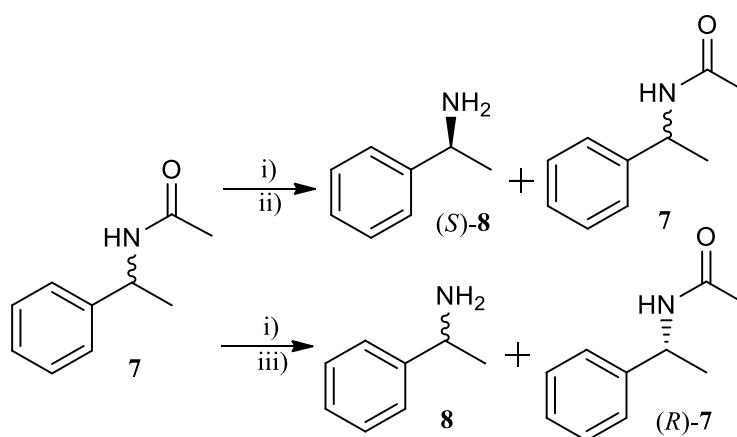
Figure 5: Current and emerging biocatalytic routes for chiral amine synthesis.²⁴

1.2.3 Kinetic resolution

Kinetic resolution of racemic alcohols, carboxylic acids and amines by hydrolytic enzymes has been studied in great detail. Hydrolytic enzymes offer the advantage of being able to carry out resolutions in low/non aqueous conditions, allowing transformations of hydrophobic substrates.^{25,26} The first report of the enzymatic resolution of chiral amines by hydrolases was reported in the late 1980s by Kitaguchi *et al.*²⁷ They subjected a panel of commercially available lipases and proteases for the resolution of various different racemic amines *via* acylation with trifluoroethyl butyrate. The commercially available lipase, Subtilisin, was selected for solvent screening and it was found that there was a strong effect on solvent choice with the enantioselectivity of

the reaction. When 3-methyl-3-pentanol was used, enantioselectivities of 99% could be achieved, highlighting the importance of solvent screening in hydrolytic processes to maximise the yield and *e.e.*

Shell developed the work of Kitaguchi *et al.*, for the synthesis of enantiomerically pure 1-phenylethylamine **8** and the corresponding amide **7** using whole cells from an *Arthrobacter sp.* (Scheme 3). Even though high enantioselectivities (> 99.5% *e.e.*) were obtained, the use of whole cells required longer reaction times making the reaction undesirable.²²



Reagents and conditions: i) *Arthrobacter sp.* ii) Potassium phosphate buffer, 30 °C, 6 hr. iii) Potassium phosphate buffer, 30 °C, 4 days.

Scheme 3: Shell's enantioselective synthesis of (S)-1-phenylethylamine **8** and (R)-acetamide **7** using whole cells from *Arthrobacter sp.*

Researchers investigated the enantioselective acetylation of racemic amines in one step by carrying out the kinetic resolution in the presence of the acetylating agent. Acquiring conditions which are not detrimental to the biocatalyst can be challenging, however BASF managed to demonstrate the multi-ton production of a number of different enantiomerically pure chiral amines in the presence of an acyl donor, isopropyl methoxyacetate.²²

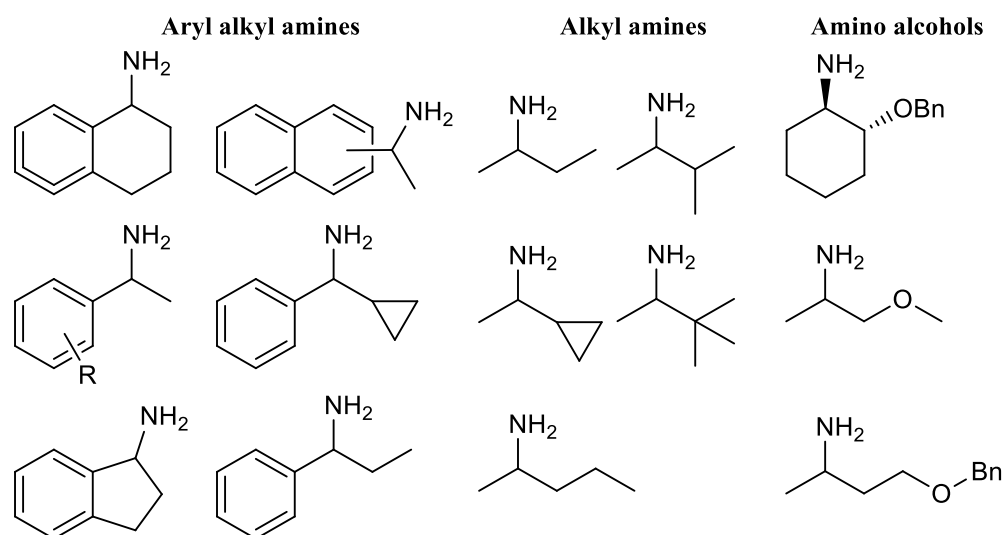


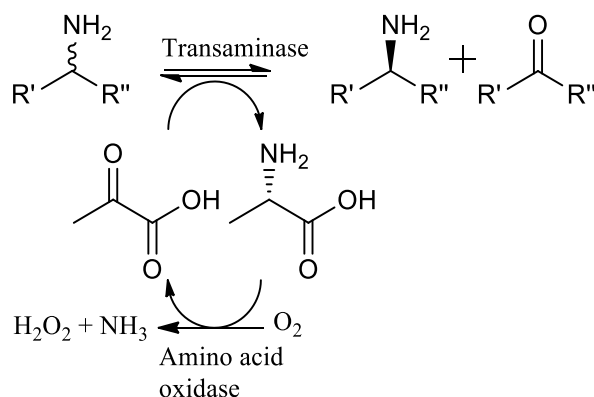
Figure 6: Substrates for the BASF lipase catalysed resolution using CAL-B.²²

The lipase catalysed resolution produced free amines (Figure 6) and the corresponding acetamides in high enantiomeric excess. After separation either by distillation or extraction, the acetamide was released by basic hydrolysis without racemisation. BASF have the facilities to carry out this process on > 3000 tonnes/year and the unreacted enantiomer can be recycled *via* racemisation with metal catalysts (such as Pd/C) and any unreacted acyl donor recovered to help lower the overall cost.

Recently, research into the use of transaminases for the resolution of racemic amines has been undertaken as the deamination reaction is thermodynamically more favoured than the asymmetric synthesis.²⁸ Shin *et al.*, developed a biphasic system to overcome inhibition of the enzyme by the product ketone.²⁹ A cyclohexane/aqueous two phase system was successful in the ω -transaminase catalysed resolution of 500 mM racemic 1-phenylethylamine. Pyruvate was used as a keto acceptor and the process obtained enantiomerically pure (*R*)-1-phenylethylamine in > 95% *e.e.* Unfortunately enzyme inactivation was observed due to an emulsion forming at the interface of the organic/aqueous phase and product inhibition by the acetophenone produced was still observed. Further work to build on the concept of the biphasic system was investigated using an enzyme membrane reactor and a hollow fibre membrane contactor for minimisation of enzyme inactivation by emulsion formation and continuous removal of acetophenone respectively.³⁰

Truppo *et al.*, proposed a dual enzyme system for the resolution of a number of different racemic amines utilising commercially available transaminases and an amino acid oxidase.³¹ Scheme 4 shows the transaminase catalysed deamination of a racemic amine

which yields alanine, the unreacted amine enantiomer and the corresponding ketone. Alanine undergoes oxidation back to pyruvate catalysed by the amino acid oxidase in the presence of molecular oxygen. This serves the purpose of minimising the amount of pyruvate in the reaction (which is known to inhibit the transaminase) as catalytic amounts can be used and also help drive the equilibrium to product formation. A range of amines were produced in 50% conversion and > 99% for both enantiomers by using enzymes with opposite selectivities.



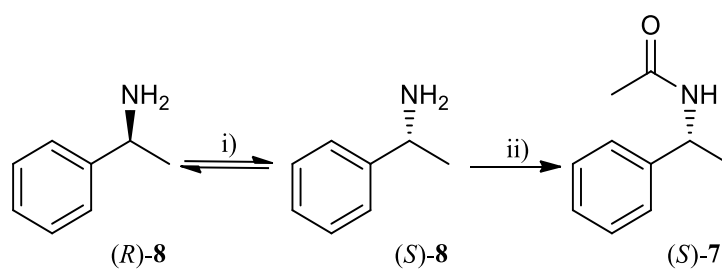
Scheme 4: Transaminase catalysed kinetic resolution of racemic amines employing an amino acid oxidase to recycle pyruvate.

These processes are only able to produce a maximum 50% yield; higher yields require the racemisation of the unreacted enantiomer.

1.2.4 Dynamic kinetic resolution

Dynamic kinetic resolution (DKR) involves the *in situ* racemisation of the starting material with the faster reacting enantiomer being removed from the system by a separate reaction, allowing access to 100% yield.¹⁵ However racemisation conditions can often be detrimental to the biocatalyst and acquiring conditions that are optimum for both the biocatalyst and the racemisation catalyst can be difficult.

One of the first examples of a DKR of an amine was demonstrated by Reetz *et al.* Palladium was used as the catalyst for the racemisation of racemic 1-phenylethylamine **8** in the presence of a lipase from *Candida Antarctica*.³² After a prolonged reaction time of 8 days, the amide (*S*)-**7** was isolated in > 99% *e.e.* and 67% yield (Scheme 5).



Reagents and conditions: i) Pd/C, H₂, Et₃N ii) Novozyme 435, EtOAc, 50-55 °C, 8 days.

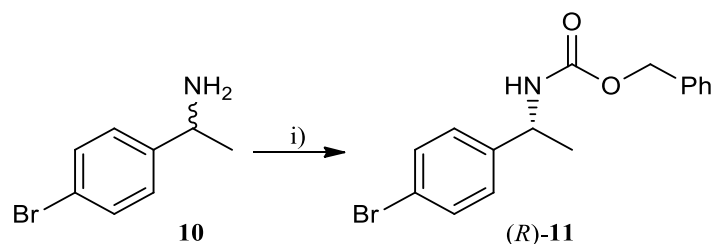
Scheme 5: Dynamic kinetic resolution of racemic 1-phenylethylamine **8** for the production of enantiomerically pure amide **7**.

Parvulescu *et al.*, built on the concept of using palladium and a lipase for the DKR of 1-phenylethylamine. They investigated palladium supported on alkaline earth salts instead of charcoal.³³ BaSO₄ was shown to be the optimum support as the best conversions and selectivities were seen when compared to other alkaline earth salts. The choice of acyl donor and hydrogen pressure was found to be important for the optimisation of reactions conditions. The BaSO₄ process offers the advantage of fewer by-products (e.g. unwanted imines) when compared to using Pd/C as the racemisation catalyst.

Kim *et al.*, investigated the use of a palladium nanocatalyst entrapped in aluminium hydroxide for the resolution of primary amines.³⁴ In a one pot reaction a wide range of amides were synthesised in high yield and *e.e.* using a commercially available lipase at 70 °C for 24 hours. The palladium nanocatalyst could be reused ten times without any significant loss of activity. The same group recently reported an improved version of the catalyst which had a reduced palladium nanoparticle size compared to the original racemisation catalyst.³⁵ The corresponding DKR in the presence of 1 mol% of new palladium nanocatalyst proceeded to completion in a faster reaction time of 12 hr.

Bäckwall and co-workers developed a Ru-catalyst for the racemisation of primary and secondary amines which allowed for high functional group tolerance.³⁶ They later developed a DKR method for the production of enantiomerically pure aliphatic and benzylic amides employing commercially available CAL-B in conjunction with the Ru-catalyst.³⁷ However, to gain access to the free amine, harsh reaction conditions are required, such as high temperatures and the use of concentrated hydrochloric acid for long periods of time. The same group developed a new method which formed carbamates, instead of amides, that can easily be removed at room temperature.³⁸ Scheme 6 shows the synthesis of carbamate **11** which was produced in 98% *e.e.* and a

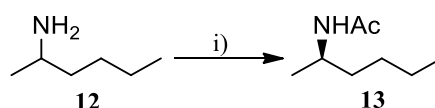
yield of 95%; the carbamate was removed using Pd/C at room temperature for 0.5 hrs under hydrogen conditions with full retention of the *e.e.*



Reagents and conditions: i) Ru-catalyst, CAL-B, Na₂CO₃, toluene, dibenzylcarbamate, 90 °C, 72 hrs.

Scheme 6: Dynamic kinetic resolution of racemic 4-bromo-1-phenylethylamine **10** for the production of enantiomerically pure carbamate **11**.

The use of less expensive transition metal catalysts, such as nickel, to replace palladium or ruthenium based catalysts is advantageous.³⁹ Scheme 7 shows the Raney Ni and CAL-B catalysed DKR for the production of amide **13** by Parvulescu *et al.*⁴⁰ As a one pot reaction, amide **13** could be produced in 95% yield and 97% *e.e.*, but if this reaction was applied for the synthesis of 1-phenylethylamine, a two pot resolution followed by racemisation had to be carried out due to Raney Ni deactivating the biocatalytic reaction. Cobalt was also tried as a racemisation catalyst but low activity and poor operational stability meant it was unsuitable for use. The Raney Ni system offers the advantage of lower reaction costs with regards to the racemisation catalyst and also because of the lower temperatures required for operation.

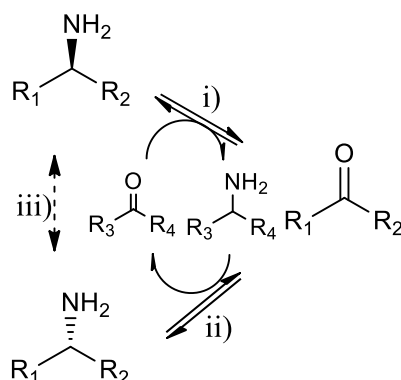


Reagents and conditions: i) Raney Ni, CAL-B, ethyl methoxyacetate, toluene, 70 °C, 4 day.

Scheme 7: Dynamic kinetic resolution of racemic 2-hexylamine **12** for the production of enantiomerically pure amide **13**.

Poulhès *et al.*, have investigated metal free DKR using radical racemisation methods. Recently they reported a low temperature reaction (38-40 °C) to produce non benzyl primary amines in range of enantiopurities (56-99% *e.e.*).⁴¹ Octanethiol was used as the racemisation agent using photochemical irradiation at 350 nm and, after acyl donor screening, methyl β-methoxypropanoate was selected due to its volatility and ease of removal from the reaction medium.

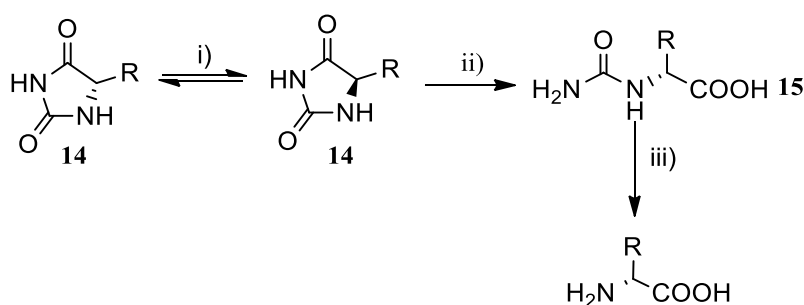
Recently Koszelewski *et al.*, demonstrated the use of transaminases for the enzymatic racemisation of chiral amines.⁴² By utilising two enantio-complimentary transaminase enzymes, a racemic amine and an amine acceptor, interconversion of the amine enantiomers could be observed (Scheme 8).



Reagents and conditions: i) (*R*)-Transaminase ii) (*S*)-Transaminase, iii) Enzymatic racemisation, 100 mM phosphate buffer, pH 7, 30 °C, 24 hours.

Scheme 8: Enzymatic racemisation employing two enantio-complementary transaminase enzymes.

However, the number of enzymatic racemisation processes are limited and few examples have been seen on an industrial scale.⁴² An example of one such reaction is the hydantoinase process. This is a three step whole cell DKR of 5-monosubstituted hydantoins **14**.⁴³ Enzymatic racemisation of hydantoin allows for complete conversion to *D*-*N*-carbamoyl amino acids **15** using *D*-hydantoinases. These are further hydrolysed to yield *D*-amino acids using a *D*-carbamolyase enzyme (Scheme 9). Directed evolution of hydantoinase has optimised this reaction. Naturally occurring *L*-carbamolyase and *L*-hydantoinase has allowed for the production of *L*-amino acids *via* the same route. This method has been used on an industrial scale for the production of both *L* and *D*-amino acids and unfortunately cannot be applied for the synthesis of amines.

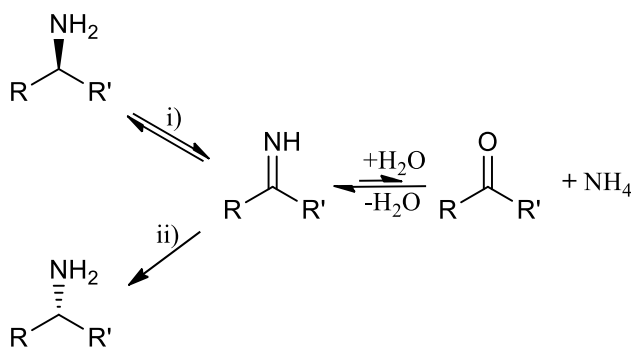


Reagents: i) Racemase ii) *D*-Hydantoinase and iii) *D*-Carbamolyase.

Scheme 9: Production of α -amino acids using hydantoinase and carbamoylase enzymes.

1.2.5 Deracemisation

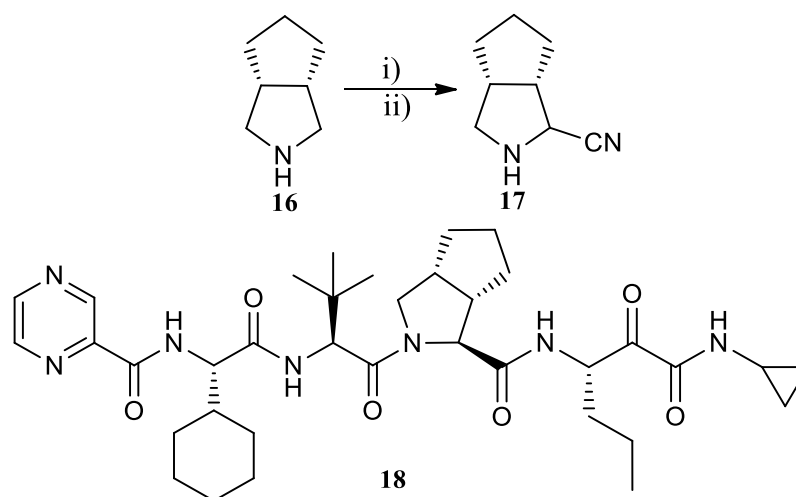
Amine oxidases catalyse the oxidation of an amine to an imine which spontaneously hydrolyses in the presence of water to the corresponding aldehyde or ketone. Schilling *et al.*, identified and cloned a flavin dependant monoamine oxidase (MAO) from *Aspergillus niger*.^{44,45} Turner and co-workers built on the activity and sequence data obtained and developed a high through-put assay for the detection of MAO activity.⁴⁶ They subjected active mutants to a deracemisation reaction with 1-phenylethylamine; if oxidation of the amine to the corresponding imine was observed in the presence of a suitable reducing agent, such as ammonia borane, the unreacted amine enantiomer was accumulated in high enantiomeric excess (Scheme 10). This method produced (*R*)-1-phenylethylamine in 77% yield and 93% *e.e.*



Reagents and conditions: i) MAO-N ii) NH_3BH_3 , 1 M Phosphate buffer pH 7.8.

Scheme 10: Monoamine oxidase deracemisation of chiral amines in the presence of ammonia borane.

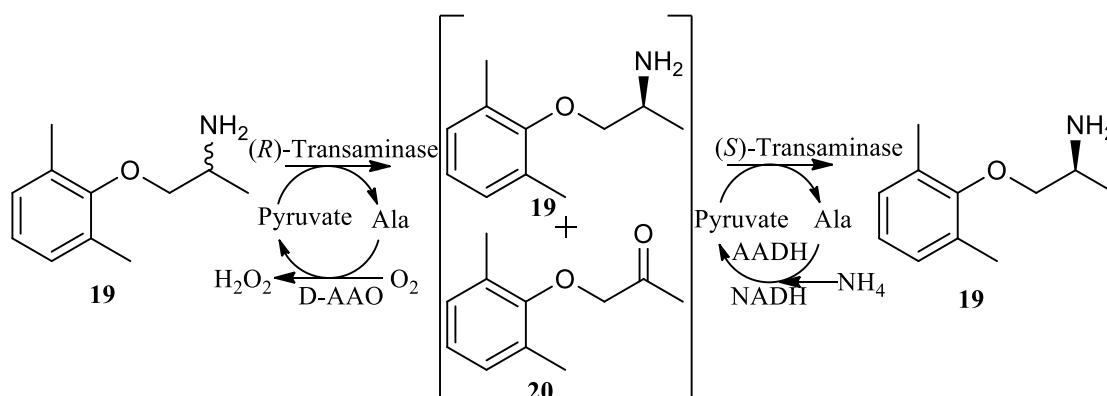
Since then, the crystal structure of the MAO-N has been solved⁴⁷ and several rounds of mutagenesis have been carried out to increase the reactivity of the enzyme towards a number of different secondary amines.⁴⁸ Köhler *et al.*, screened a wide range of secondary amines for activity with a MAO-N mutant D5.⁴⁹ Pyrrolidine **16** undergoes the MAO-N oxidation reaction, followed by cyanide addition, to give the corresponding α -amino nitrile **17** with a *d.r.* ratio 96:4 (Scheme 11). α -Amino nitrile **17** then undergoes hydrolysis in the presence of HCl to yield the corresponding amino acid (after recrystallisation) in 40% yield, *d.r.* 150:1 with a *e.e.* 98%. The 3,4-substituted proline analogue is found in hepatitis C virus protease inhibitors Telaprevir **18**.



Reagents and conditions: i) MAO-N D5, O₂ atmos., potassium phosphate buffer ii) TMSCN, MeOH and DCM.

Scheme 11: Monoamine oxidase synthesis and TMSCN addition to produce α -amino nitrile **17** which is hydrolysed to the corresponding amino acid for the synthesis of Telaprevir **18**.

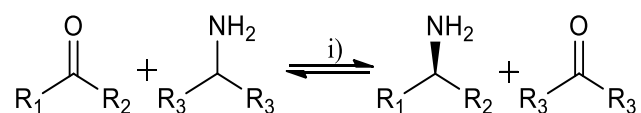
Koszelewski *et al.*, investigated the ω -transaminase catalysed deracemisation and asymmetric synthesis of Mexiletine **19**, a chiral orally effective antiarrhythmic agent, in a two-step one pot reaction.⁵⁰ Scheme 12 shows the reaction scheme for the transaminase catalysed reaction resulting in (*S*)-Mexiletine **19** being produced in > 99% *e.e.* and 97% isolated yield. (*R*)-Mexiletine **19** can be synthesised in equally high yield and enantiopurity by simply switching the order of transaminases used.



Scheme 12: Transaminase catalysed deracemisation and asymmetric synthesis of Mexiletine **19** in a two-step one pot reaction.

1.2.6 Asymmetric synthesis

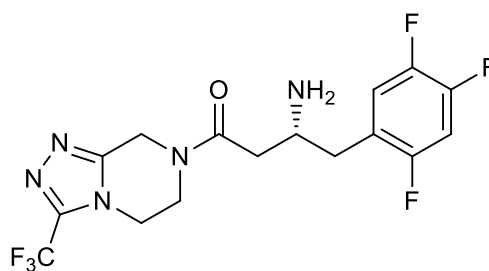
Asymmetric synthesis of chiral amines is mainly achieved by the use of transaminase enzymes (Scheme 13). In 1964 Kim reported the identification of an α -ketoglutarate transaminase which could deaminate terminal diamines utilising pyruvate or α -ketoglutarate.⁵¹ Transaminases have been used for the industrial production of amino acids but were not utilised for industrial application of simple amines until the end of the 1980s when Celgene published patents for both the kinetic resolution and asymmetric synthesis of aromatic and aliphatic amines using *R* and *S*-selective transaminase enzymes.^{52–54} The reaction starts with a prochiral ketone (for example acetophenone) and an amine donor (in this case isopropylamine (IPA)) resulting in the corresponding chiral amine and acetone respectively. Utilising both reagents at different concentrations to help drive the equilibrium, this process has been achieved on a 2.5 m³ scale giving high *e.e.* values for both *R* and *S*-amines.



Reagents and conditions: i) Transaminase, pyridoxal 5'-phosphate, buffer.

Scheme 13: General asymmetric synthesis of chiral amines using transaminases as the biocatalysts.

Codexis recently demonstrated how powerful a tool biocatalysis can be for industrial production of pharmaceutical compounds. Savile *et al.*, carried out several rounds of mutagenesis on a ω -transaminase from a *Arthrobacter sp.* to improve the transamination of a Sitagliptin diketone using IPA as an amine donor.⁵⁵ High concentrations of both the keto acceptor and the amine donor were required to make the process an industrial viable option, the addition of DMSO co-solvent was needed to solubilise the starting material. Mutations were required to stabilise the protein in conditions which did not mimic its natural environment. After 27 rounds of mutagenesis an increase in productivity (53%) and a decrease in waste (20%) were observed when using the ω -transaminase compared to the chemical route. Sitagliptin **41** (Figure 7) was produced in 99.95% *e.e.* and 92% assay yield.



41

Figure 7: The structure of the pharmaceutical compound Sitagliptin **41** synthesised using ω -transaminases by Codexis.

A major disadvantage to the use of transaminases for the asymmetric approach is the need for stoichiometric or large excesses of amine acceptor to drive reaction equilibrium toward product formation. Even though Codexis managed to achieve the conditions required to drive the equilibrium, it involved 27 rounds of mutagenesis to develop a biocatalyst to withstand those conditions. Unless high through put screening methodologies are available, screening for new enzymes/mutagenesis libraries is a slow process.

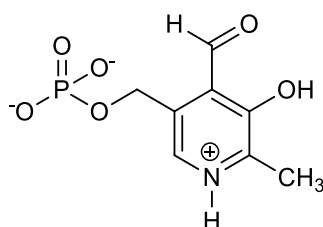
1.3 Transaminases

Transaminases are a class of pyridoxal 5'-phosphate (PLP) dependant enzymes that catalyse the reversible transfer of ammonia from an amine donor (e.g. alanine) to a keto acceptor (e.g. acetophenone). In 1932 H. A. Krebs first observed the deamination of amino acids in tissue slices but lack of adequate instrumentation at the time hampered the full characterisation of the reaction.

In 1979 the international union of biochemistry named 'aminotransferases' in the official Enzyme Nomenclature and they were termed 'transaminases' for every day usage.⁵⁶ Transaminases are attractive to the chemical community as they can be utilised for asymmetric synthesis of amines from prochiral or *meso* ketones, giving access to chiral amines with a theoretical yield of 100%. Today transaminases are used for the industrial production of natural and unnatural amino acids.

1.3.1 Pyridoxal 5'-phosphate and the transaminase active site

PLP **21** (also known as vitamin B₆, Figure 7) is a cofactor which plays a vital role in biocatalytic reactions such as decarboxylation, transamination, aldol condensation and racemisations.⁵⁷ Transaminases, alongside other PLP dependant enzymes, have two highly conserved amino acid residues: a lysine, which forms an internal aldimine with the aldehyde group of the PLP and secondly, a carboxylate side chain (usually glutamate or aspartic acid) which is positioned within hydrogen bonding distance of the pyridine nitrogen of the cofactor.⁵⁸



21

Figure 8: Pyridoxal 5'-phosphate.

A recent publication by Humble *et al.*, on the crystal structure of the ω -transaminase from *Chromobacterium violaceum* (CV2025) revealed a homodimer which has an active site at the dimeric interface.⁵⁹ Each monomer contributes amino acids to the

active site and it was found upon PLP binding major structural changes were observed. To give the active form, major refolding of the secondary structure occurs in both monomers (but predominantly on one side of the active site whereas the other side is ridged).

Detailed studies looking at the active site of transaminases have attempted to explain the stereoselectivity and understand the substrate range. Kim *et al.*, proposed a two-binding site model (Figure 8) based on the substrate structure-reactivity relationship.⁶⁰ They suggested two binding pockets, a small 'S' pocket and a large 'L' pocket. A strong electrostatic repulsion for carboxylates and steric constraint is observed in the 'S' pocket (anything larger than an ethyl group showed decreased activity), resulting in stereoselectivity and substrate specificity. Even the 'L' pocket showed a limitation to the size of substituent as anything more sterically demanding than a hexyl group was inactive towards the enzyme.

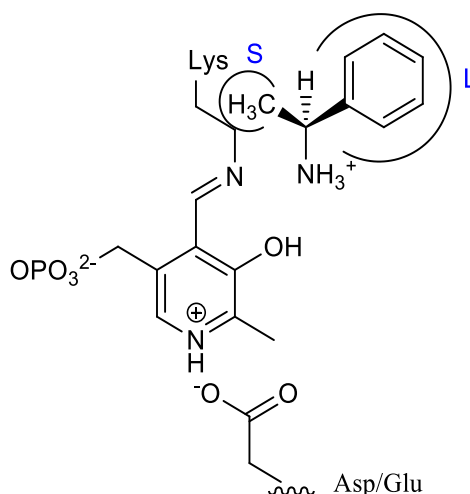
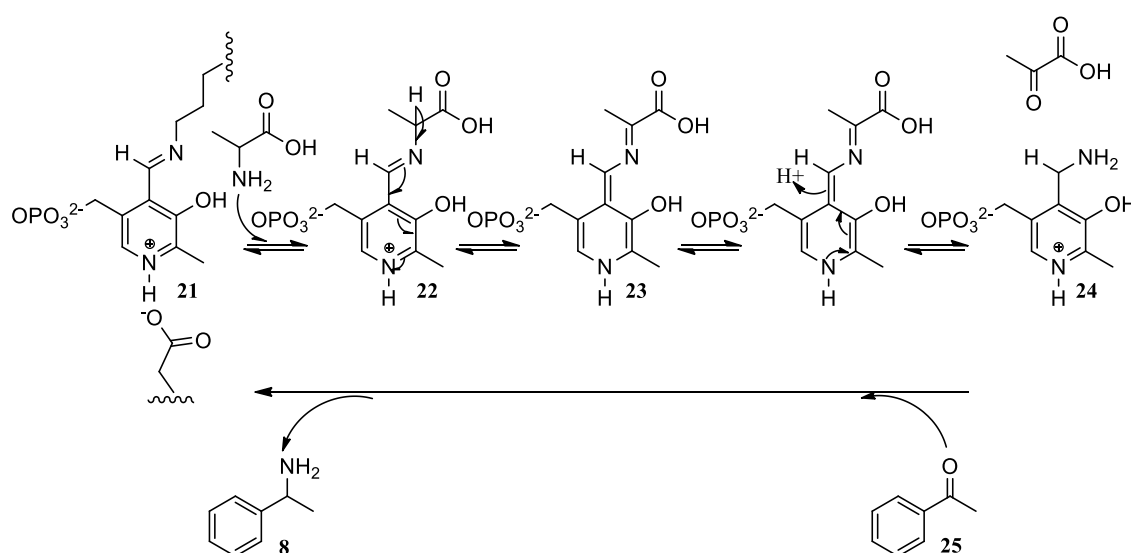


Figure 9: Active site model proposed by Kim *et al.*⁶⁰

Distefano *et al.* produced an artificial transaminase by binding a pyridoxamine derivative to the active site of an intestinal fatty acid binding protein *via* a disulphide bond.⁶¹ Point mutations were carried out in order to place a lysine group in close proximity to the aldehyde group of the cofactor, and catalytic activity was seen with good enantioselectivity within the range of 84-94% *e.e.* Further work to stabilise the positive charge on the synthetic pyridoxamine ring was investigated.⁶² A carboxylate group was inserted into the active site of the enzyme but this resulted in the mutants being unstable. An alternate route using a chemically synthesised *N*-methylated pyridoxamine to create a cationic cofactor proved to be more successful.

1.3.2 Transaminase mechanism

The transaminase mechanism is known as a ping-pong bi-bi mechanism and is composed of two half reactions which regenerates the PLP cofactor (Scheme 14).⁵⁶ An internal schiff base is formed between an internal lysine and the aldehyde group of the PLP. The alanine amine donor forms an imine with the PLP by replacing the active site lysine, forming an external aldamine **22**. A [1-3]-proton shift (catalysed by the lysine residue released in the previous step) of the substrates α -proton results in the formation of a ketamine **23**. Hydrolysis of the intermediate releases a ketone (in this case pyruvate) and forms pyridoxamine 5'-phosphate **24** (PMP). The formation of a Michaelis-complex between the PMP **24** bound to the enzyme and a amine acceptor **25** results in the second reverse reaction to proceed and hence regenerates the enzyme bound PLP **21**.^{63,64}



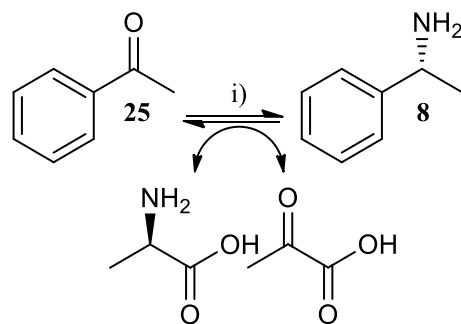
Scheme 14: Transaminase ping-pong bi-bi mechanism.

1.3.3 Methods to overcome transaminase challenges

Transaminases are known to have high stereoselectivity,⁶⁵ and work efficiently under mild reaction conditions,⁶⁶ and their ability to catalyse asymmetric reactions means they show great potential as industrial biocatalysts. However, transaminases have considerable limitations which has hampered their use within industry for the synthesis of chiral amines, such as the equilibrium strongly favouring kinetic resolution rather than asymmetric synthesis of amines and enzyme inhibition by both products and

starting material.⁶⁷ Some of these limitations and methods to overcome these challenges will be discussed below.

Transaminase reactions are well known to suffer from poor equilibrium constants. This is because there is very little change in the Gibbs free energy of the reaction, due to reactions being reversible and the substrates/products resembling each other in structure with equilibrium constants for the reaction being ~ 1 .⁶⁸



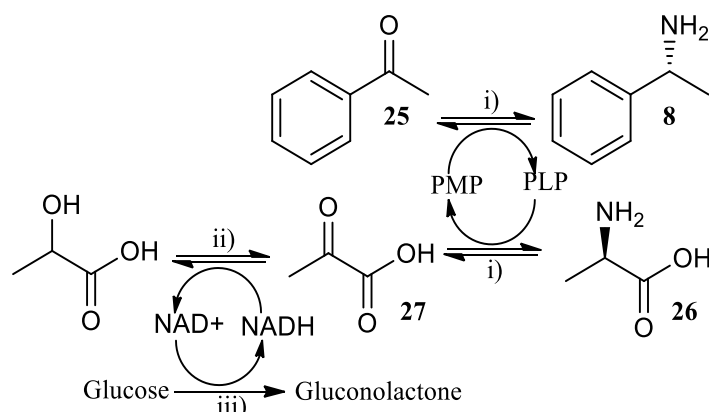
Reagents: i) Transaminase

Scheme 15: Forward and reverse transaminase reaction.

Different methods have been used to drive the equilibrium to product formation and prevent the reversible reaction between substrates and products. Shin and Kim employed a biphasic system using the reverse transaminase biotransformation (i.e. 1-phenylethylamine **8** to acetophenone **25**, Scheme 15).²⁹ The transaminase reaction occurred mostly in the aqueous phase whilst employing an organic phase (cyclohexane) to remove acetophenone **25** and act as a reservoir for 1-phenylethylamine **8**. This method helped drive the equilibrium to product formation by controlling the concentration of acetophenone and 1-phenylethylamine **8** in the aqueous phase which also helped prevent substrate/product inhibition of the transaminase.

Other methods which have been used to drive equilibrium involve the use of co-enzymes to remove one or both products. Truppo *et al.*, proposed a three enzyme system to remove pyruvate **27** which serves the dual purpose of driving the equilibrium to product formation and preventing inhibition of the transaminase.⁶⁹ The transaminase catalysed the reaction of acetophenone **25** to 1-phenylethylamine **8** employing D-alanine **26** as an amine donor (Scheme 16). Pyruvate **27** was then reduced by lactate dehydrogenase (LDH) and glucose dehydrogenase (GDH) was used to recycle the cofactor NADH, which is essential for LDH activity. The production of gluconic acid

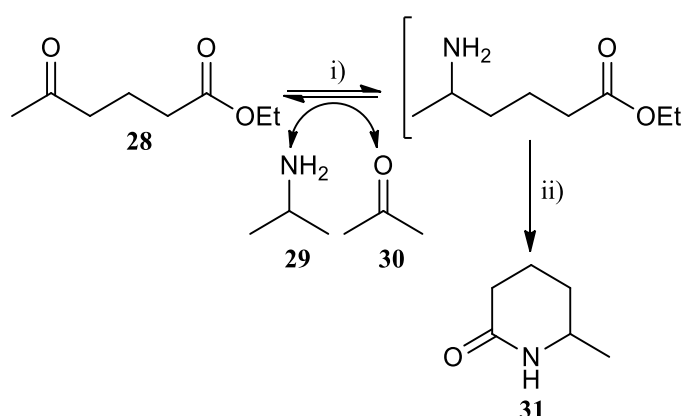
resulted in a drop in pH allowing for rapid screening using the indicator dye phenol red. The colour change can be monitored spectrophotometrically at 560 nM.



Reagents and conditions: i) Transaminase, ii) Lactate dehydrogenase and iii) Glucose dehydrogenase, 100 mM potassium phosphate buffer, 30 °C.

Scheme 16: Transaminase catalysed reaction of acetophenone **25** employing the LDH/GDH system purposed by Truppo *et al.*

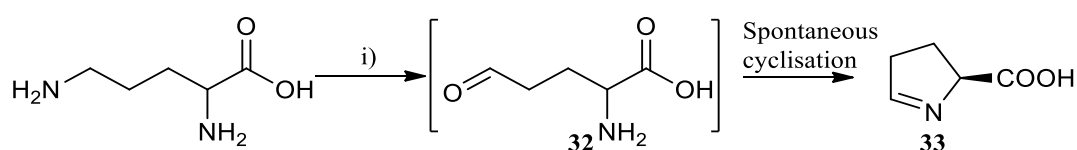
Another means of driving the equilibrium towards product formation is the use of spontaneous cyclisation of one or both transaminase products. This method can also be utilised to remove products which are inhibiting to the transaminase enzyme. Truppo *et al.*,⁷⁰ ran 50 g/L scale reactions starting from ethyl 4-acetylbutyrate **28** with an excess of IPA **29** utilising the commercially available Codexis enzymes ATA-117/113. The reactions proceeded in > 99% conversion and > 99% *e.e.* after < 15 hours the cyclised product (6-methyl-2-piperidone **31**) was isolated in > 90% yield (Scheme 17).



Reagents and conditions: i) Transaminase, ii) Spontaneous cyclisation, 100 mM potassium phosphate buffer, 30 °C.

Scheme 17: Transaminase catalysed reaction of ethyl 4-acetylbutyrate **28** with spontaneous cyclisation of the amine product to yield 6-methyl-2-piperidone **31** in high *e.e.* developed by Truppo *et al.*

A coupled reaction between an α -transaminase and a δ -transaminase for the synthesis of Δ -pyrroline-(*S*)-carboxylic acid **33**, by recycling 2-ketoglutaric acid with the α -transaminase, was investigated by Tao *et al.*⁷¹ The δ -transaminase catalyses the deamination of L-ornithine forming L-glutamic acid semialdehyde **32**, using 2-ketoglutaric acid as the keto acceptor. L-glutamic acid semialdehyde then spontaneously cyclises, driving the equilibrium to product formation (Scheme 18). The overall yield of the amino acids from both reactions increased by around 40% compared to using both systems individually.



Reagents: i) Ornithine- δ -transaminase.

Scheme 18: Spontaneous cyclisation to produce Δ -pyrroline-(*S*)-carboxylic acid **33** from the coupled transaminase reaction by Tao *et al.*

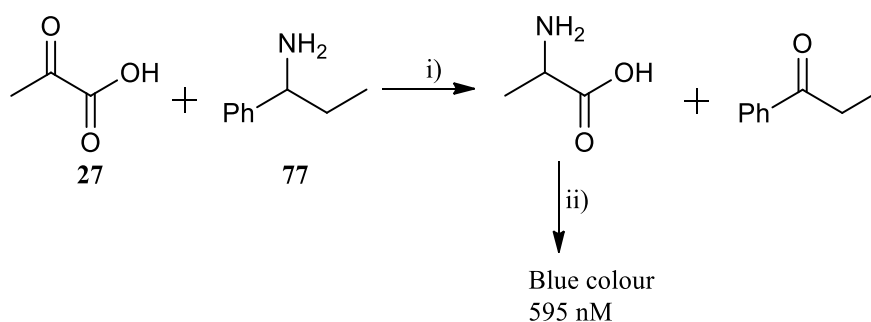
Höhne *et al.*, investigated the transaminase catalysed asymmetric synthesis of four different chiral amines utilising alanine as an amine donor.⁷² The use of a pyruvate decarboxylase (PDO) was explored to help drive the equilibrium to product formation by the breakdown of pyruvate to acetone and CO₂. A PDO was employed because it does not require for an external cofactor, unlike the LDH system which requires NAD⁺. An excess of alanine (110 mM, 22 equivalents) helped drive the transaminase reaction to above 80% conversion, which otherwise showed poor conversions of between 5.5-6% using an equimolar ratio without the PDO.

The highlighted examples show the potential of transaminases for the industrial asymmetric synthesis of chiral amines in high yield and *e.e.* They overcome problems with equilibrium by driving the reaction to completion by removing one of both of the products. An excess of amine donor can also be utilised to push the reaction equilibrium and spontaneous cyclisation can serve the dual purpose of driving the reaction, and also creates a secondary product which is not inhibitory to the enzyme.

1.3.4 Screening of transaminase enzymes

In order to detect new transaminase activity or to screen a library of mutants, a high throughput assay (the ability to screen 10^4 - 10^6 variants)¹² is desirable. The most widely used methods for the detection of transaminase activity involve conventional analytical techniques such as HPLC or GC. These are time consuming and limit the number of enzymes which can be screened, therefore, either a 96-well based assay or a solid phase screen is required to allow screening of large libraries.

In 2004 Hwang *et al.*, developed a 96-well microtiter plate (MTP) spectrophotometric method using $\text{CuSO}_4/\text{MeOH}$ for the detection of ω -transaminase activity.⁷³ Scheme 19 shows the concept of the assay, a keto acceptor (e.g. pyruvate, **27**) and a amine donor (e.g. 1-phenylethylamine, **77**) is subjected to an ω -transaminase from *Vibrio fluvialis* to produce the corresponding α -amino acid and ketone or aldehyde. In the presence of CuSO_4 the α -amino acid forms a copper complex resulting in a blue colour which is detectable at 595 nM. A wide range of amino donors were screened utilising this method and the selectivity of the enzyme could be calculated by using a chiral amine donor. However formation of phosphate-copper complexes means the assay solution has to be centrifuged and cell cultures have to be dialysed before being screened due to phosphates salts present in the cell culture, and endogenous amino acids can give negative results. Another drawback of the methodology is that it is only an endpoint assay; unfortunately the assay solution inhibits the enzyme and therefore cannot be used to determine kinetic data.



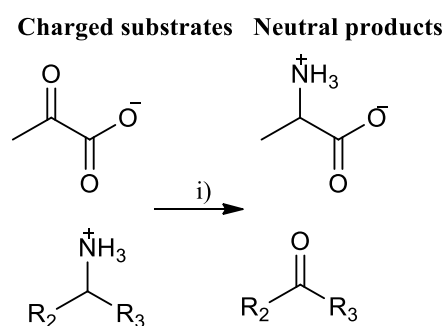
Reagents and conditions: i) Transaminase, 100 mM phosphate buffer, pH 7, ii) $\text{CuSO}_4/\text{MeOH}$.

Scheme 19: Spectrophotometric assay developed by Hwang *et al.*, for the detection of α -amino acid formation by forming a copper complex.

Schätzle *et al.* built on this concept but instead of using a copper staining solution they monitored the production of acetophenonespectrophotometrically at 245 nM.⁷⁴ As long

as low wavelength UV absorbing ketones/aldehydes or keto acids are used as a co-substrate with 1-phenylethylamine then kinetic data can be recorded for the transamination. However, this assay is limited to screening transaminases with 1-phenylethylamine and is limited to low concentrations as too high a concentration overloads the detector and therefore kinetic parameters cannot be measured.

To overcome the limitation of only one amine donor being screened Schätzle *et al.* developed a conductometric method for the detection of transaminase activity.⁷⁵ Utilising pyruvate as the keto acceptor and any amine donor, a decrease in the conductivity can be observed if transaminase activity is present as demonstrated in Scheme 20. Low conducting buffers have to be used as only a slight change is observed in the conductivity of the reaction, thus phosphate buffer had to be replaced with tricine buffer.



Reagents and conditions: i) Transaminase, 20 mM Tricine buffer, pH 4-8.

Scheme 20: Conductometric transaminase assay which can be used to carry out an amino donor profile.

Recently Sehl *et al.*, have published a colourimetric assay for the detection of ω -transaminase activity with substrates with 2-hydroxy ketone **35** motifs (Figure 10).⁷⁶ 2,3,5-Triphenyltetrazolium chloride (TTC) was used to detect a wide range of different aliphatic, aliphatic-aromatic and aromatic 2-hydroxy ketones **35** using either 1-phenylethylamine **8**, benzylamine **34** or alanine **26** as the amine donors. Upon conversion of the 2-hydroxy ketone to the corresponding amine, TTC is reduced to 1,3,5-triphenylformazan (TFP) which produces a colour change from an intense red colour to colourless which can be detected spectrophotometrically at 510 nm.

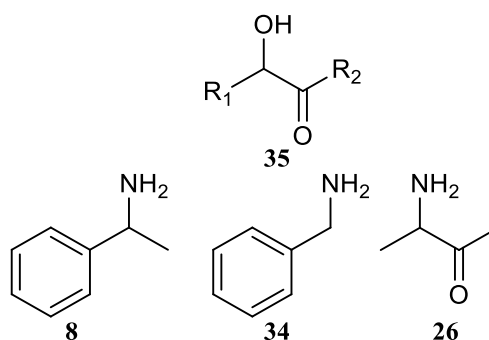


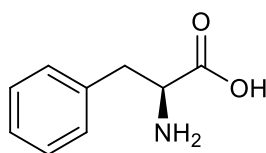
Figure 10: 2-Hydroxy ketone **35** and three different amine donors utilised for the TTC assay developed by Sehl *et al.*

Although the above methods offer higher through-put than standard HPLC/GC detection techniques, they do not generate the outcome that a solid phase assay would provide, meaning the ability to screen large libraries of transaminases is often time consuming.

1.3.5 Transaminases for chiral amine synthesis

Transaminases offer many advantages over other available enzymes for the industrial production of chiral amines. Transaminases possess high turnover rates, have no requirement for external cofactor recycling, have a broad substrate specificity and the ability to catalyse asymmetric synthesis giving access to a wide range of chiral amines in a theoretical quantitative yield.⁵⁶ Because of these factors, transaminases have attracted increased attention by research scientists to exploit new routes for the large scale industrial production of chiral amines.

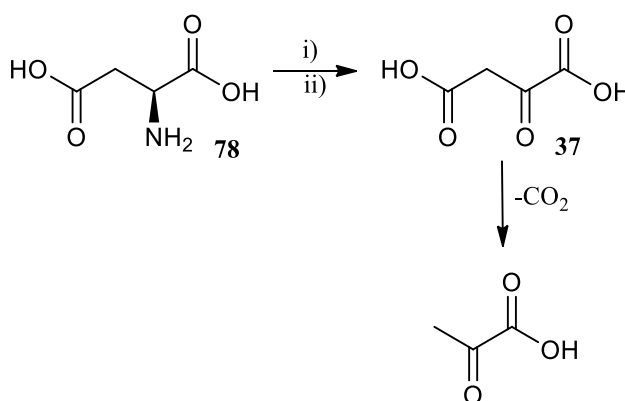
Transaminases are already well established for the industrial production of α -amino acids. The synthesis of both D and L-amino acids employing microbial amino acid transaminases as the biocatalyst has proven very successful with greater than 99.9% *e.e.*⁷⁷ Production of L-phenylalanine **36** (Figure 11) from phenylpyruvic acid utilising an immobilised recombinant *E.coli* expressing transaminase (SW0209-52) was investigated by Leng *et al.*⁷⁸ The average productivity was 1.85 g/L/h, with an average of 85% conversion over 40 days, making this process relevant for industrial applications. However, the addition of the expensive cofactor PLP was required for high transaminase activity; this would have to be addressed prior to large scale commercial processes.



36

Figure 11: Structure of L-phenylalanine **36**.

A tyrosine aminotransferase (E.C 2.6.1.5) has been used for the large scale production of L-thienylalanine from 2-hydroxy-3-thienylacrylic acids. L-Thienylalanine is an important building block of the bradykinin antagonist HOE-140 which is used as an anti-inflammatory and anti-allergenic agent.⁷⁹ The use of L-aspartate **78** as an amine donor served to drive the equilibrium as upon production of the equivalent keto acid **37** by the transaminase, decarboxylation occurred as demonstrated in Scheme 21.

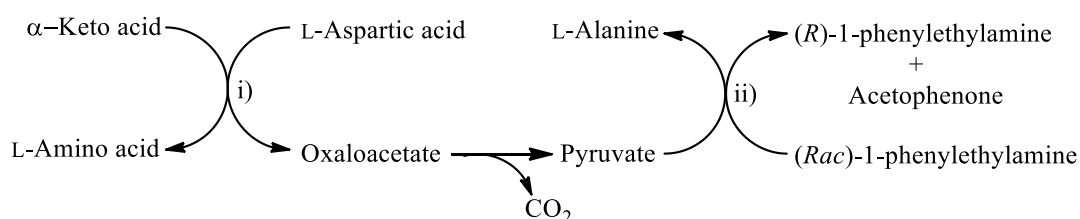


27

Reagents: i) Transaminase (ATCC 11303), ii) L-thienylalanine

Scheme 21: Decarboxylation of keto acid **37** to pyruvate **27**.

An ω -transaminase from *Vibrio fluvialis* JS17 and an α -transaminase from the (*avtA*) gene of *E. coli* K-12 were employed for the simultaneous synthesis of (*S*)-amino acids and (*R*)-amines as shown in Scheme 22.⁸⁰ The decarboxylation of oxaloacetate helps drive the α -transaminase reaction to completion but also provides the keto acceptor (pyruvate) for the ω -transaminase reaction. This process produced L-amino acids and (*R*)-1-phenylethylamine in high conversion and *e.e.*

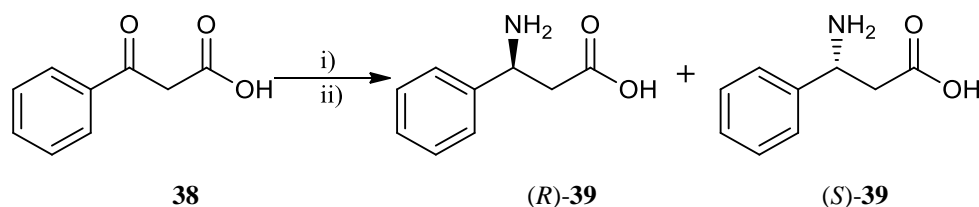


Reagents: i) α -Transaminase, ii) ω -Transaminase

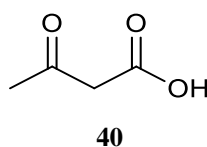
Scheme 22: Dual transamination reaction for the production of enantiomerically pure L-amino acids and (R)-1-phenylethylamine.

As the use of transaminases for the production of α -amino acids has been successful on an industrial scale, the use of transaminases for the synthesis of β -amino acids has also been investigated. β -Peptides show a higher resistance to protease degradation when compared to α -peptides making them valuable physiologically active compounds.^{81,82}

A novel β -transaminase from *Mesorhizobium* sp. Strain LUK⁸³ was identified for the asymmetric synthesis of 3-amino-3-phenylpropanoic acid **38** in high *e.e.* The transformation utilised 3-aminobutyric acid as the amino donor to help drive the equilibrium to product formation as the by-product that is formed (acetoacetic acid **40**) spontaneously decomposes into acetone and CO₂ (Scheme 23). A dual enzymatic system was required because the substrate had to be synthesised *in situ* (because the acid was prone to decarboxylation) using a lipase from the corresponding ester.



Reagents: i) β -Transaminase ii) 3-aminobutyric acid



Scheme 23: Asymmetric synthesis of 3-amino-3-phenylpropanoic acid **39** employing a β -transaminase from *Mesorhizobium* sp. as the biocatalyst and the by-product acetoacetic acid **40** before spontaneous decomposition.

Truppo *et al.*, demonstrated the use of IPA in high concentrations to push the equilibrium of the transamination of acetophenone to (R) and (S)-1-phenylethylamine using the commercially available transaminases ATA-117 and 113.⁶⁹ The reactions were carried out on a 25 mL scale in the presence of 20 mM acetophenone. The

reactions went to 95% conversion in greater than 99% *e.e.* for both enantiomers. This system shows great promise for the industrial production of chiral amines as IPA is cheaper to use as an amine donor than alanine.

Even though transaminases present problems as industrial biocatalysts, the above methods show some possible solutions for resolving these problems. Whether it is the use of coenzymes or a large excess of the amine donor to drive the equilibrium, chiral amines can be produced at industrially relevant concentrations using the above methodologies. Codexis demonstrated that whilst wild-type transaminases may not be active under desired process conditions, it is possible to engineer the enzyme to tolerate the reaction environment.

1.4 Aims of the project

The aim of this project is to develop transaminases for the synthesis of enantiomerically pure chiral amines. Firstly a suitable screening methodology will be developed for the detection of novel transaminase activity utilising chiral amines and a keto acceptor. The screen must have the ability to detect the selectivity of the enzyme (i.e. whether the enzyme is *R* or *S* selective).

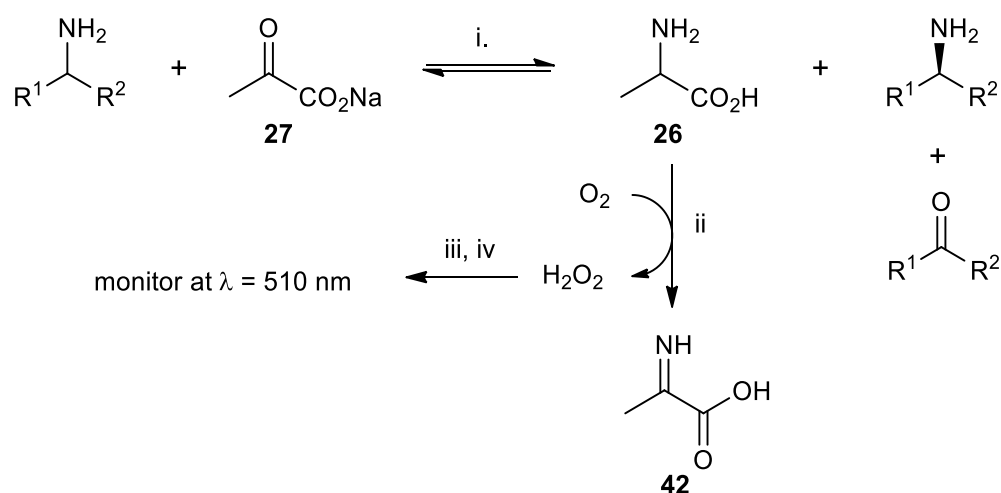
Transaminases identified by this approach will be cloned and expressed in *E. coli* and characterised for their ability to convert keto acids to optically active amines of industrial importance. Desirable characteristics that will be looked for include high enantioselectivity and also high catalytic activity against a range of different substrate keto acids.

The identified enzymes of interest will be subjected to preparative biotransformations in order to address the issues associated with scale-up, particularly substrate/product concentrations and also enzyme stability under the reaction conditions.

2. Results and discussion- Colourimetric assay

In order to detect the transamination of chiral amines and sodium pyruvate, a high-throughput screen was required. Current methods of screening transaminase activity have been based upon monitoring pH changes using the indicator dye phenyl red,⁶⁹ formation of coloured copper–alanine complexes,⁷³ an elegant UV spectrophotometric protocol⁷⁴ and recently a 96-well colourimetric assay for the detection of 2-hydroxyamines.⁷⁶ However, reaction time and sample preparation can often be time consuming. Herein describes a simple colorimetric-based method and it has been demonstrated that this method can be used to determine both the activity and enantioselectivity of a wide range of transaminase substrates.

A three-enzyme colourimetric assay was developed for the detection of transaminase activity; amines are treated with a transaminase and sodium pyruvate **27**. Successful substrates result in the conversion of sodium pyruvate **27** to L- or D-alanine **26** which can be detected by the addition of an amino acid oxidase (L- or D-AAO respectively) to the reaction mixture. Oxidation of alanine **26** to the imine **42** by AAO results in the production of H₂O₂ which can be detected colourimetrically by the addition of a reporter dye (in this case pyrogallol red) and horse radish peroxidase. Provided that all subsequent enzymes and reagents are added in excess; the transaminase step becomes rate-limiting and hence its activity with respect to the amine substrate of interest can be determined. Scheme 24 shows the assay which is adapted from previous reported screens for the use with oxidase enzymes.^{46,84}



Scheme 24: Overview of the colourimetric assay.

Reagents and conditions: i) ATA-117, ii) D-AAO, iii) PGR, iv) HRP, 30 °C, pH 7.5, 510 nm.

2.1 Path length determination

In order to calculate the extinction coefficient of PGR, the path length of a sample in a 96-well MTP requires calculation. A flavin adenine dinucleotide (FAD) solution (17 mM) in 100 mM phosphate buffer (pH 7.7) was used due to its known extinction coefficient ($11300 \text{ M}^{-1}\text{cm}^{-1}$).

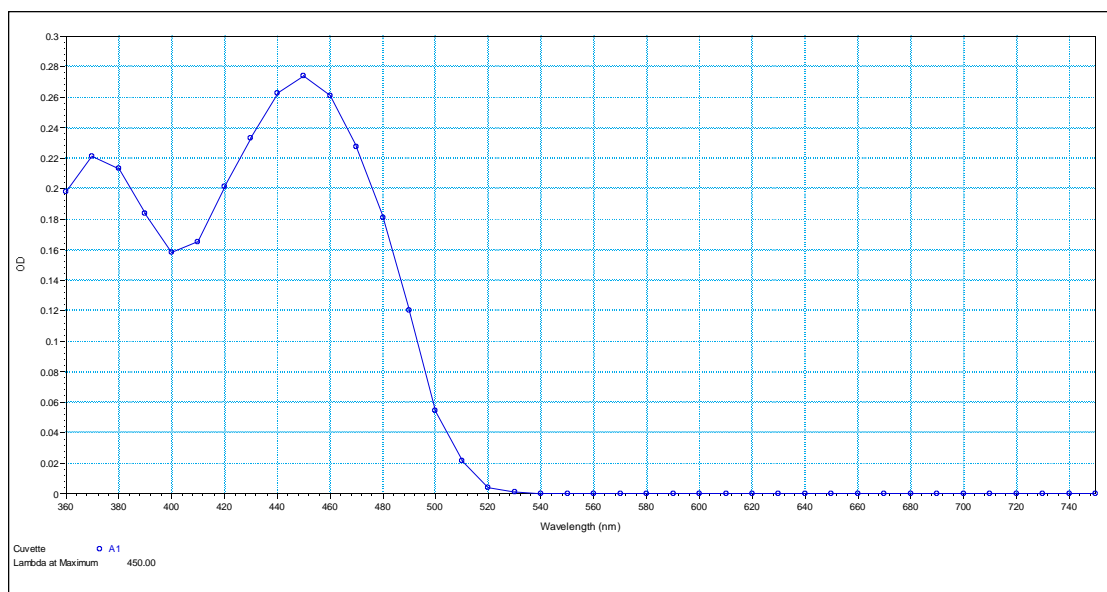


Figure 12: Absorbance spectrum of a FAD solution over the range of 360-750 nm.

Figure 12 shows that the absorbance maximum of the FAD solution is 450 nm, therefore, samples were run in both a 1 cm cuvette and a flat bottom 96-well MTP at 450 nm. Measurements were taken in a 1 cm cuvette using 100 mM potassium phosphate buffer (pH 7.7) as a standard, followed by a series of volumes in a MTP (Table 1). The path length was calculated by using Equation 1.

Equation 1: Path length (cm).

$$\text{Path length} = \text{OD 96 well MTP} \div \text{OD 1 cm cuvette}$$

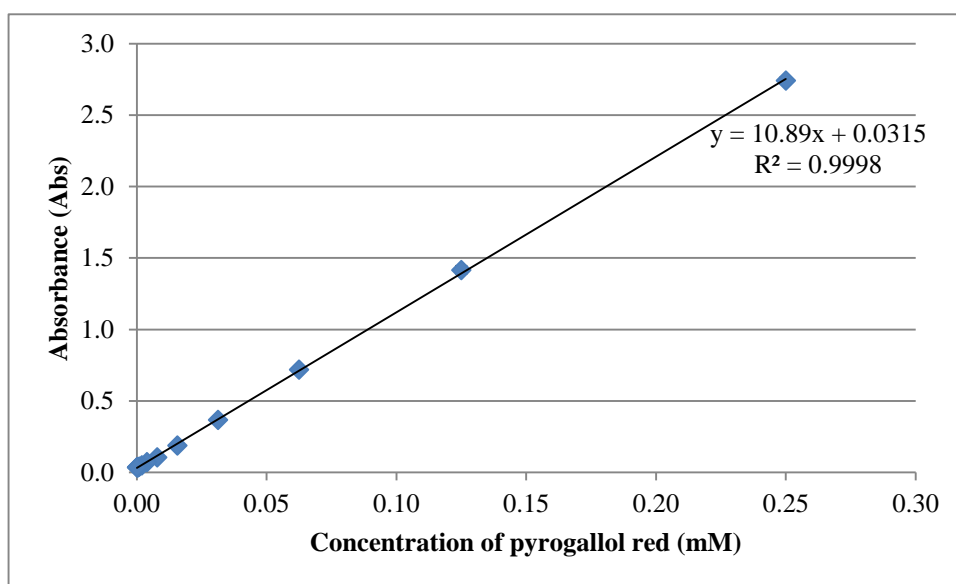
$$\text{OD} = \text{Optical Density (AU}\lambda\text{)}$$

Table 1: Calculated path length of four different volumes in a flat bottom 96-well MTP.

Volume (μL)	Path length (cm)
200	0.61
132.5	0.41
122.5	0.37
100	0.31

2.2 Determination of extinction coefficient of pyrogallol red

In order to determine the extinction coefficient and maximum wavelength (λ_{max}) of PGR, the absorbance spectrum was measured between the wavelengths 300 nm and 700 nm. The maximum wavelength (λ_{max}) was determined to be 540 nm (Appendix 8.1.3). The concentration of PGR was then varied to produce a standard curve (Figure 13).

**Figure 13:** Linear range of the PGR standard curve at 540nm.

The linear range at 540 nm of a standard curve gives a gradient which is equal to the extinction coefficient \times the path length. According to the Beer-Lambert law (Equation 2) for a 100 μL solution this gives an extinction coefficient for PGR of 35.1 $\text{mM}^{-1}\text{cm}^{-1}$.

Equation 2: The Beer-Lambert law.

$$A = \varepsilon \times c \times L$$

A = Absorbance ($\text{AU}\lambda$), ε = extinction coefficient ($\text{M}^{-1}\text{cm}^{-1}$), C = concentration (M) and L = path length (cm).

2.3 Background activity of Pyrogallol red

Background activity of PGR in the colourimetric solution phase screen was determined by carrying out a series of blank reactions. Experiments were carried out using the optimised assay conditions utilising 1-phenylethylamine as the amine donor and individual components removed were replaced by the addition of 100 mM phosphate buffer (Table 2).

Table 2: Components of each individual reaction investigated.

	Components		
	1-Phenylethylamine	D-AAO	ATA-117
Reaction	✓	✓	✓
Blank 1		✓	✓
Blank 2	✓	✓	
Blank 3	✓		✓

Figure 14 shows that there is minimal background activity which does not interfere with the most active of substrates. The effect of background activity on the data from the screen can be minimised by removing a blank from the substrate data. The highest background activity was obtained when ATA-117 was removed. This result suggests that upon the addition of the amine an increase in background activity can be observed. All control experiments were therefore measured without the addition of ATA-117/113.

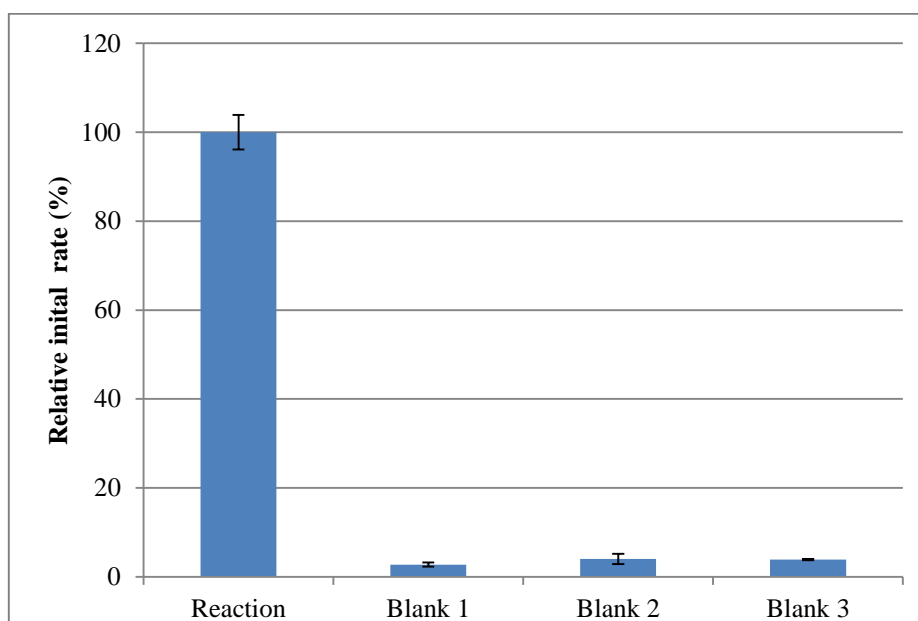
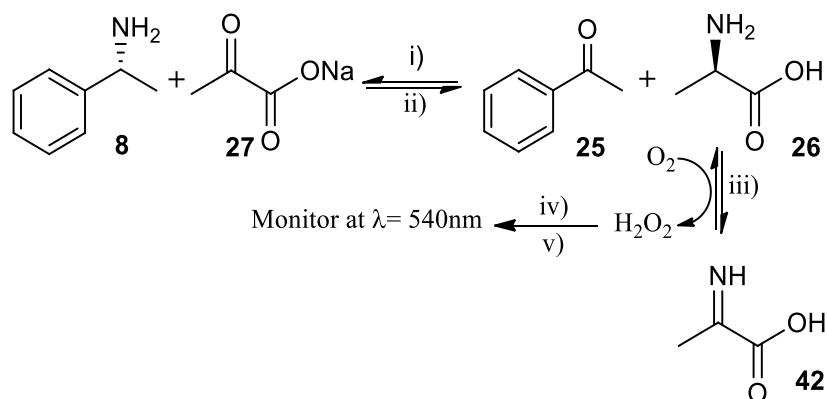


Figure 14: Determination of pyrogallol red background activity.

2.4 Screening of amine substrates

A selection of amine donors were screened and the relative initial rates calculated to determine if the liquid phase assay (Scheme 25) could be used to discriminate between different amine donors. This was achieved by comparison of the different rates with ATA-117 and therefore, their acceptance by the transaminase enzyme.



Reagents and conditions: i) Forward reaction, ii) Reverse reaction, iii) D-AAO, iv) HRP, v) PGR, 30 °C, 540 nm, pH 7.5.

Scheme 25: Transamination reaction using ATA-117.

Previous studies have indicated that ATA-117 has good activity with 1-phenylethylamine **8**, therefore relative initial rates of substrates screened were compared to 1-phenylethylamine **8**.

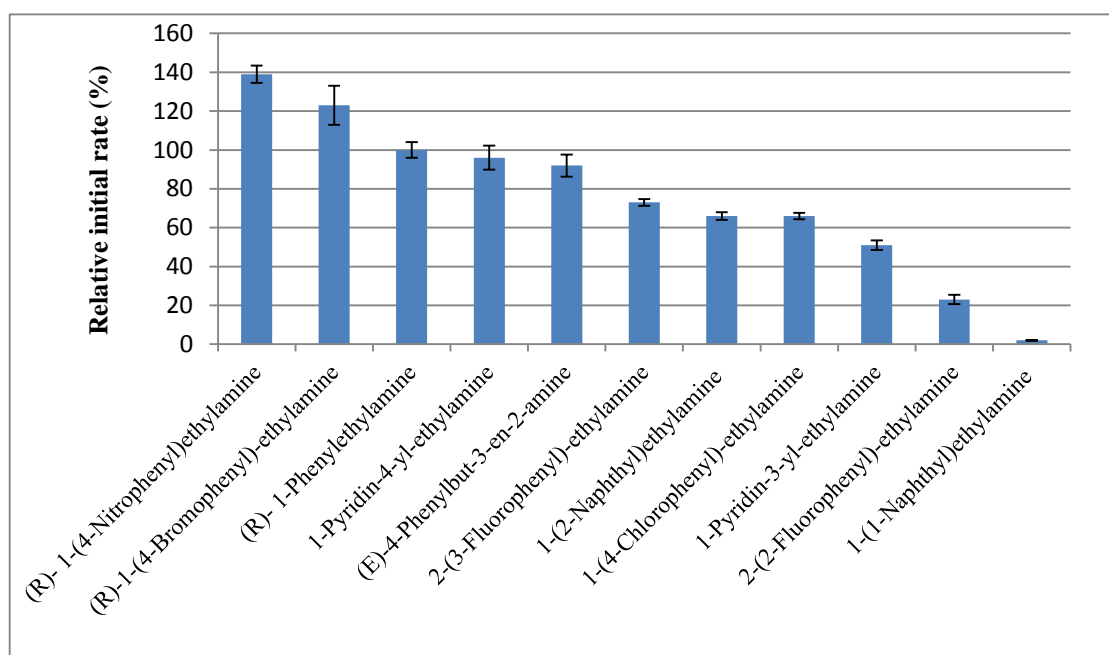


Figure 15: Different amine substrates screened and the relative initial rates compared to 1-phenylethylamine. Control experiments were carried out for each reaction utilising the same reaction conditions but without the transaminase present.

Five different β -amino acids were also screened (3-amino-4-phenylbutanoic acid, 3-aminobutyric acid, 3-amino-2-methylpropanoic acid, 3-aminopentanedioic acid and 3-aminopropanoic acid), however no activity was observed with any of the compounds. As seen in Figure 15 the assay was able to measure initial rates with ATA-117 with various substrates.

2.5 Varying ATA-117 concentration

Optimisation of the colourimetric assay conditions was required, therefore, investigation into the effect of varying ATA-117 concentration was carried out. A series of dilutions of ATA-117 were prepared and using 1-phenylethylamine as a substrate, previous conditions were kept constant (see Section 6). Experiments were carried out at 30 °C and analysed spectrophotometrically.

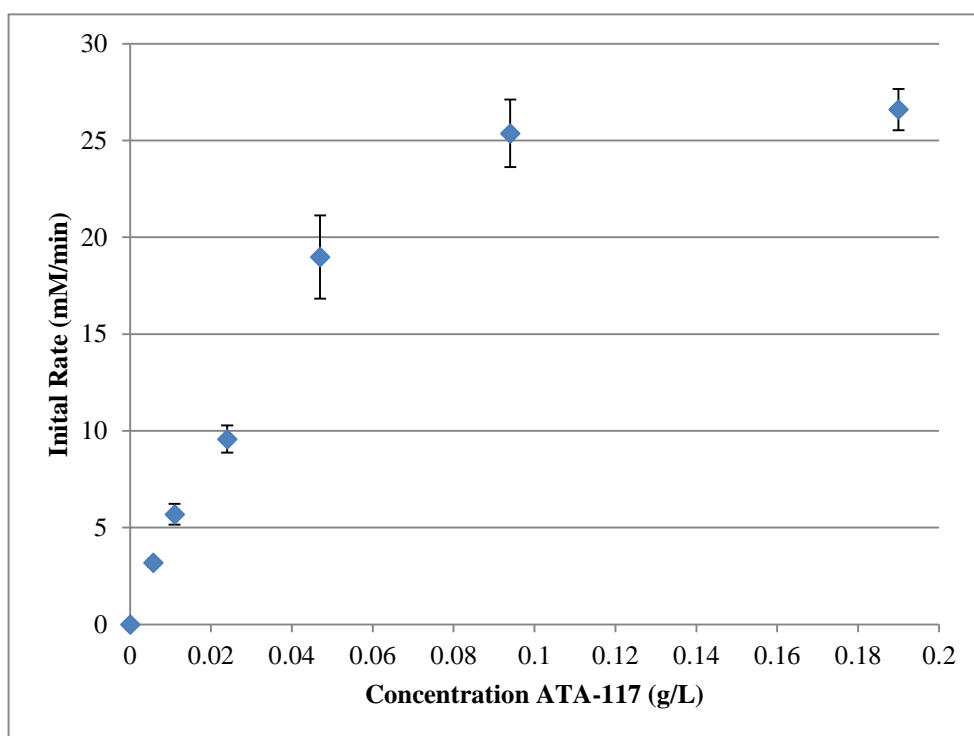


Figure 16: The effect of changing ATA-117 concentration, each experiment was carried out in triplicate and analysed *via* the colorimetric assay.

Figure 16 shows that as the concentration of ATA-117 increases above 0.05 g/L, the transamination step is no longer rate limiting. Therefore, in order to obtain accurate kinetic data the concentration of ATA-117 used in the assay must be within the linear range (i.e. no higher than 0.05 g/L).

Further investigations into changing both ATA-117 and D-AAO concentrations were carried out to confirm the above results. As the concentration of D-AAO was increased from 4.5 U to 9 U, the initial rate also increased (Figure 17). This result suggests that the transamination step was not rate limiting when using 4.5 U of D-AAO. However, as the concentration of D-AAO was increased from 9 U to 18 U, the rate, which was still in the linear range (i.e. up to 0.01 g/L of transaminase) did not increase. The transamination step is therefore rate limiting under the concentrations of the oxidase enzyme employed within the assay.

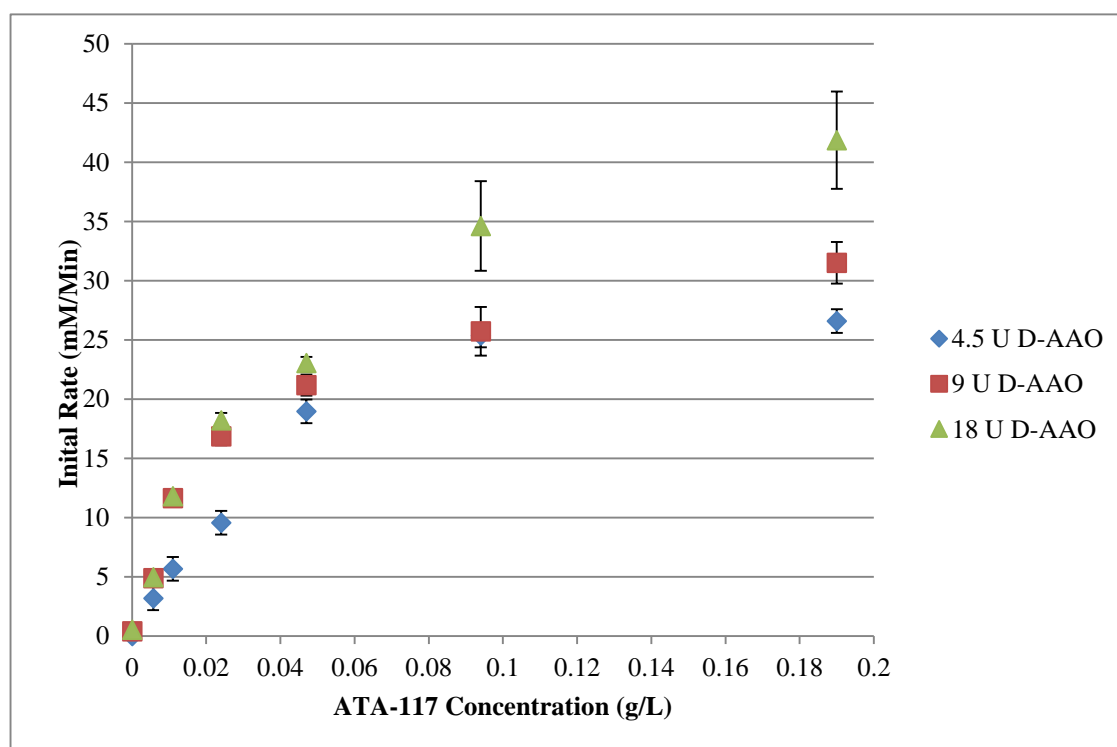


Figure 17: Effect of changing both ATA-117 and D-AAO concentration.

Experiments were carried out to analyse the kinetics of the transaminase reaction using 9 U of D-AAO and 0.01 g/L of ATA-117 (i.e. to ensure that the transaminase step is the rate limiting step whilst, D-AAO and HRP are in excess). Alternatively, when screening for activity towards different substrates where the transaminase concentration is not critical (if a substrate is accepted by a specific transaminase enzyme), the amount of transaminase employed in the reaction was 0.09 g/L and the AAO concentration was lowered to 3 U.

Using the optimised reaction conditions described above, the specific activity of ATA-117 can be calculated assuming a ratio of 1:1 between PGR oxidation and the rate of D-alanine formation. Specific activity measurements for different substrates can be determined and the differences in observed activity are a result of the acceptance of the substrate by the transaminase being the rate-limiting step in the reaction.

2.6 Effect of adding external pyridoxal-5'-phosphate

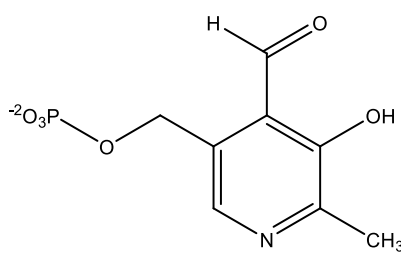
**21**

Figure 18: The structure of the cofactor PLP.

Previous research has found that PLP **21** is covalently bound to an internal lysine group of the transaminase active site; suggesting that no external cofactor would be needed for the transaminase reaction to proceed. The effect of supplementing the assay with PLP **21** (Figure 18) was therefore investigated. Experiments were run using the optimised assay conditions both with and without external PLP **21**.

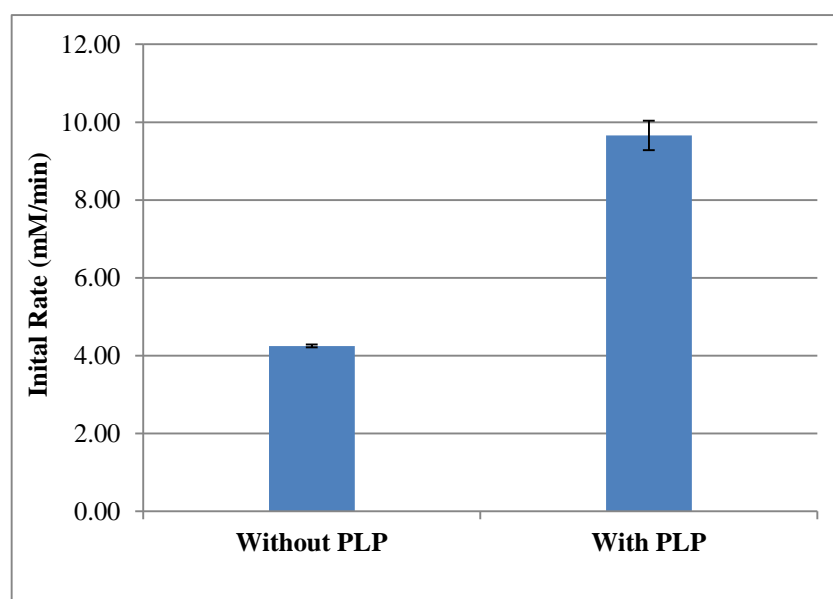
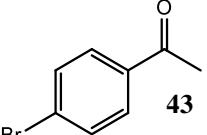
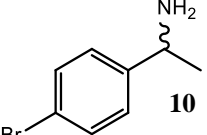
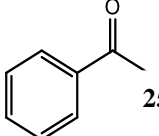
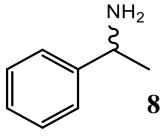
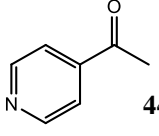
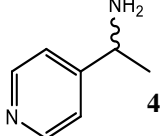
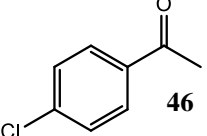
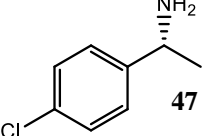
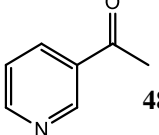
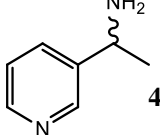


Figure 19: Effect on addition of external pyridoxal-5'-phosphate.

From Figure 19 it can be seen that supplementing the assay with PLP **21** more than doubles the initial rate of the detected reaction. As a result, reactions can be run without the addition of external PLP **21** but in order to reduce the reaction time for screening purposes PLP **21** was added at a concentration of 0.05 g/L.

Table 3: List of the different keto acceptors and the corresponding amines.

Ketone	Amine
 43	 10
 25	 8
 44	 45
 46	 47
 48	 49

Inspection of the data in Figure 20 reveals that there is good correlation between the GC data and the colorimetric assay for all five of the substrates. This demonstrates that the assay can be employed to predict the initial rate for the forward transaminase reaction. Experiments monitored consumption of PGR for the reverse transaminase reaction *via* plate spectrophotometry and observation of conversion for the corresponding forward reaction was monitored by GC.

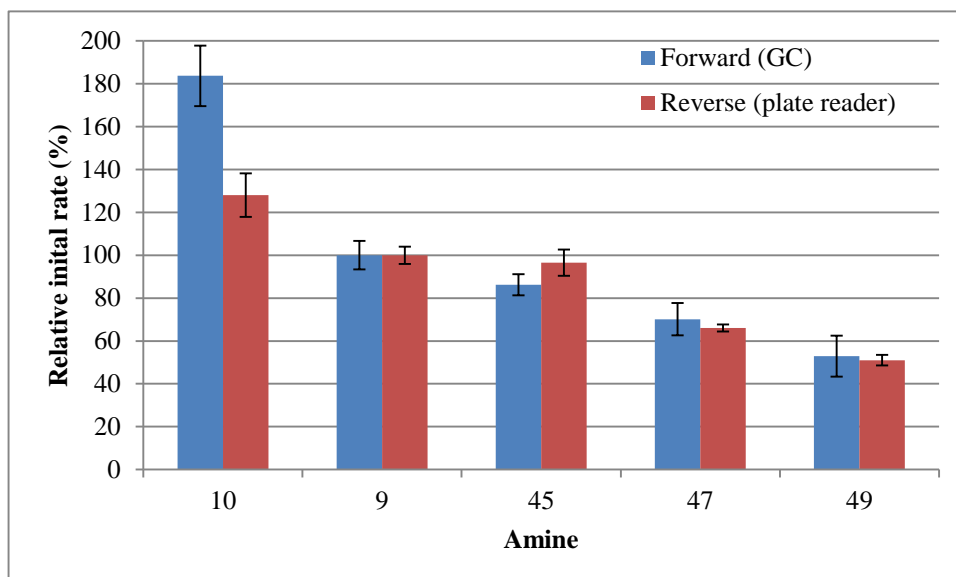


Figure 20: Comparison of the relative initial rates (compared to 1-phenylethylamine) for the forward (GC) and reverse (plate reader) transaminase reaction.

2.8 Determination of enantioselectivity

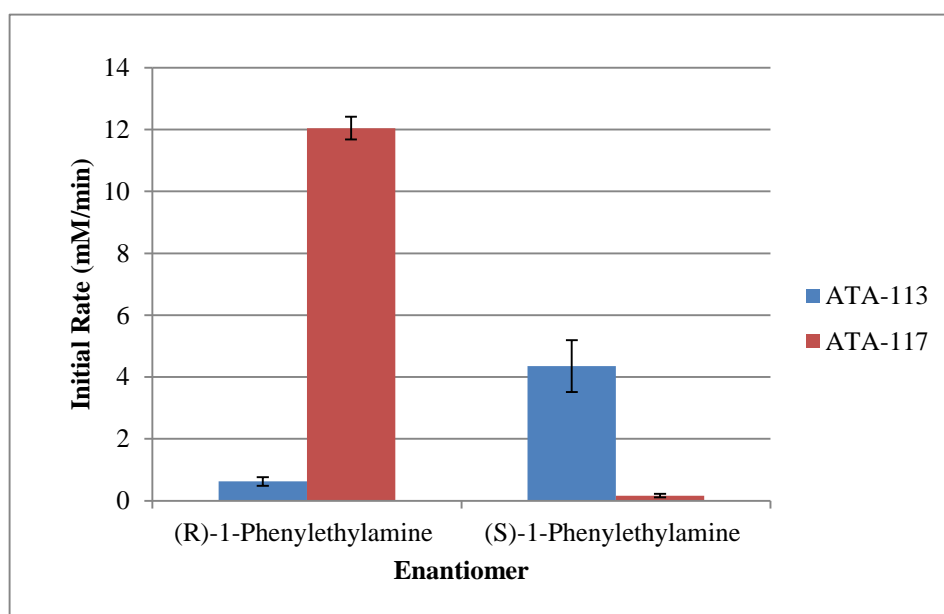


Figure 21: The selectivity of two different transaminase enzymes (ATA-113 and ATA-117) with the two enantiomers of 1-phenylethylamine.

Investigations into whether the assay could be used to distinguish enzymes that showed the opposite enantioselectivity compared to ATA-117 (i.e. a preference for (*S*)-enantiomers over (*R*)-enantiomers) were conducted using two different commercially available transaminase enzymes with known selectivity (ATA-113 (*S*)-selective and ATA-117 (*R*)-selective). To detect activity of the (*S*)-enantiomer, D-AAO

was replaced in the colourimetric screen with L-AAO, since the transaminase reaction with (*S*)-selective transaminase enzymes generates the L-amino acid. Control experiments showed that both L-AAO and D-AAO were selective for L-alanine and D-alanine respectively. Inspection of Figure 21 reveals that by changing the amine donor enantiomer and the AAO, transaminases with opposite selectivity can be detected.

2.9 pH Stability

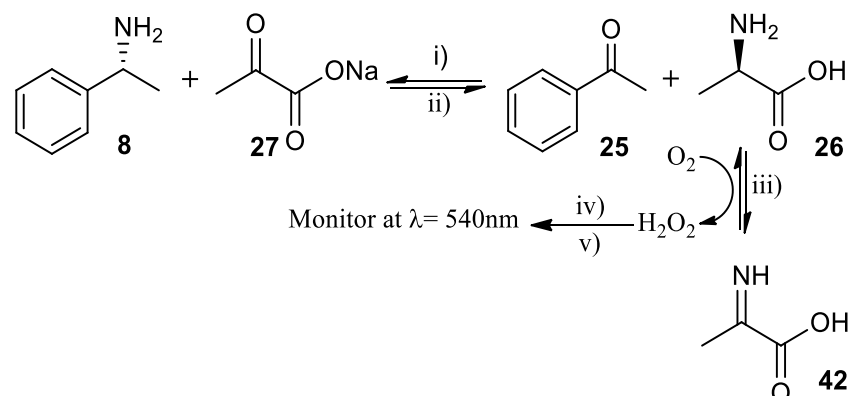
The pH stability of the colorimetric screen was monitored to establish if there was an effect on initial rate by a change in the pH. Reactions were run in eppendorf tubes using the colorimetric assay conditions (Section 6) scaled up 10 fold (a total volume 1.325 mL). pH readings were taken on a MultiMax reactor system at time zero and ten minutes to allow for full consumption of the PGR (monitored by a plate spectrophotometer).

Table 4: pH of both the sample and the blank at time 0 and 10 minutes.

Time (Min)	0	10
pH of blank	8.09	8.07
pH of sample	8.09	8.06

It can be seen from Table 4 that the pH throughout the reaction is stable. The slight change in pH between 0-10 minutes could be attributed to the error on the MultiMax pH probe (1/100th of a pH unit). The amount of product produced is minimal, therefore should not have a direct effect on the pH.

2.10 Screening of whole cell transaminases

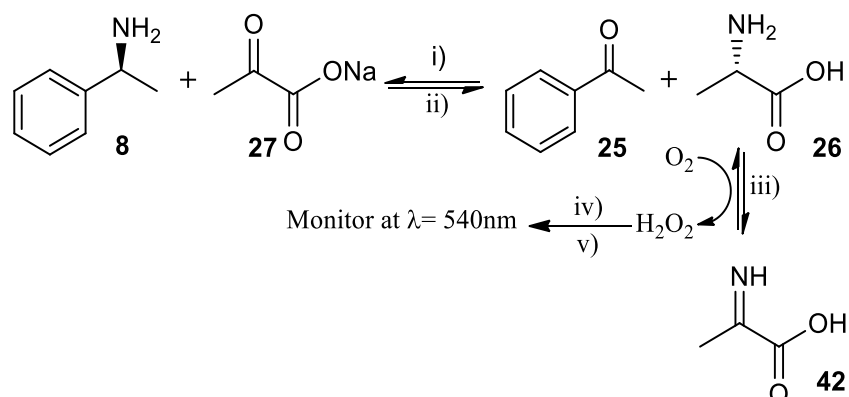


Reagents and conditions: i) Forward reaction, ii) Reverse reaction, iii) L-AAO, iv) HRP, v) PGR, 30 °C, pH 7.5, 540 nm.

Scheme 27: Transamination reaction using *Chromobacterium violaceum*.

The solution phase screen (Scheme 27) was then tested to see if transaminase activity could be detected from whole cell microorganisms. It has been previously reported,⁸⁶ that *Chromobacterium violaceum* (LGC standards, accession number 9131, ATCC 12472) has (*S*)-transaminase activity and this microorganism was assayed using the solution phase screen. When a colony of *C. violaceum* was re-suspended in the assay mixture utilising 1-phenylethylamine **8** as the amine donor and left for 24 hours no conversion could be detected. This result suggests that the levels of conversion were too low to detect. Moreover, the organism was grown in LB media until an OD₆₀₀ of 5 was reached. The cells were subsequently harvested and re-suspended in the assay mixture containing 1-phenylethylamine **8** as the amine donor. As soon as the cells were re-suspended a colour changed occurred from red to yellow, this was also observed in the negative control (pET-16b in *E.coli* BL21 (DE3)). It was concluded that amino acids in the cell were giving a false positive and therefore the screen cannot be utilised for whole cell transaminase screening.

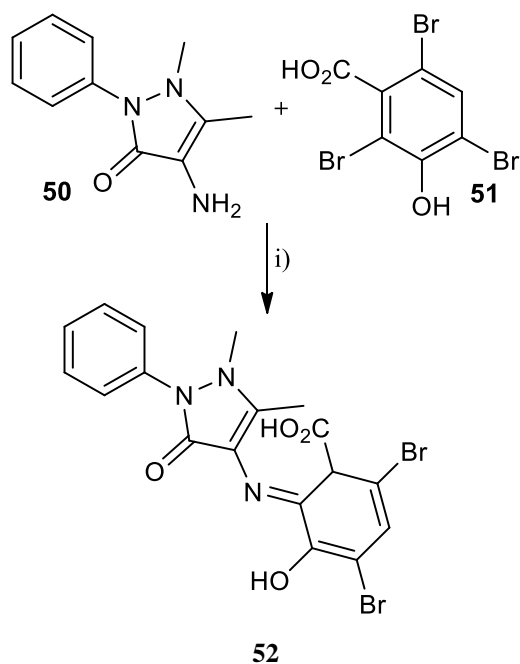
2.11 Transaminase activity with purified enzyme



Reagents and conditions: i) Forward reaction, ii) Reverse reaction, iii) L-AAO, iv) HRP, v) PGR, 30 °C, pH 7.5, 540 nm.

Scheme 28: Transamination reaction using Cv TA1.

Due to the unsuccessful screening of whole cell transaminases, screening of the purified enzyme was investigated (Scheme 28). Cloning and expression of the transaminase gene from *C. violaceum* into pET-16b (Appendix 8.3, PJH1) was carried out as previously reported.⁸⁶ Purification by affinity chromatography on a Ni column followed by desalting and removal of any amino acids through a PD10 column (GE healthcare-17-0851-01) afforded a pure transaminase (Cv TA1). Cv TA1 was subjected to the solution phase assay utilising 1-phenylethylamine **8** as the amine donor and sodium pyruvate **27** as the keto-acceptor. Activity was observed when using racemic 1-phenylethylamine **8** and L-AAO, however, even the negative control (empty pET16b) showed slight background activity. Previous investigations showed that the dye PGR which is currently used in the screen slowly decolourises over 24hr in the current reaction conditions with 1-phenylethylamine **8**. The background activity of PGR results in the dye being unsuitable for lower activity systems. For this reason, investigations into an alternative dye were carried out. TBHBA **51** coupled with 4-AAP **50** (Scheme 29) has been previously analysed as co-substrate indicators that can be used in HRP based assay systems.^{85,87} TBHBA **51** and 4-AAP **50** do not produce a coloured product until H₂O₂ oxidises 4-AAP **50** in the presence of HRP. The oxidised form of 4-AAP **50** subsequently reacts with TBHBA **51** to produce the dye quinoneimine **52** (λ_{max} 510 nm). The screen was tested with TBHBA **51** and 4-AAP **50** employing organisms with known transaminase activity (*C. violaceum*).



Reagents: i) HRP and H₂O₂.

Scheme 29: HRP coupled assay producing the dye quinoneimine.

The use of TBHBA 4-AAP resulted in no background activity when the negative control (blank pET-16b) was used. The dye was therefore changed to allow screening for lower activity systems.

The assay was then applied for the screening of 32 different amine donors using sodium pyruvate as the keto-acceptor. The results of the screen are depicted in Figure 22.

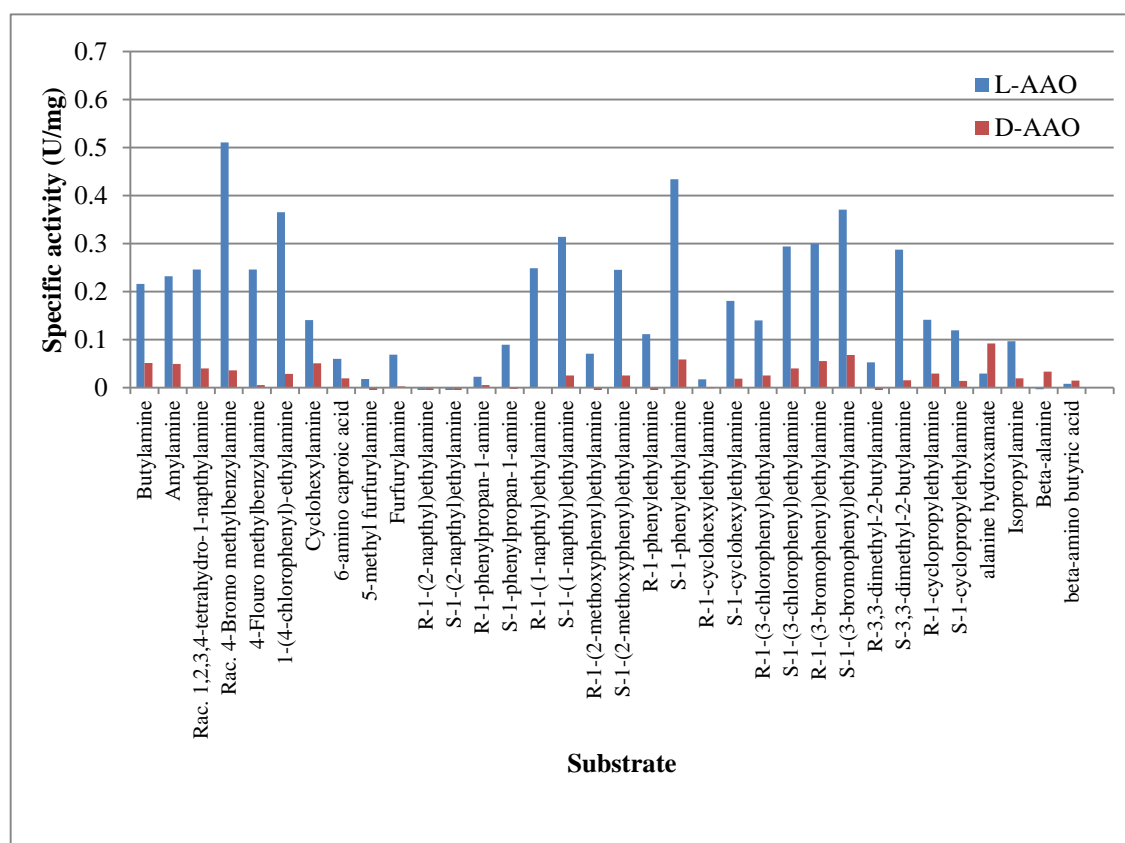


Figure 22: Different amine substrates screened with purified Cv TA1 with L and D-AAO.

Inspection of Figure 22 reveals that the enzyme displayed (*S*)-selectivity towards the majority of the compounds assayed and showed slight preference for *para*-substituted aromatics over *ortho* or *meta*- substitution. β -Alanine and β -amino butyric acid showed little or no activity compared to the best amine donor, 4-bromo-1-phenylethylamine. The enzyme also showed activity towards the primary amines butylamine and amylamine.

2.12 Conclusion

The aim of this research was to develop a high-throughput assay for the detection of transaminase activity in the deamination direction. The coupling of AAO, HRP and transaminase (which was an adaptation of an oxidase screen previously reported) allows for the screening of a wide range of chiral amines and the determination of the enantioselectivity of the enzyme by replacing D-AAO with L-AAO (*R*) and (*S*) selectivity respectively). The use of the commercially available Codexis enzymes (ATA-117 and ATA-113) allowed the development of the assay and it was applied to screen a wide range of chiral amines with the (*R*)-transaminase (ATA-117) and D-AAO

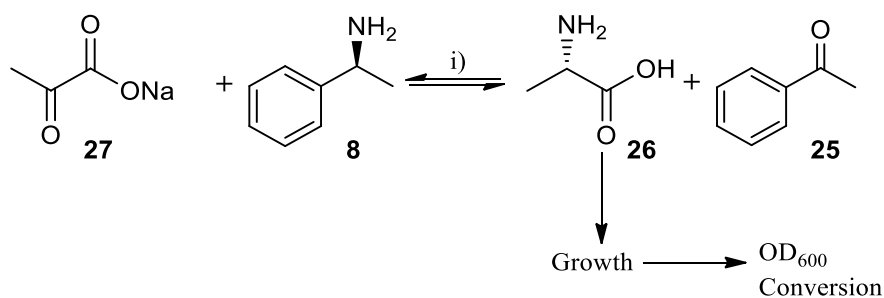
on one plate in under an hour. It has also been used to show the difference in selectivities of the two enzymes (which has already been pre-determined) and prove that there is no need to add external PLP. Unfortunately, the screen was unusable for screening whole cell microorganisms for transaminase activity by the re-suspension of a colony of *C. violaceum* as the activity is too low. Re-suspension of harvested cells was also unsuccessful because the background activity was too high whilst using AAO with the amino acids from the cell or media. Furthermore, the assay was used to screen transaminases which were over expressed. A *C. violaceum* transaminase (Cv TA1) was cloned and expressed and the purified (affinity chromatography and PD10 column) CFE was used in the assay.

PGR was switched for TBHBA and 4-AAP to remove the background activity which occurred with PGR. A full substrate spectrum was obtained for the transaminase and the enantioselectivity was determined. The disadvantage of the solution phase screen is the cost of the oxidase enzymes (in particular L-AAO). The overall cost can be minimised by reducing the loading of the transaminase and hence the loading of the oxidase enzyme can be lowered (as long as the transaminase step remains rate limiting). Producing stocks of L-AAO was not possible as only the D-AAO can be expressed in *E.coli* due to L-AAO being toxic to the cell in which it is expressed. Although the cost of the oxidase enzymes is high, the screen can be used to assay a wide range of chiral amines in a short period of time, removing the need for long HPLC/GC runs and laborious extractions. The screen is currently being developed onto a solid phase format which will allow a high-throughput method for mutagenesis studies with a lower screening cost for large libraries.

3. Results and discussion- Cloning identification and characterisation of two transaminase enzymes

There has been an increase in demand for chiral amines as intermediates for the pharmaceutical industry and new efficient synthetic methodologies are being investigated.¹⁰ Enzymatic synthesis of chiral amines is performed on a multi-ton scale per annum by employing kinetic resolutions using hydrolytic enzymes which give the resulting amine in high enantiomeric excess.⁸⁸ Recently, the use of lipases (e.g. CAL-B) for the DKR of racemic amines employing metal catalysts for the racemisation, such as palladium or ruthenium, has achieved high *e.e.* (> 99%) and high yields (80-90%). Unfortunately, acquiring conditions which are suitable for the chemo- and bio-catalyst to work together has proven to be challenging.²⁴ The recent emphasis on applying a biocatalyst for the asymmetric synthesis of prochiral or *meso* substrates provides a more attractive approach. Transaminases catalyse the reaction of a prochiral ketone with an amine donor (e.g. alanine) to give access to a wide range of chiral amines and often show high enantioselectivity and broad substrate specificity without the addition of external cofactors. This class of enzymes are therefore suitable for industrial applications.

Increasing demand for novel ω -transaminases has been represented by the extensive number of publications which include transaminases from *Vibrio fluvialis* JS17,⁸⁹ *Alcaligenes denitrificans* Y2k-2,⁹⁰ *Arthrobacter sp.* KNK168,⁹¹ *Mesorhizobium sp.* LUK⁸³ and more recently, a transaminase from *Pseudomonas fluorescens* KNK08-18.⁹² The number of ω -transaminases which show potential for industrial application are limited, and most ω -transaminases reported to date are (*S*)-selective, resulting in the search for (*R*)-selective transaminases. To screen for potential transaminase activity in *wt* organisms, a sensitive, accurate and high-throughput screen is required. Without such a screen, identifying transaminase activity can be labour-intensive and also time-consuming. Previously, there have been reports^{69,93} of solution phase screens which have been utilised to select *wt* microorganisms with transaminase activity. In this study the use and optimisation of a previously developed minimal media based selection screen for the detection of transaminase activity from *wt* organisms is reported.²⁹



Reagents and conditions: i) Transaminase, 30 °C, 250 rpm, pH 8.

Scheme 30: Principle of solution phase screen for the detection of TA activity utilising (*S*)-1-phenylethylamine as the sole nitrogen source.

A minimal media screen reported by Shin and Kim²⁹ (Scheme 30) for the detection of transaminase activity in *wt* organisms was investigated. The screen omits the standard ammonia source (usually NH₄Cl) from the growth media and replaces it with (*S*)-1-phenylethylamine **8**. The media is also supplemented with a carbon source (glycerol). If transaminase activity is observed, conversion of (*S*)-1-phenylethylamine **8** to acetophenone **25** and production of L-alanine **26** can be detected and an increase in OD₆₀₀ will be observed. The assay was adapted to include sodium pyruvate **27** as a carbon source and the screen can also be used to screen for (*R*)-selective transaminases by simply replacing (*S*)-1-phenylethylamine **8** with (*R*)-1-phenylethylamine **8**.

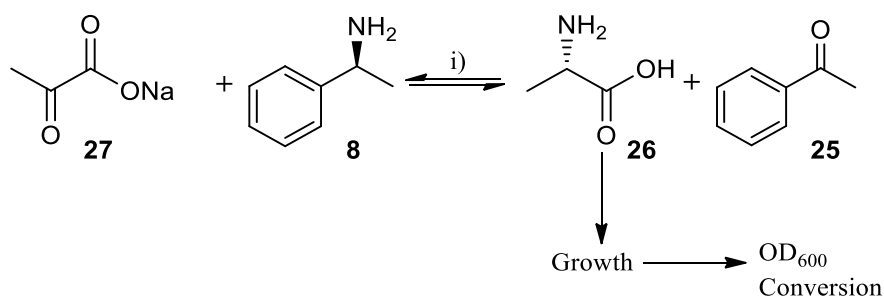
Herein the isolation, purification and characterisation of two different transaminases from *C. violaceum* (CMCC 104818, Cv TA2) which has a 95% sequence identity to that of the previously published *C. violaceum* (CMCC 105910, Cv TA1)⁸⁶ and a new *O. anthropi* transaminase (CMCC 104240, Oa TA1) is reported.

3.1 Initiation of screen

To ascertain whether the screen was reliable for detecting transaminase activity, a recombinant transaminase, overproduced in *E. coli* BL21 (DE3) was screened first. *C. violaceum* was purchased from LG standards (9131) and deposited into the Chirotech Microbial Culture Collection (CMCC) and given the accession number CMCC 105910. The genomic DNA was isolated and a PCR carried out using previously reported⁸⁶ primers which introduced *Xho*I and *Nde*I restriction sites for sub-cloning into the expression vector pET-16b. The PCR product was gel purified, initially cloned into a Zero blunt TOPO cloning vector and then used to transform *E. coli* XL1 blue. Restriction digests were performed and the gene was cloned into pET-16b using the

*Xho*I and *Nde*I restriction enzyme sites present on the plasmid to create pJH1 (Appendix 8.3). The resulting plasmid was used to transform *E. coli* BL21 (DE3).

As the first step, initial proof of principle experiments were carried out using *E. coli* BL21 (DE3) pET-16b (negative control) and *E. coli* BL21 (DE3) pJH1, employing three different carbon sources (1. sodium pyruvate **27**, 2. glycerol and 3. sodium pyruvate and glycerol – demonstrated in Scheme 31). This was to identify conditions that would allow the growth of a bacterium expressing a transaminase when using the defined combination of nutrients. 250 mL culture flasks containing minimal media were inoculated with 2.5 mL of starter culture and incubated at 37 °C and 250 rpm. Samples were taken periodically to monitor growth and conversion.



Reagents and conditions: i) Whole cell transaminase, 30 °C, 250 rpm, pH 8.

Scheme 31: Principle of solution phase screen for the detection of TA activity utilising (S)-1-phenylethylamine as the sole nitrogen source and sodium pyruvate a carbon source.

As expected no growth or conversion of (S)-1-phenylethylamine to acetophenone was observed with *E. coli* BL21 (DE3) pET-16b when grown on any of the three carbon sources. *E. coli* BL21 (DE3) pJH1 showed acetophenone production after 20 hours and reached an OD₆₀₀ of 1.4 after 185 hours when a combination of both glycerol and sodium pyruvate were used as the carbon sources (Figure 23).

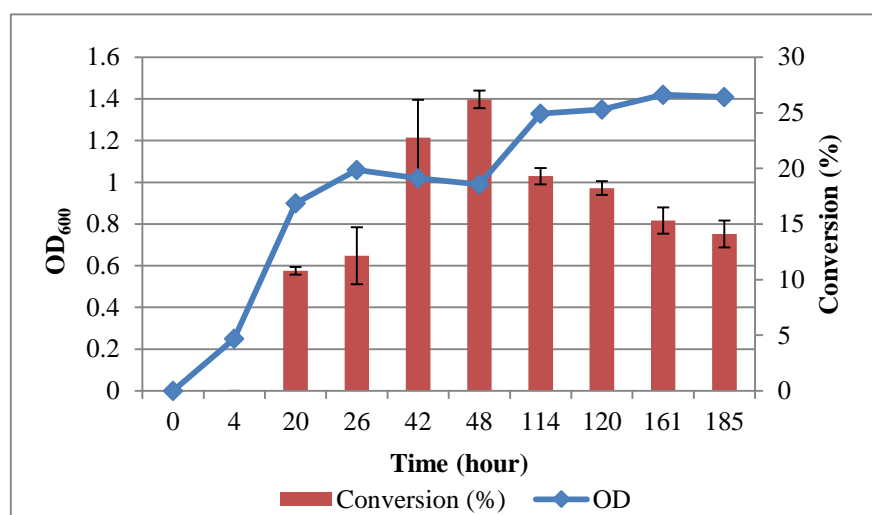


Figure 23: *E. coli* BL21 (DE3) pJH1 utilizing a combination of both glycerol and pyruvate as the carbon source. Conversion (%) was calculated by chiral GC analysis.

The above results demonstrate that the screen could be utilised for transaminases in recombinant systems. The next step was to see if the assay could be applied for the identification of transaminase activity in *wt* organisms. A *C. violaceum* was purchased from LG standards (NCIMB 9178, ATCC 12472) and was deposited into the CMCC under CMCC 105910 and was used as a test organism as it is known to possess transaminase activity.⁸⁶ The CMCC already contained an additional *C. violaceum* (CMCC 104818) which was screened for comparison of transaminase activity. Again three different types of minimal media containing three different carbon sources were inoculated with 2.5 mL of starter culture and OD₆₀₀ measurements and GC samples taken to monitor conversion.

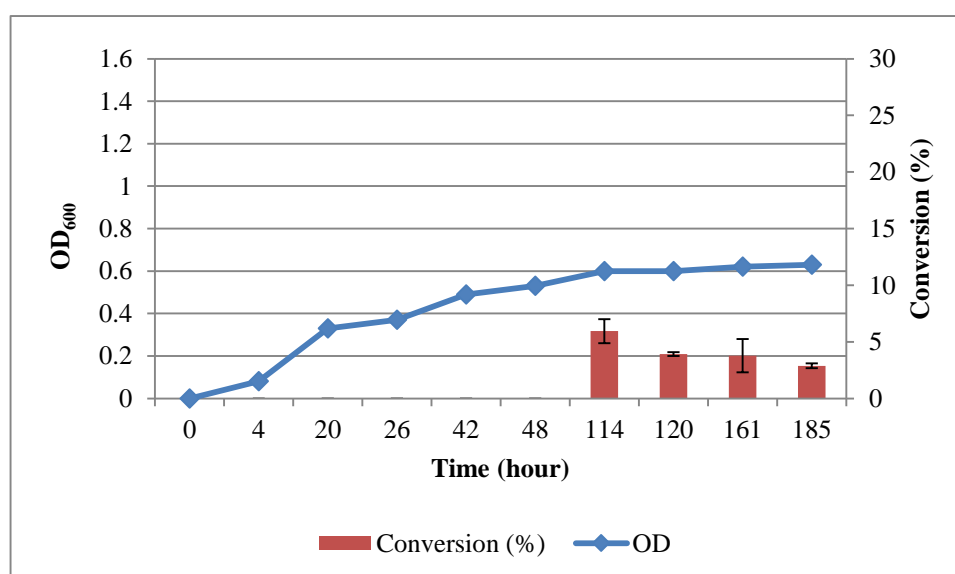


Figure 24: *C. violaceum* (CMCC 105910) employing both glycerol and pyruvate as the carbon source.

Figure 24 shows the conversion (%) of (*S*)-1-phenylethylamine to acetophenone whilst taking OD₆₀₀ measurements over a period of 185 hours. The data shows good correlation between increase in OD₆₀₀ and percentage conversion. Upon inspection of Figure 25, *C. violaceum* CMCC 104818 shows slightly higher activity and better growth compared to *C. violaceum* CMCC 105910 after 185 hours.

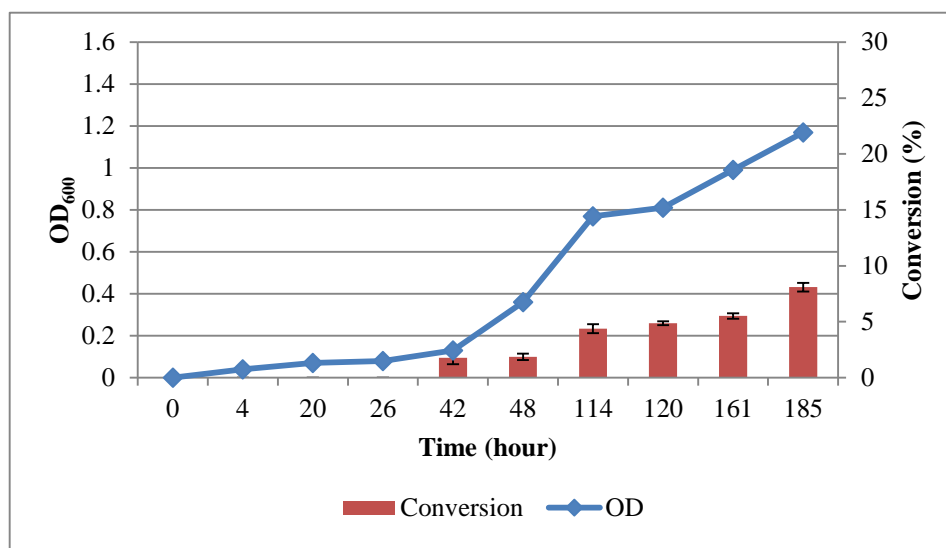


Figure 25: *C. violaceum* (CMCC 104818) employing both glycerol and pyruvate as the carbon source.

The liquid phase minimal media screen was then used to assay a selection of unknown microorganisms from the CMCC. Eight strains were selected from the CMCC on the basis that they were previously screened for α -transaminase activity but not screened for ω -transaminase activity. Below in Table 5 is the list of the eight unknowns screened and the results for the three different carbon sources that were used.

Table 5: List of CMCC screened for transaminase activity employing three different carbon sources.

CMCC reference	Carbon Source		
	Sodium Pyruvate	Glycerol	Sodium pyruvate and glycerol
104236 (T ₂ C18)			
104247 (T ₂ M30)	✓	✓	✓
104241 (T ₂ M24)		✓	✓
104240 (T ₂ S148)	✓	✓	✓
104332 (T ₂ S112)	✓	✓	✓
104263 (T ₂ C6)			
104284 (T ₂ S57)			
104337 (T ₂ S128)			

✓ = growth

Out of eight unknowns screened, four showed potential transaminase activity with (*S*)-1-phenylethylamine. To achieve higher throughput, a solid phase screen was developed.

3.2 Solid phase screen

Solid phase screening has a higher throughput than that of liquid phase screens due to the decrease in manual handling, resulting in more microorganisms that can be screened in a shorter period of time. Shin and Kim²⁹ reported a solid phase assay using the minimal media mentioned above in Section 3.1 but with the addition of 1% agar. Plates were supplemented with different carbon sources (sodium pyruvate and glycerol) and incubated at 30 °C. Colonies were visualised only with microorganisms that express transaminase activity for (*S*)-1-phenylethylamine and hence produce L-alanine for growth.

A selection of unknowns were picked for screening from the CMCC which have been previously screened for α -transaminase activity. Table 6 shows the results when comparing the two different carbon sources glycerol and sodium pyruvate. A combination of both glycerol and pyruvate was tested but the combinations of carbon sources resulted in crystals forming in the agar.

Table 6: Screening results for several unknown microorganisms from the CMCC.

CMCC reference	Carbon Source	
	Sodium Pyruvate	Glycerol
BL21 pET16b (Blank)		
BL21 pJH1 (Positive control)	✓	
104245 (T ₂ M28)	✓	✓
104248 (T ₂ M31)		
104231 (T ₂ C13)		
104235 (T ₂ C17)	✓	✓
104241 (T ₂ M24)	✓	✓
1042338 (T ₂ C20)		
104345 (T ₂ S144)		
104234 (T ₂ C16)		

Three out of eight unknown microorganisms screened showed growth after five days at 30 °C, suggesting that they have potential transaminase activity with (*S*)-1-phenylethylamine. The three unknowns which had activity (CMCC 104235, 104241, 104245) showed better growth when the media was supplemented with

glycerol rather than sodium pyruvate (only a few colonies visualised) compared to the control experiment *E. coli* BL21 (DE3) pJH1 which only showed growth with media supplemented with sodium pyruvate. CMCC 104241 was screened on both liquid phase and solid phase to confirm the reliability of both screens and a good correlation was found between the two assays.

3.3 Identification of unknown microorganisms

To determine whether the potential transaminase activity discovered in Section 3.2 was novel, 16S rRNA sequencing was carried out. This was used to identify what classification of species the microorganisms were. 16S rRNA sequencing uses generic primers to amplify the 16S gene, encoding the ribosomal RNA (in prokaryotes) to provide a PCR product which can be sequenced by conventional methods. The sequencing results can be entered into a database (for example ExPASy BLAST) to determine the species of the microorganism. Table 7 shows the results of the 16S rRNA sequencing and BLAST searches.

Table 7: 16S rRNA sequencing results and the top match from ExPASy BLAST searches.

Chirotech Microbial Culture Collection accession number	Organism
104241 (T2M24)	Unable to identify
104240 (T2S148)	<i>Ochrobactrum anthropi</i>
104235 (T2C17)	<i>Elizabethkingia sp.</i>
104247 (M30)	<i>Elizabethkingia sp.</i>
104332 (S112)	<i>Ochrobactrum anthropi</i>
104245 (T ₂ M28)	Unable to identify
104236 (T2C18)	Unable to identify

3.4 Protein identification

To identify any potential transaminase enzymes from the *wt* organisms *Elizabethkingia sp.* (CMCC 104247) and *Ochrobactrum anthropi* (CMCC 104240), protein identification was carried out. The organisms were grown in LB broth with 1-phenylethylamine and isopropylamine overnight at 37 °C. The cells were harvested and semi-purified using a butyl His-trap column. Samples were then analysed *via* SDS-PAGE (Figure 26) and separated proteins sent for protein identification. Samples

were sent to the Facility of Life Sciences for Biomolecular Analysis and identification experiments were performed by Emma-Jayne Kevil. A trypsin digest was performed followed by tandem MS/MS analysis (MALDI-TOF/TOF) and the data was processed using Proteome Softwear.

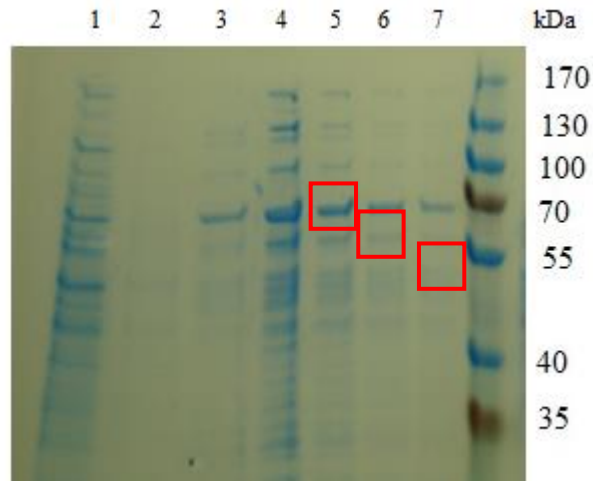


Figure 26: SDS-PAGE analysis of *Ochrobactrum anthropi* transaminase production and purification when grown on selection media. Lane 1: Flow through, Lane 2: Wash, Lane 3: Elution 1 mL, Lane 4: Elution 2 mL, Lane 5: Elution 3 mL, Lane 6: Elution 4 mL, Lane 7: Elution 5 mL. The red boxes indicate the samples sent for protein identification.

Analysis of the *Elizabethkingia sp.* showed that there was no potential transaminase protein, however, the *O. anthropi* revealed potential transaminase protein at 55 kDa. The protein sequence fragments (not a full sequence due to the trypsin digest) received from the identification were entered into ExPASy BLAST and a full protein sequence was obtained from *O. anthropi* (ATCC 49188, Figure 27). One of the sequence fragments was at the N-terminal end of the protein sequence, and from this the DNA sequence from the protein in the database was obtained and primers were designed for the 5' end to see if the transaminase gene could be isolated from the genomic DNA of *O. anthropi* (CMCC 104240).

```

MQFIDLGAQR ARIEDRLNAA ISKVVAEGRY ILGPEVAEFE KKLGEYLGVE HVIACANGTD
ALQMPLMARG IGPGDAVFVP SFTFAATAEV VALVGAEPVF IDVDADTYNL NIEQLEAAIA
AIRKEGRLQP KAIIPVDLFG LAADYNRISA IADREGLFVI EDAAQSIGGK RDNVMCGAFG
HVGATSFYPA KPLGCGYDGG AMFTNDAELA DTLRSVLFHG KGETQYDNVR IGINSRLDTI
QAAVLLLEKLA ILEDEMEARD RIAKRYNEAL KDVVKVPALP AGNRSAWAQY SIESENRDGL
KAHLQAEGIP SVIYYVKPLH QQTAYKHYPV APGGLPISES LPNRILSLPM HPYLSEADHD
KIIGAIRGFH GKKA

```

O. anthropi (strain ATCC 49188 / DSM 6882 / NCTC 12168)

Figure 27: Protein sequence of *O. anthropi* transaminase in the ExPASy database. The red fragments were those obtained from protein identification of the SDS-PAGE bands from *O. anthropi* (CMCC104240).

3.5 Cloning and expression of *Ochrobactrum anthropi*

Primers were designed based on the N-terminal sequence of an *O. anthropi* (ATCC 49188) transaminase which is published on ExPASy. Primer walking was carried out to obtain the full DNA sequence of the potential transaminase gene from *O. anthropi* CMCC 104240. This was translated and the protein sequence was aligned to the published protein sequence to which it showed 95% sequence identity. Primers were designed to amplify the target sequence, also introducing *Bam*HI and *Xho*I restriction enzyme recognition sites. These restriction sites were chosen as the gene sequence does not contain either *Bam*HI or *Xho*I restriction enzyme sites which are found in the multiple cloning site of the expression vector pET-16b. The gene was amplified by PCR and initially cloned into Zero blunt TOPO cloning vector (Invitrogen- K2830-20) and the resulting construct used to transform *E. coli* XL1 blue. To see if the cloning was successful, the transformants were screened by conducting a PCR using the primers described above.



Figure 28: PCR product from TOPO cloning. Potential *O. anthropi* transaminase can be seen at 1 kb.

Figure 28 shows the cloning was successful as PCR fragments could be visualised at 1 kb, hence, a double digest was performed on the DNA obtained from the transformants. Restriction endonucleases, *Bam*HI and *Xho*I were used to clone the gene into pET-16b to create pJH3 and the construct was subsequently used to transform *E. coli* BL21 (DE3) (Appendix 8.3). Clones were confirmed by sequencing using T7 forward/reverse primers and expression studies were carried out in LB ampicillin at; 25 °C, 30 °C and 37 °C with induction at OD₆₀₀ 0.6 using 1 mM IPTG. Samples were taken at different time points to monitor the expression and analysed by SDS-PAGE (Figure 29). *E. coli* BL21 (DE3) pJH3 was grown and the transaminase was purified by affinity chromatography followed by PD-10 buffer exchange to give pure a transaminase (Oa TA1).

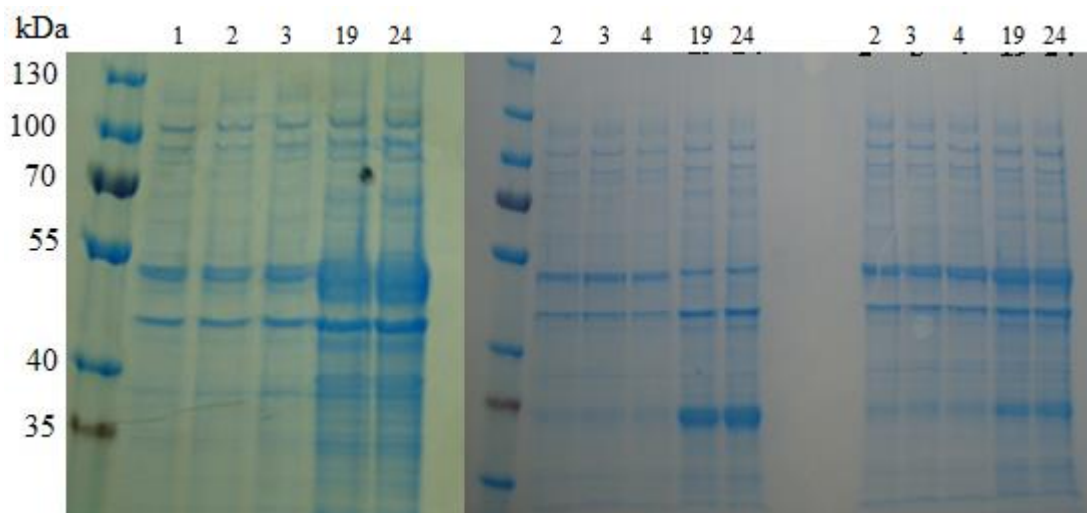


Figure 29: SDS-PAGE of expressed pJH3, protein appears at 54 kDa. The gel on the left hand side is at 30 °C and different time points (hours), the gel in the middle is 37 °C and the gel on the right is 25 °C.

A higher level of protein expression was observed when grown at 30 °C, 19 hours. The protein was not visible in the insoluble fractions and the smaller band at 50 kDa was not present after purification with a Ni column. A western blot of the expressed protein at 30 °C revealed the His-Tag was present on the band at 54 kDa (Figure 30).

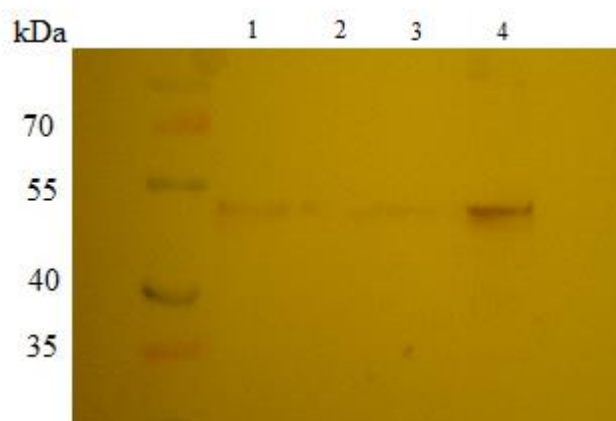


Figure 30: Western of potential transaminase from Oa TA1, protein appears at 54 kDa.

After purification the protein was filtered through a PD-10 column to exchange imidazole with HEPES buffer and also to remove small amino acids present in the solution. The enzyme was then screened to investigate the activity and substrate scope using the solution phase assay developed in Section 2.

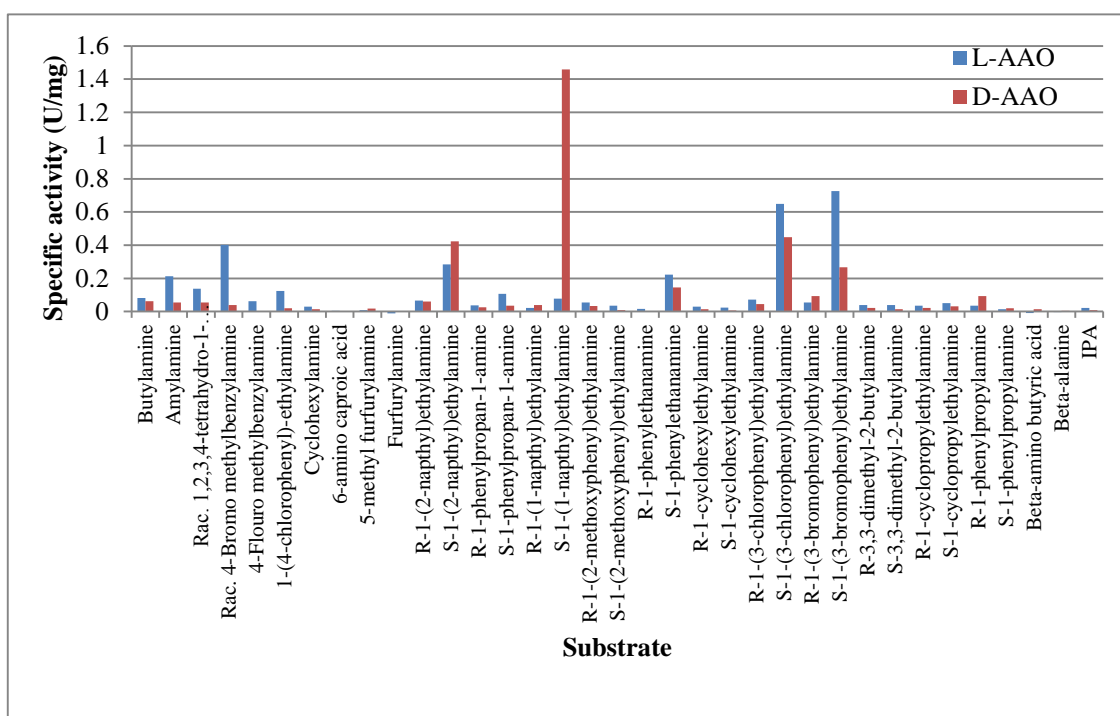


Figure 31: Different amine substrates screened with Oa TA1 with L and D-AAO using the TBHBA 4-AAP solution phase assay. 1U = is defined as 1nmol/min.

Investigation of the data in Figure 31 revealed Oa TA1 does not show selectivity for alanine production but does have slight activity with (*R*)-amines. The enzyme displayed activity with naphthylethylamines, 3-(chloro) and 3-(bromophenyl)ethylamine and primary amines butylamine and amylamine. No activity was seen with the β -amino acids and isopropylamine.

Transaminases are known to use different keto acceptors such as acetone and keto acids similar to sodium pyruvate. The screen was adapted for the use of α -keto-glutarate **53** instead of sodium pyruvate to give L/D-glutamic acid **54**. L/D-AAO was replaced with glutamate oxidase, which in the presence of molecular oxygen yields hydrogen peroxide and an imine **55** (Scheme 32). Commercially available L-glutamate oxidase (Sigma G5921, D-glutamate oxidase is not commercially available) was used to test this screen. However, one major drawback was that only the production of L-glutamic acid **54** could be monitored.

The gene was then cloned into Zero blunt TOPO vector (Invitrogen- K2830-20) to create TOPO JH2 (Appendix 8.3) and used to transform *E. coli* XL1 blue. To confirm the cloning was successful, *Eco*RI restriction sites were chosen to perform a digest. This restriction enzyme site was chosen as it is located on either side of the cloned gene. No sequence data was available at this point so it was not known if the gene itself contained any *Eco*RI restriction sites. If the cloning was successful products at 3 kb and 1.5 kb would be expected.

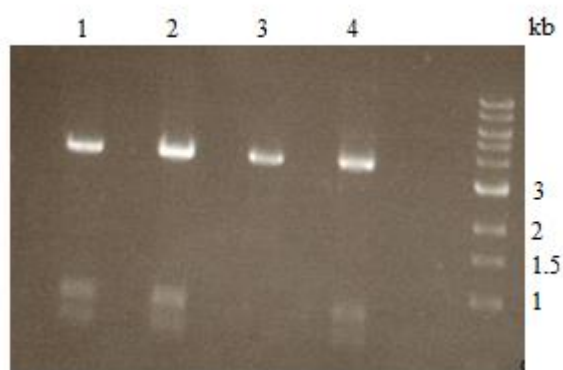


Figure 33: *Eco*RI Digest, Lane 1: TOPOJH2 4:1 with DMSO* Lane 2: TOPOJH2 4:1 Lane 3: TOPOJH2 1:1 with DMSO* Lane 4: TOPOJH2 1:1.

Inspection of Figure 33 should show a product at 3 kb and 1.5 kb but it reveals that there was an unexpected *Eco*RI restriction site within the gene, resulting in three fragments at 3, 0.9 and 0.6 kb. The gene was then sent for sequencing and subsequently cloned into pET-16b and the resulting construct (pJH2) used to transform *E. coli* BL21 (DE3). The sequence of the transaminase protein produced in *E. coli* BL21 (DE3) pJH2 (referred to herein as Cv TA2) was aligned to the known published sequence of Cv TA1.

		1	50
CV 104818	(1)	MQKQRTTSQWRELDAAHHLHPFDTASLNQAGARVMTRGEGIYLWDS	DGN
CV 2025	(1)	MQKQRTTSQWRELDAAHHLHPFDTASLNQAGARVMTRGEGVYLWDS	DGN
		51	100
CV 104818	(51)	KIIDGMAGLWCNVVGYGRKDFAEVARRQMEELPFYNTFFKTTHPAVVELS	
CV 2025	(51)	KIIDGMAGLWCNVVGYGRKDFAEVARRQMEELPFYNTFFKTTHPAVVELS	
		101	150
CV 104818	(101)	RLLAEVTAGFDHVFYTNSSGSESVDTMIRMVRRYWDVQGGKPEKKTIGRW	
CV 2025	(101)	RLLAEVTAGFDHVFYTNSSGSESVDTMIRMVRRYWDVQGGKPEKKTIGRW	
		151	200
CV 104818	(151)	NGYHGSTIGGASLGGMKYMHEQQDLPIPGMAHIEQPWWYKHGKDMTPDEF	
CV 2025	(151)	NGYHGSTIGGASLGGMKYMHEQQDLPIPGMAHIEQPWWYKHGKDMTPDEF	
		201	250
CV 104818	(201)	GVVAARWLDEKIQEIGADKVAAFVAEPIQGAGGVIIPPATYWPETIERICR	
CV 2025	(201)	GVVAARWLEKILEIGADKVAAFVGEPIQGAGGVIIPPATYWPETIERICR	
		251	300
CV 104818	(251)	KEDVLEVADEVICGFGRTGEWFGHQHFGFQPDLFATAAKGLSSGYLPIGAV	
CV 2025	(251)	KEDVLEVADEVICGFGRTGEWFGHQHFGFQPDLFATAAKGLSSGYLPIGAV	
		301	350
CV 104818	(301)	FVGKRVAEGLIAGGDFNHGFTYSGHPVCAAVAHANVALRDEGIVQRVKD	
CV 2025	(301)	FVGKRVAEGLIAGGDFNHGFTYSGHPVCAAVAHANVALRDEGIVQRVKD	
		351	400
CV 104818	(351)	DIGPYMQKRWRETFSSQFEHVDDVRGVLQAFTLVKNKAKRELFPDFGEV	
CV 2025	(351)	DIGPYMQKRWRETFSSRFEHVDDVRGVMVQAFTLVKNKAKRELFPDFGET	
		401	450
CV 104818	(401)	GTLCRDIFFRNNLIMRACGDHIVCSPLVMTRAEVDEMLVAARCLAEFE	
CV 2025	(401)	GTLCRDIFFRNNLIMRACGDHIVSAPPLVMTRAEVDEMLVAERCLAEFE	
		451	
CV 104818	(451)	QALKARGLA	
CV 2025	(451)	QTLKARGLA	

Figure 34: Alignment of Cv TA1 (CV2025) with Cv TA2 (CV 104818). The yellow indicates conserved regions, green represents conservative amino acids with respect to physical properties and white indicates mutations for amino acids with different physical properties.

Figure 34 shows the aligned sequences of the two *C. violaceum* transaminases have 95% sequence identity. Overall there are 22 mutations in the transaminase gene from Cv TA2 compared to Cv TA1; 10 code for amino acids with similar chemical properties and 12 code for amino acids which are different in physical properties from the parental amino acid. To see if the mutations cause any difference in the activity between the two enzymes, *E. coli* BL21 (DE3) pJH2 was grown in LB containing ampicillin for selection at 37 °C, 250 rpm and induced at an OD₆₀₀ of 0.6 with 1 mM IPTG for the overproduction of Cv TA2. Different time points were taken to monitor the expression by SDS-PAGE. As shown in Figure 35 the protein (Cv TA2) was produced at a high level 2 hours post-induction.

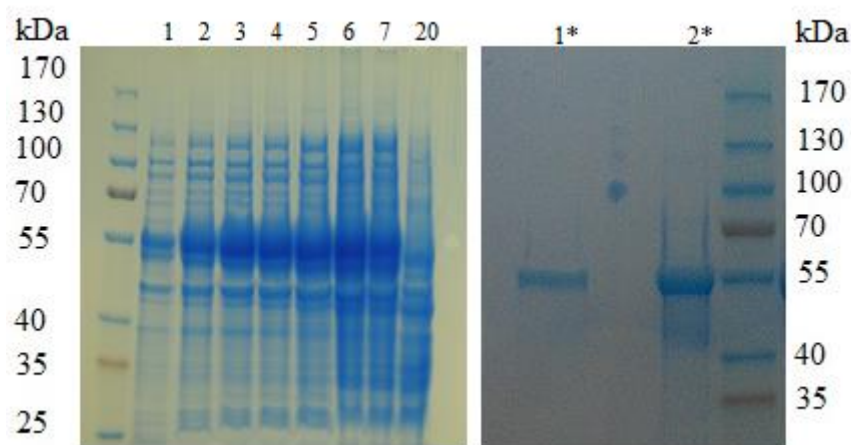


Figure 35: SDS-PAGE of produced Cv TA2, protein appears at 55 kDa. The gel on the left hand side is pre-purification at different time points (hours), the gel on the right is post His-tag purification (1*) followed by PD-10 buffer exchange (2*).

The enzyme was then assayed to determine the activity and substrate scope using the solution phase assay developed in Section 2. The purified protein was filtered through a PD-10 column to remove imidazole, exchange the elution buffer from the purification with HEPES buffer and also to remove small amino acids present in the solution. The data was also compared to the liquid phase assay carried out on Cv TA1 in Section 2.

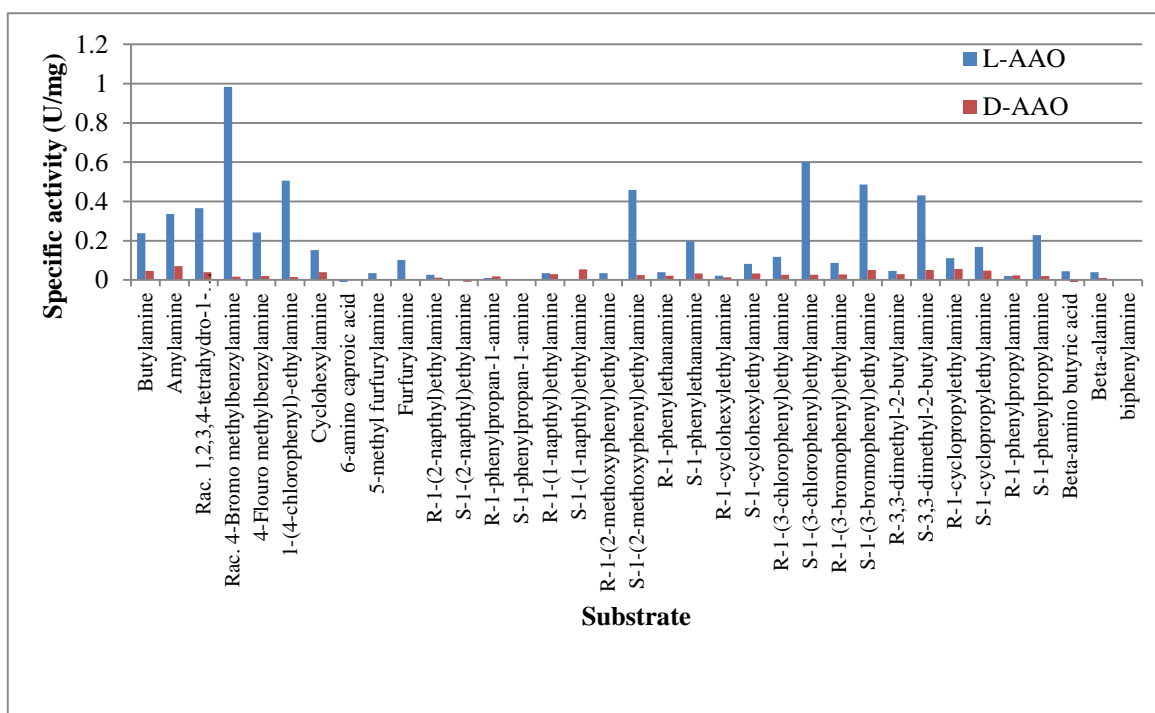


Figure 36: Different amine substrates screened with Cv TA2 with L and D-AAO using the TBHBA 4-AAP solution phase assay. 1U is defined as 1 nmol/min.

The data revealed (Figure 36) that Cv TA2 displayed (*S*)-selectivity towards all compounds assayed and showed a preference for substituted aromatics over non-substituted. β -Alanine and β -amino butyric acid afforded 5% relative initial activity compared to the best amine donor, 4-bromo-1-phenylethylamine. The enzyme also demonstrated activity towards the primary amines butylamine and amylamine.

When comparing the data of the two *C. violaceum* transaminases the specific activity varied slightly. Cv TA2 showed higher activity with 4-bromo-1-phenylethylamine but lower activity with (*S*)-1-phenylethylamine when compared to Cv TA1. Interestingly, Cv TA1 was less selective for alanine and also showed activity with some of the (*R*)-enantiomers of the amines screened when utilising L-AAO.

3.7 Homology modelling of the *Chromobacterium violaceum* transaminases

To gain a better understanding where the difference in activity of the two *C. violaceum* transaminases originated, homology modelling based on Cv TA1 was investigated. Prof. Jenny Littlechild from the University of Exeter provided PDB files for three different crystal structures of Cv TA1.⁹⁴ The structures are the enzyme in three different forms; holoenzyme (PLP bound enzyme), apoenzyme (no PLP bound enzyme) and inhibitor bound enzyme (gabaculine). Previous crystal structures⁹⁵ revealed that the PLP binding site is located at the interface of two subunits. Most of the residues which are involved in cofactor binding come from the subunit which is covalently bound to PLP and this is the case for all ω -transaminases. Interestingly, the main difference between the holoenzyme and apoenzyme is that the apoenzyme has a more open active site than the holoenzyme which can be attributed to a flexible N-terminal loop. Upon PLP binding, the loop completes the enzyme active site by binding to the phosphate group of PLP in the holoenzyme. This loop could play a major part in substrate specificity as it projects a phenylalanine (Phe22) directly into the active site region.

Models of Cv TA2 were constructed by Dr. Simon Willies with Accelrys Discovery Studio 3.1, using the X-ray crystal structure of CV TA1 (PDB code 4AH3) which was crystallised in the holo state. This was a more relevant form of the enzyme due to this being the active state of the enzyme with PLP bound in the active site. Homology modelling could not identify any significant differences between the two models, due to the very high similarity in the two sequences. Therefore, MD simulations were carried

out using a standard dynamics cascade with the CHARMM forcefield implemented in Accelrys Discovery Studio 3.1. There were three mutations which altered the structure marginally, Gly225Ala, Cys424Ser and Ser425Ala. All the mutations were approximately 9Å (2nd/3rd sphere residues) from the PLP so they are not directly involved in substrate binding but they are close enough that they could have an effect on the shape or size of the cavity.

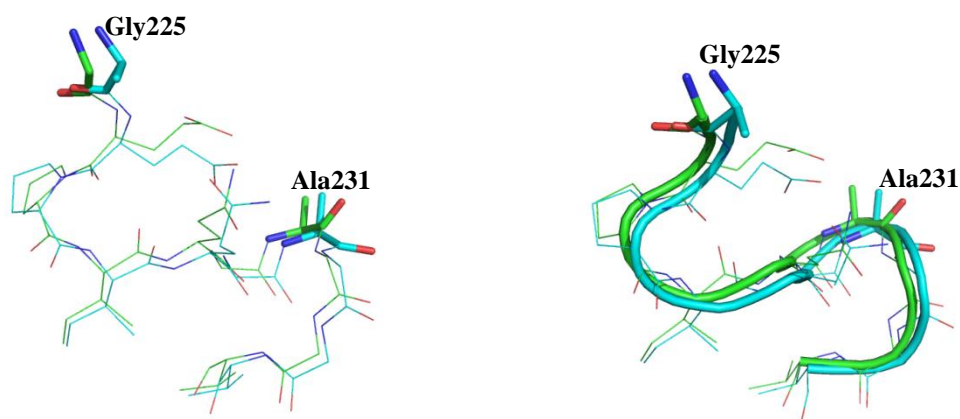


Figure 37: Comparison of holoenzyme and Cv TA2 structures. Region 229-233, Gly225Ala and Ala231 highlighted. Green: Holoenzyme and blue: Cv TA2.

The mutation Gly225Ala in Cv TA2 alters the confirmation of the loop leading up to Ala231. Ala231 forms part of the active site pocket but does not directly bind to PLP in the holoenzyme structure. Figure 37 shows a slight shift in the loop leading up to Ala231 in the Cv TA2 model. Ala231 has shifted by 1.7Å which could account for the increased activity with *para*-substitued compounds in Cv TA2.

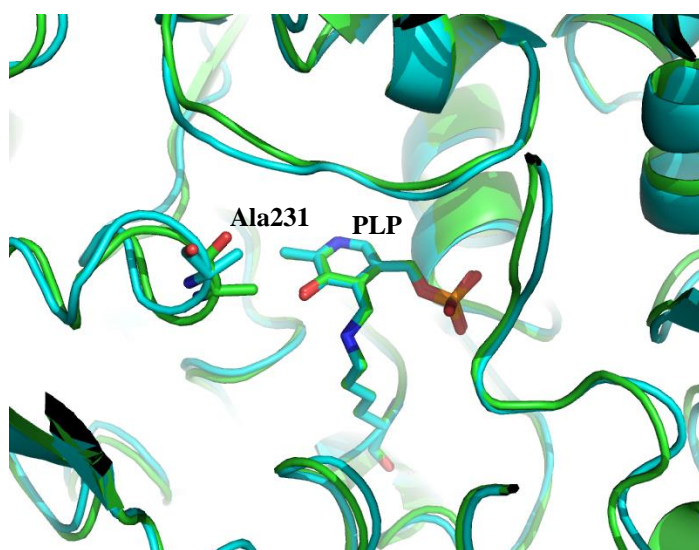


Figure 38: Comparison of holoenzyme and Cv TA2 structures. Active site cavity shown with PLP bound. Green: Holoenzyme and blue: Cv TA2.

All the other mutations demonstrated no major differences in the structure between the two proteins. Inspection of Figure 38 shows a slight shift in the loops that form the active site but nothing significant enough to account for the differences in selectivity for alanine or (*R*)-enantiomers of the amine donors between the two enzymes. The calculated RMSD for the structure is 0.794 Å which suggests that overall there is no significant difference in the two structures.

3.8 Conclusion

The aim of this work was to identify novel transaminase enzymes for the synthesis of enantiomerically pure chiral amines. The work was initiated by screening eight microorganisms from the CMCC, previously shown to have α -transaminase activity, for ω -transaminase activity using a solution phase and solid phase assay which was developed by Shin *et al.*,²⁹ for ω -transaminase activity. Screening with the solution phase assay containing 1-phenylethylamine, sodium pyruvate and glycerol was investigated and organisms which showed conversion of 1-phenylethylamine to acetophenone (analysed *via* GC) and an increase in OD₆₀₀ were subjected to 16S rRNA sequencing for classification of species.

Elizabethkingia sp. and *O. anthropi* were identified as the soil microorganisms possessing potential transaminase activity. Samples were then sent for protein identification to ascertain the enzyme which displayed the potential transaminase activity. *Elizabethkingia sp.* did not produce a transaminase which was detectable by protein identification, however, a transaminase was found at 55 kDa *via* SDS-PAGE in *O. anthropi*. Primers were designed based on the published sequence in ExpASY BLAST and a gene was isolated from the genomic DNA. The protein sequence was aligned to the published *O. anthropi* and the identity was 95% on a protein level. The expression of the *O. anthropi* transaminase was investigated in pET-16b and *E. coli* BL21 (DE3) at three different temperatures with 1 mM IPTG. The gene was successfully cloned into *Bam*HI and *Xho*I restriction enzyme sites of pET-16b and soluble protein could be obtained after 19 hours incubation at 30 °C. The activity and substrate scope was investigated using the solution phase assay developed in Section 2 but the enzyme only showed good activity with naphthylethylamine type compounds. When sodium pyruvate was exchanged for α -keto-glutarate, to try and achieve better activity, no turnover by the enzyme was observed.

C. violaceum CMCC104818 was found in the CMCC and was subjected to the minimal media based assay. Conversion of (*S*)-1-phenylethylamine to acetophenone was observed alongside an increase in OD₆₀₀. DNA primers were designed based on a published transaminase (Cv TA1) and a PCR product was obtained which had a 95% sequence identity to the Ward *et al.*,⁸⁶ transaminase (Cv TA1). The gene was cloned into pET-16b using the restriction sites *Xho*I and *Nde*I and expressed in *E. coli* BL21 (DE3) at 30 °C for 5 hours. After His-trap purification Cv TA2 was subjected to the solution phase assay described in Section 2, the results were compared to substrate scope obtained for Cv TA1. Cv TA2 showed higher activity with 4-bromo-1-phenylethylamine but lower activity with (*S*)-1-phenylethylamine when compared to Cv TA1. Interestingly, Cv TA1 was less selective for alanine but also showed activity with some of the (*R*)-enantiomers of the amines screened when utilising L-AAO.

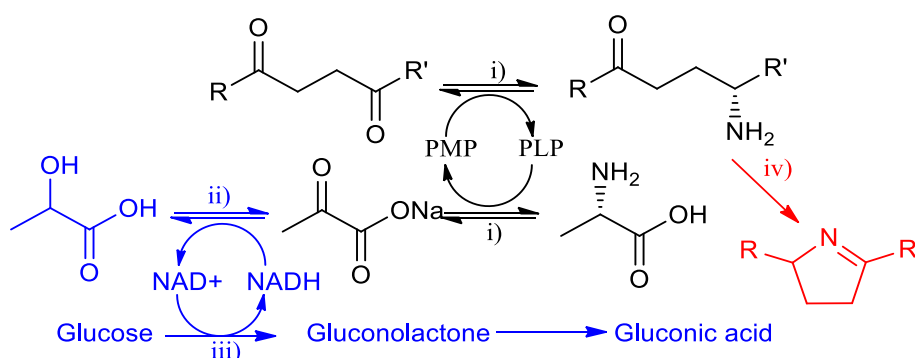
Dynamic simulations did not reveal any significant differences between the holoenzyme form of Cv TA1 and the model of Cv TA2. The only differences observed were three mutations; Gly225Ala, Cys424Ser and Ser425Ala (the mutations closest to the active site) which marginally altered the structure of the enzyme. All the mutations were approximately 9 Å from PLP so they are not directly involved in binding of substrate but they are close enough that they could have an effect on the shape or size of the cavity. A shift in the active site Ala231 was caused by a mutation Gly225Ala and a slight change in where the loop (229-233) sits. Ala231 had shifted by 1.7 Å which could explain the slight differences in activity between the two compounds.

Further work would be to investigate the differences in activity by carrying out a series of mutations with Cv TA2. Firstly, the three mutations Gly225Ala, Cys424Ser and Ser425Ala should be mutated both singly and combinatorially back to the original sequence of *E. coli* Cv TA1 and a comparison of activity investigated. Another interesting mutation to perform would be to switch Ala231 for glycine and see if this alters the active site cleft and substrate preference and/or activity

4. Results and discussion- Biotransformations using transaminases

Regulations that require strict testing of both enantiomers of racemic compounds^{4,96} before release for sale is resulting in an increase of the approval of single enantiomer drugs worldwide.⁹⁷ Biocatalysts have the potential to offer a cost effective, environmentally benign route to chiral molecules owing to their inherent enantioselectivity. For this reason Dr Reddy's (Chirotech Technology Centre) are investigating new biocatalytic methods for the synthesis of enantiomerically pure chiral amines and transaminase enzymes provide an attractive approach by employing asymmetric catalysis from a prochiral ketone.

Within this project is described the synthesis of a number of different chiral primary and secondary amines using two different transaminase enzymes (a commercially available (*R*)-selective transaminase from Codexis and the overproduced recombinant (*S*)-selective transaminase from *C. violaceum*) to catalyse a reductive amination reaction. Scheme 33 describes two different methods which were used to help drive the equilibrium; (i) LDH/GDH⁶⁹ system in which the LDH serves to drive the equilibrium by the removal of pyruvate (known to inhibit transaminase) and the GDH recycles the NADH cofactor for the LDH and (ii) spontaneous cyclisation of the initial amine produced to remove it from the system and therefore drive the reaction.



Reagents and conditions: i) Transaminase ii) LDH, iii) GDH, 30 °C, 100 mM potassium phosphate or HEPES pH 7.5, 20% DMSO.

Scheme 33: GDH recycle system (blue) and spontaneous cyclisation (red) for the production of enantiomerically pure chiral amines.

4.1 4-Bromoacetophenone

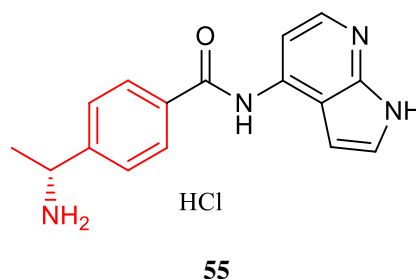
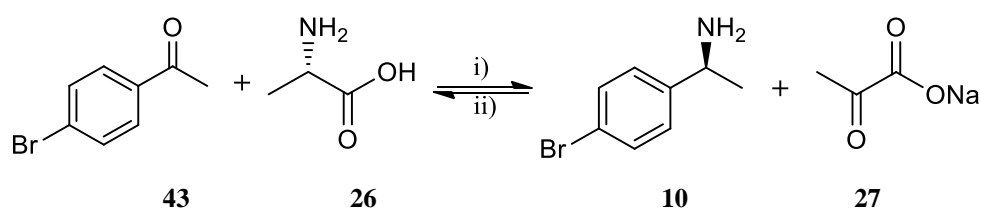


Figure 39: Y-39983, a Rho-associated protein kinase inhibitor for the treatment of ophthalmic treatment of glaucoma.

Y-39983 compound **55** (Figure 39) is a Rho-associated coil-forming protein kinase inhibitor (ROCK inhibitor) for the potential ophthalmic treatment of glaucoma.⁹⁸ One of the steps in the synthesis of Y-39983 is the carbonylation of (*S*)-4-bromo-1-phenylethylamine.^{99,100} It was envisaged that (*S*)-4-bromo-1-phenylethylamine could be synthesised from the corresponding ketone, 4-bromo-acetophenone, by utilising Cv TA2. In Section 2 the enzyme was assayed against a panel of 35 different amine donors for activity in the reverse deamination direction. Cv TA2 displayed the highest activity with (*S*)-4-bromo-1-phenylethylamine when using sodium pyruvate as a keto acceptor. If alanine **26** is used as the amino donor then it should be possible to aminate 4-bromo-acetophenone **43** to synthesise (*S*)-4-bromo-1-phenylethylamine **10** and pyruvate **27** (Scheme 34). A solvent screen showed that DMSO was the best co-solvent when compared to MeOH, acetone and acetonitrile, therefore this was the co-solvent selected for all future biotransformations.



Reagents and conditions: i) Forward transaminase reaction: transaminase, LDH, GDH, glucose, 30 °C, 100 mM potassium phosphate pH 7.5, 20% DMSO ii) Reverse transaminase reaction.

Scheme 34: Biotransformation employing (*S*)-TA Cv TA2 for the production of (*S*)-4-bromo-1-phenylethylamine.

Different enzyme preparations of Cv TA2 were investigated to try and achieve the optimum biotransformation conditions for the conversion of 4-bromo-acetophenone to (*S*)-4-bromo-1-phenylethylamine. Reactions were performed on a 1 mL scale (5 mM) at

30 °C using whole cell, lysed whole cell, cell free extract and purified protein preparations and monitored for up to 24 hours via chiral GC analysis. The data in Figure 40 revealed the best activity was seen when utilising purified Cv TA2.

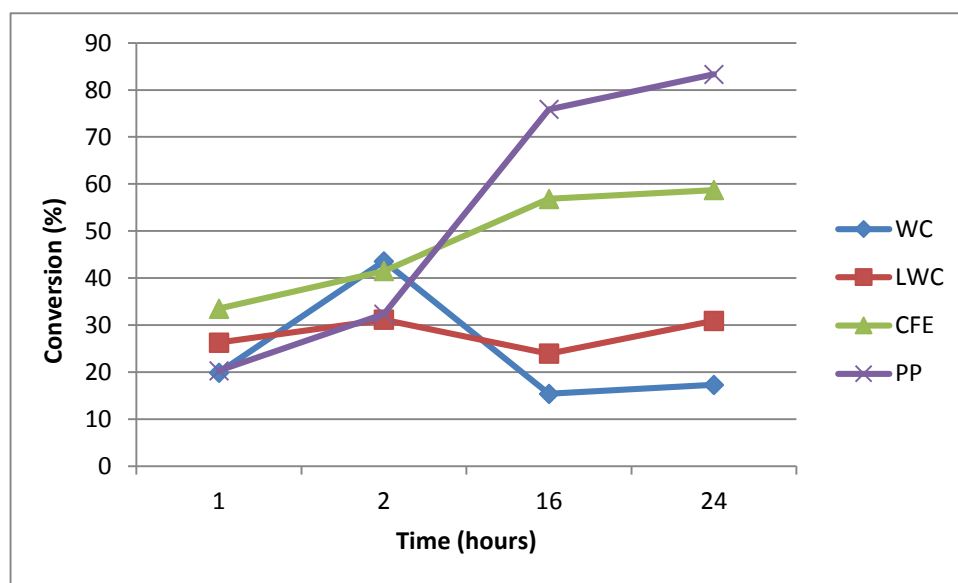


Figure 40: Biotransformation of 5 mM 4-bromo-acetophenone using Cv TA2 utilising L-alanine as a amine donor. Reactions were prepared from 1g of wet cell (the same batch) to control the amount of protein in the reactions. WC = Whole cell, LWC = lysed whole cell, CFE = Cell free extract and PP = purified protein.

Initial scale up of the biotransformation was investigated using the Mettler-Toledo Multi-Max reactor system (5 mM 4-bromo-acetophenone, 20 mL total volume). Conversion was monitored by chiral GC and the automated addition of 2 M NaOH to maintain the pH at 7.5 (a drop in pH should be observed upon conversion from 4-bromo-acetophenone to (*S*)-4-bromo-1-phenylethylamine due to the production of gluconic acid by the GDH in the recycling system) using purified protein enzyme preparations. No conversion was observed after 24 hours even when the reaction was repeated and the rpm of the paddle stirring reduced. To investigate whether the paddle stirring was denaturing the enzyme a different method of agitation was tried. Reactions were carried out on a 20 mL scale at 5 mM 4-bromo-acetophenone in a sealed conical flask and shaken at 250 rpm in a 30 °C incubator. Two different buffers (potassium phosphate and HEPES) were also employed based on the results obtained from a pH profile for Cv TA2 (Appendix 6) and previous investigations by Ward and co-workers showing that using HEPES instead of potassium phosphate increased the activity of Cv TA1.⁸⁶

Table 8: Results from two different buffered systems carried out with a different agitation method.

72 hours	Potassium phosphate	HEPES
Conversion	89%	97%
<i>e.e.</i>	> 99% (<i>S</i>)	> 99% (<i>S</i>)

The data in Table 8 shows that HEPES gave the best conversion from 4-bromo-acetophenone to 4-bromo-1-phenylethylamine and it was concluded that paddle stirring is not suitable for this reaction as the biotransformation went to completion after 24 hours with orbital shaking. The maximum substrate loading for the reaction was investigated next by carrying out the reaction at different concentrations. At 15 mM it was noted that the conversion was greatly decreased (Table 9). This reduction in conversion could be due to the low solubility of the starting material even in the presence of 20% DMSO and also a build-up of the product amine could lead to inhibition of the transaminase.

Table 9: Different substrate loadings of 4-bromo-acetophenone using purified protein enzyme preparations.

48 hours	5 mM	10 mM	15 mM	20 mM
Conversion	94%	96%	40%	20%
<i>e.e.</i>	> 99%	> 99%	> 99%	> 99 %

To overcome the problem of substrate solubility, a product accumulation experiment was carried out by the drop wise addition of a solution of 4-bromo-acetophenone (113.92 mg, 18 mM) in DMSO (20% reaction volume) over a period of 72 hours. The reaction proceeded to 90% conversion (based on GC analysis) and the product was isolated (yield 92%) and analysed by NMR. However, when the reaction was repeated and a higher concentration of 4-bromo-acetophenone was added to the solution (total 30 mM), the rate of reaction greatly decreased beyond 25 mM substrate concentration. Investigation into the reason for decreased activity was carried out using the solution phase assay in the deamination direction as discussed in Section 2. Varying concentrations of 4-bromo-(*S*)-1-phenylethylamine were assayed to assess the effect of change in concentration upon specific activity.

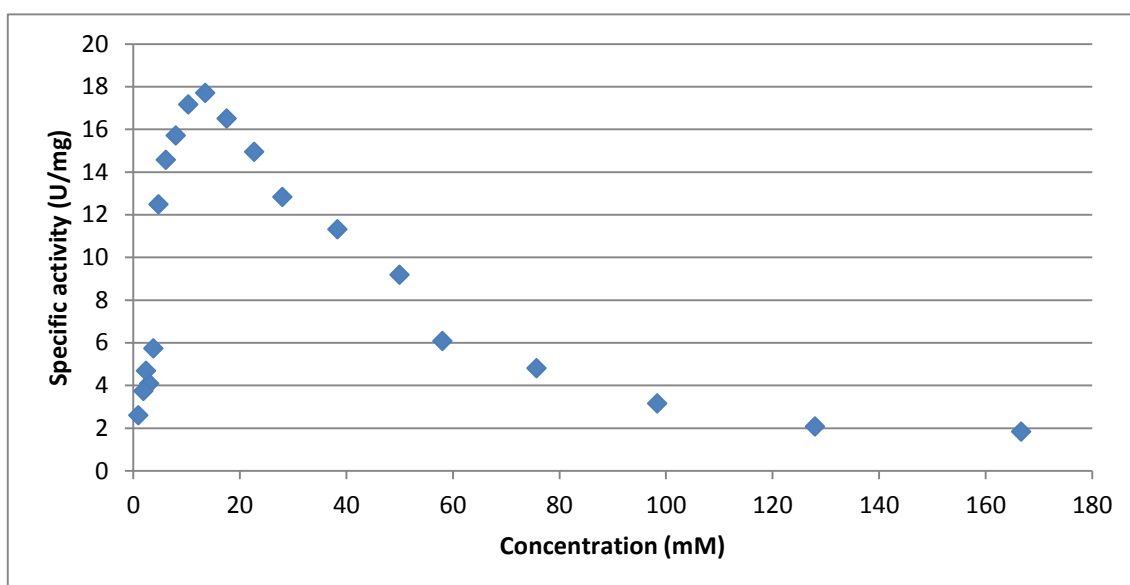


Figure 41: Concentration curve employing the solution phase screen (TBHBA 4-AAP) with (*S*)-4-bromo-1-phenylethylamine. 1U = is defined as 1nmol/min.

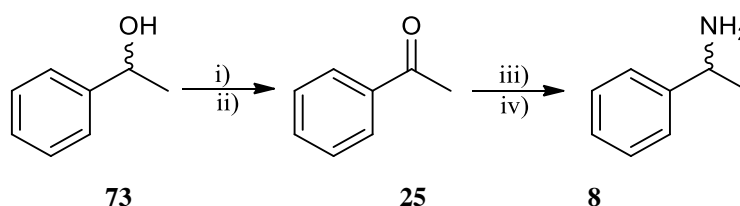
Inspection of Figure 41 reveals a reaction profile for the deamination reaction which is indicative of substrate inhibition. At concentrations of 4-bromo-(*S*)-1-phenylethylamine above 17 mM a significant decrease in activity was observed. This observation helps explain the decreased reaction rate for the forward transaminase reaction because accumulation of 4-bromo-(*S*)-1-phenylethylamine occurs in the solution. However additional sources of inhibition must be present to explain the significant loss of activity, most likely to be caused by the substrate 4-bromo-acetophenone. Investigations into whether 4-bromo-acetophenone causes substrate inhibition in the forward transaminase reaction is required, however, increasing the amount of substrate loading produces more 4-bromo-(*S*)-1-phenylethylamine which itself causes inhibition, therefore a method of product removal must be investigated first. There have been many methods developed for product removal in transaminase reactions including the use of resins,⁷⁰ cosolvents²⁹ and spontaneous cyclisation⁷⁰ of the amine product to help drive the equilibrium and reduce the concentration of the product inhibitor within the solution. Investigation into the above methods to study the inhibition effects of 4-bromo-acetophenone and hence eventually increase the substrate loading was unfortunately outside the timeframe of this project.

4.2 Cascade reactions

Biocatalytic cascade reactions provide an ideal approach for the synthesis of pharmaceutical compounds. The idea of a multi-step one-pot synthesis by incorporating multiple genes on one plasmid which are co-overproduced, provides an attractive approach for an organic chemist because, without requirement for intermediate isolation procedures, the process becomes environmentally benign and sustainable.¹⁰¹ Within this project, proof of principle experiments behind biocatalytic cascade reactions were investigated using purified transaminase, galactose oxidase (GO) and monoamine oxidase enzymes either sequentially or in one-pot for the synthesis of enantiomerically pure chiral amines.

4.2.1 Galactose oxidase/transaminase cascade

Galactose oxidases (GOase) is a copper dependant enzyme that catalyses the oxidation of the C6-OH in D-galactose to the respective aldehyde. A GOase variant (M₃₋₅) has been created that catalysed the kinetic resolution of racemic 1-phenylethylalcohol to acetophenone in the presence of hydrogen peroxide scavengers, HRP and catalase.⁸⁴ The recombinant GOase was overproduced in *E. coli*. BL21 Star and combined with commercially available Codexis transaminases (ATA 113 and 117) to provide an attractive approach to (*S* or *R*)-1-phenylethylamine **8** (depending on the selectivity of the transaminase enzyme used) which is demonstrated in Scheme 35.



Reagents and conditions: i) GOase ii) HRP and Catalase, iii) Transaminase and iv) GDH recycle system.

Scheme 35: Biotransformation employing a overproduced GOase and commercially available Codexis Transaminase enzymes ATA-113 and 117 for the production of (*S* or *R*)-1-phenylethylamine **8** from (*rac*)-1-phenylethylalcohol **73**.

In this process racemic 1-phenylethylalcohol **73** is initially converted to acetophenone **25** using GOase, HRP and catalase. Ideally in a one pot reaction, the transaminase (alongside the GDH recycle system) is used to carry out a reductive amination reaction

providing access to (*S* or *R*)-1-phenylethylamine **8** depending on whether an *S* or *R* selective transaminase is used.

Initial investigations were carried out in one pot using 5 mM (*rac*)-1-phenylethylalcohol on a 1 mL scale. GOase and the commercially available Codexis enzymes ATA-117 and 113 were combined with the GDH recycle system, HRP and catalase. The reactions were monitored over a period of 24 hours by chiral GC analysis but unfortunately, no conversion from the alcohol to acetophenone was observed by the GOase. In previous experiments it was noted that chemical reducing agents inhibited the GOase by possibly reducing the copper in the GOase active site. We considered that LDH in the GDH recycle system could be reducing the copper suggesting that the transaminase reaction mixture could be added to the GOase until the reaction is complete. Thus the GOase reaction was carried out individually and monitored over a period of 3 hours to make sure the kinetic resolution of 10 mM (*rac*)-1-phenylethylalcohol went to completion.

Table 10: Different substrate loadings of 4-bromo-acetophenone.

GOase	Percentage (%)
Conversion	47
<i>e.e.</i>	96

The data in Table 10 reveals that the (*R*)-selective GOase reaction went to 47% conversion in high enantiomeric excess. A solution of the transaminase in the GDH recycle system was added to the GOase reaction mixture and was monitored over a period of 28 hours by chiral GC analysis. Both the ATA 117 and 113 reactions progressed to 80% and 70% conversion respectively and in both cases greater than 99% *e.e.* as shown in Figure 42.

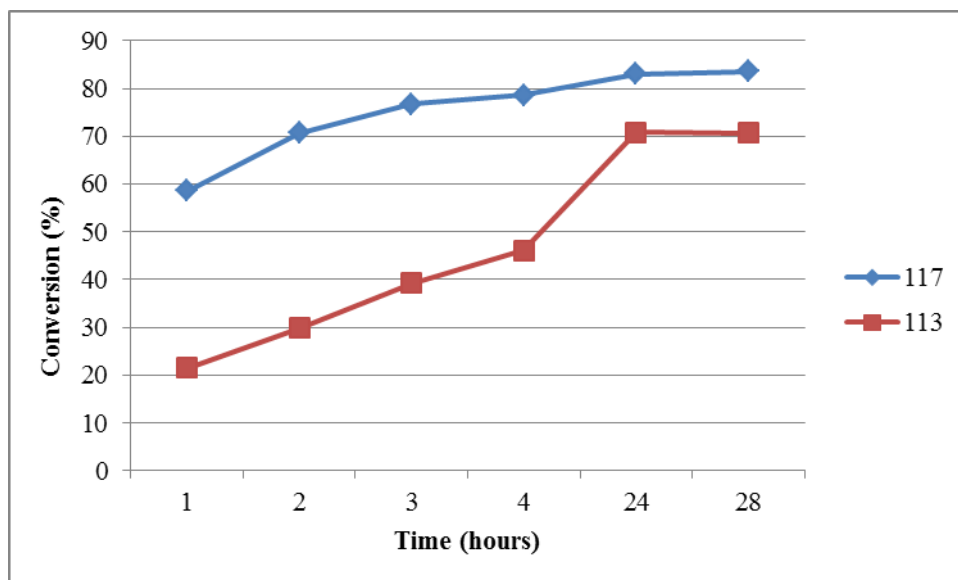


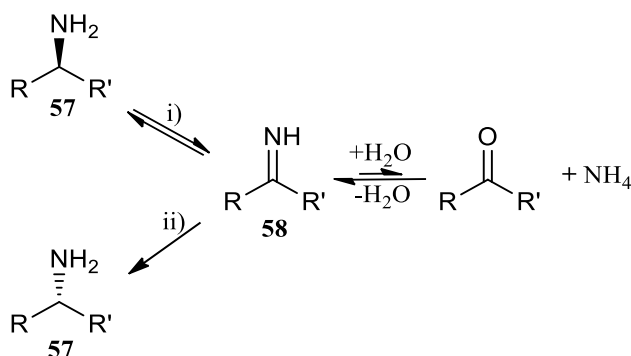
Figure 42: Conversion of acetophenone to (*S* or *R*)-1-phenylethylamine employing commercially available Codexis transaminase enzymes ATA 117 and ATA 113.

The results show the potential of combining two enzymes to carry out a synthetic sequence which would be difficult to carry out chemically. The use of GOase and transaminase in a two-step, one pot synthesis of cyclic chiral secondary amines from a *mesodiol* for the asymmetric synthesis of chiral amines in 100% yield would be the next step; unfortunately, further investigation was restricted due to the time frame of this project.

4.2.2 Monoamine oxidase and transaminase cascade

Spontaneous cyclisation helps drive the equilibrium of transaminase reactions by removing the amine product which is known to inhibit transaminase enzymes. Simon *et al.*, demonstrated the regioselective and stereoselective amination of 1,5-diketones **74** which spontaneously cyclised to give the corresponding cyclic imine **76** in high yield and *e.e.*¹⁰² Diastereoselective hydrogenations were performed utilising Pd/C to give access to *cis*-(+)-piperidines **56** in high yields (Scheme 36).

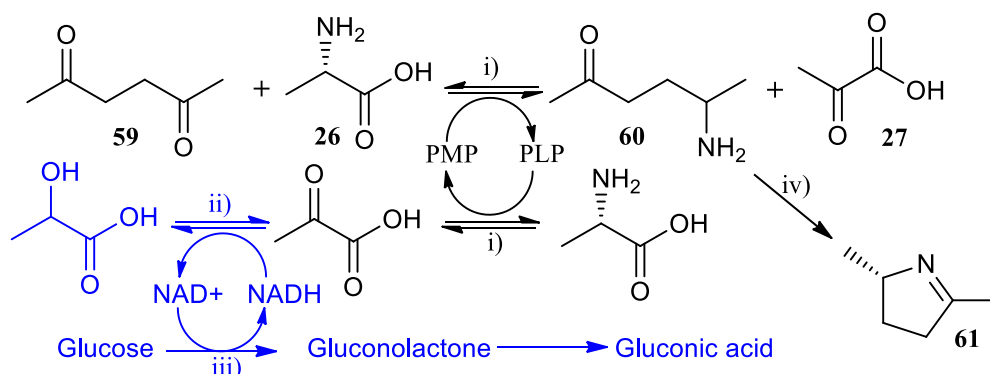
(such as NaBH_4 and NH_3BH_3) alone as only 50:50 mixtures of diastereomers would be obtained in these instances. The flavin dependant MAO from *Aspergillus niger* (MAO-N) catalyses the selective oxidation of chiral amines **57** to the corresponding imine **58**, which in the presence of a suitable reducing agent, such as ammonia borane, gives access to the unreacted amine in high enantiomeric excess as demonstrated in Scheme 37.⁴⁶ Different variants of the MAO-N can be utilised which have undergone several rounds of mutagenesis, in this study MAO-N D9 and D11 will be used.



Reagents and conditions: i) MAO-N ii) NH_3BH_3 , 1 M Phosphate buffer pH 7.8.

Scheme 38: Monoamine oxidase deracemisation of chiral amines **57** in the presence of ammonia borane.

Initial experiments were carried out with commercially available 2,5-hexanedione **59** (5 mM, Sigma 165131) to see if the formation of 2,5-dimethyl-3,4-dihydro-2*H*-pyrrole **61** could be detected (Scheme 39). Reactions were carried out using the LDH/GDH recycle system (with and without DMSO) and with the (*S*)-selective recombinant transaminase Cv TA2 and monitored over a period of 24 hours *via* GC-MS and GC-FID.



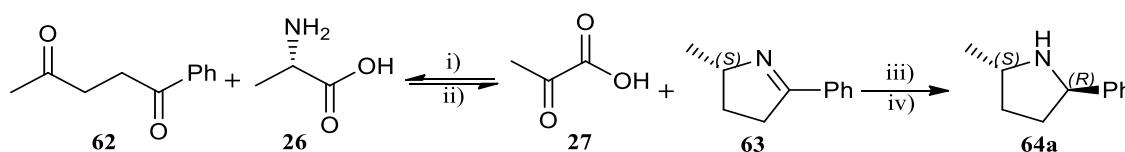
Reagents and conditions: i) Transaminase (Cv TA2) ii) LDH, iii) GDH, iv) Spontaneous cyclisation.

Glucose, 30 °C, 100 mM HEPES pH 7.5, 20% DMSO.

Scheme 39: Biotransformation employing (*S*)-transaminase Cv TA2 for the production of (*S*)-2,5-dimethyl-3,4-dihydro-2*H*-pyrrole **61** from 2,5-hexanedione **59** and (*L*)-alanine **26**.

Reactions containing 20% DMSO successfully went to 80% conversion after 24 hours compared to reactions containing no DMSO which gave very low conversions (possibly due to solubility of the substrate). The reaction containing DMSO was scaled up to 100 mM with two different transaminases, an (*R*)-selective transaminase (ATA-117) was used as well as the (*S*)-selective transaminase (Cv TA2) to generate both enantiomers of 2,5-dimethyl-3,4-dihydro-2*H*-pyrrole **61**. At 100mM the reactions went to 30% conversion and both products were isolated. ¹H NMR analysis confirmed the identity of 2,5-dimethyl-3,4-dihydro-2*H*-pyrrole **61** and equal and opposite optical rotation values (+ 3.5 and – 3.6) were obtained suggesting that different enantiomers were obtained.

Chemical reduction of imine **61** with NaBH₄ followed by oxidation catalysed by MAO-N was investigated. Unfortunately the MAO-N variants showed no activity towards either (*S*) or (*R*)-**61**. Previous studies within the Turner group have revealed that MAO-N prefers larger substituents on one side of the pyrroline ring such as ethyl, phenyl and benzyl substitutions. Therefore a reaction employing 1-phenylpentane-1,4-dione **62** as the transaminase substrate was investigated to give 2-methyl-5-phenyl-3,4-dihydro-2*H*-pyrrole **63**, which was a test substrate for the MAO-N reaction (Scheme 40).

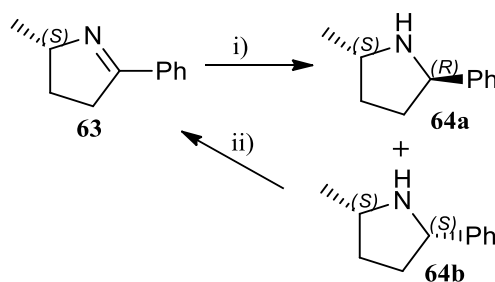


Reagents and conditions: i) Transaminase ii) Pyruvate removal system, 30 °C, 100 mM HEPES pH 7.5, 20 % DMSO iii) NaBH₄ IV) MAO-N.

Scheme 40: Biotransformation employing (*S*)-transaminase Cv TA2 and ATA-117 for the production of (*S* or *R*)-2-methyl-5-phenyl-3,4-dihydro-2*H*-pyrrole **63** followed by the MAO-N stereoselective synthesis of (2*S*,5*R*)-2-methyl-5-phenylpyrrolidine **64a**.

Reactions at 5 mM concentration were carried out employing Cv TA2 using 20% DMSO and the LDH/GDH recycle system. The reaction successfully went to 85% conversion after 24 hours as monitored by GC and chiral HPLC. The reactions were scaled up to 100 mM and both ATA-117 and Cv TA2 were utilised to generate the (*R*)- and (*S*)-enantiomers respectively of 2-methyl-5-phenyl-3,4-dihydro-2*H*-pyrrole **63**. Interestingly both transamination reactions proceeded with complete regioselectivity for the smaller substituent on the diketone (*i.e.* the methyl group in this case) resulting in only the pyrroline shown in Scheme **39** being produced. Chiral HPLC analysis confirmed both transaminase reactions proceeded in > 99% *e.e.* and the

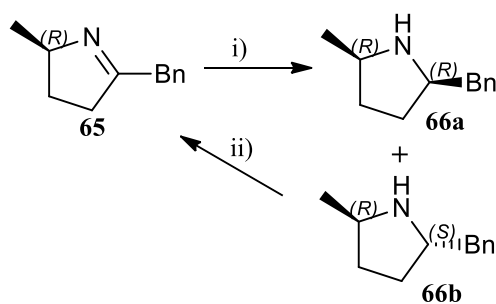
enantiopure imines were isolated, characterised and then subjected to the MAO-N (D9 mutant) catalysed reaction after reduction with ammonia borane (Scheme 41).



Reagents: i) NH_3BH_3 II) MAO-N.

Scheme 41: Biotransformation employing MAO-N for the production of (2*S*,5*R*)-2-methyl-5-phenylpyrrolidine **64a**.

The MAO-N reaction with the enantiomerically pure (*R*)-pyrroline **63** transaminase product resulted in (2*R*,5*R*)-2-methyl-5-phenylpyrrolidine **64a** in > 99% diastereomeric excess. However, the enantiomerically pure (*S*)-pyrroline transaminase product when subjected to the MAO-N reaction, only gave a diastereomeric excess of 63% for the (2*S*,5*R*)-2-methyl-5-phenylpyrrolidine **64a**. A possible explanation to this observation is that MAO-N may be also oxidising the (*S*)-methyl stereogenic centre giving access to the (*R*)-methyl diastereomer. This could prove problematic if the reaction is not monitored as 50/50 mixture of both diastereomers would be obtained resulting in a *d.e.* of 0. The MAO-N catalysed oxidation of the methyl centre is a lot slower than that of the phenyl so optimal conversion can be achieved if the reaction is stopped before oxidation of the methyl position occurs. This was demonstrated with the substrate 2-benzyl-5-methylpyrrolidine **65** (Scheme 42) which was generated by the transaminase catalysed amination of the corresponding ketone. Figure 43 shows that after 3 hours with the MAO-D9 mutant the reaction is complete with > 99% *d.e.* However after prolonged reaction times (74 hours) the *d.e.* goes to 0. If the D11 mutant is used the reaction progresses much slower and the *d.e.* after 74 hours is 85%.



Reagents: i) NH₃BH₃ II) MAO-N.

Scheme 42: MAO-N stereoselective synthesis of (2*R*,5*R*)-2-benzyl-5-methylpyrrolidine **66a**.

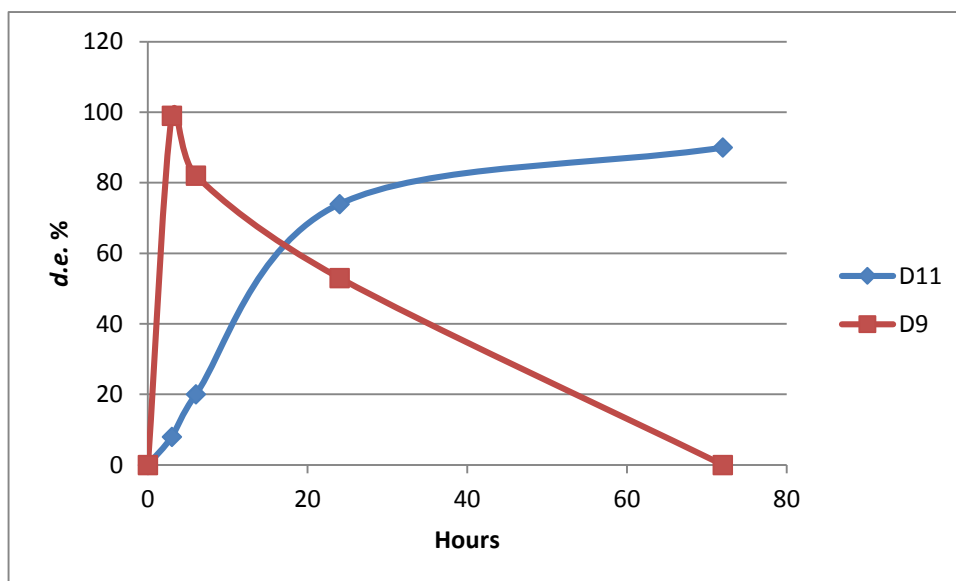


Figure 43: MAO-N stereoselective synthesis of (2*R*,5*R*)-2-benzyl-5-methylpyrrolidine **66a**.

Table 11 shows all the diketones (which were either commercially available or synthesised by Diego Ghislieri) screened and the results from the sequential transaminase then MAO-N reaction.

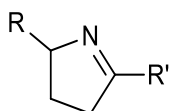


Figure 44: Structure of the di-substituted pyrroline.

Table 11: Table of di-substituted pyrrolines and the *e.e.* values after oxidation with MAO-N.

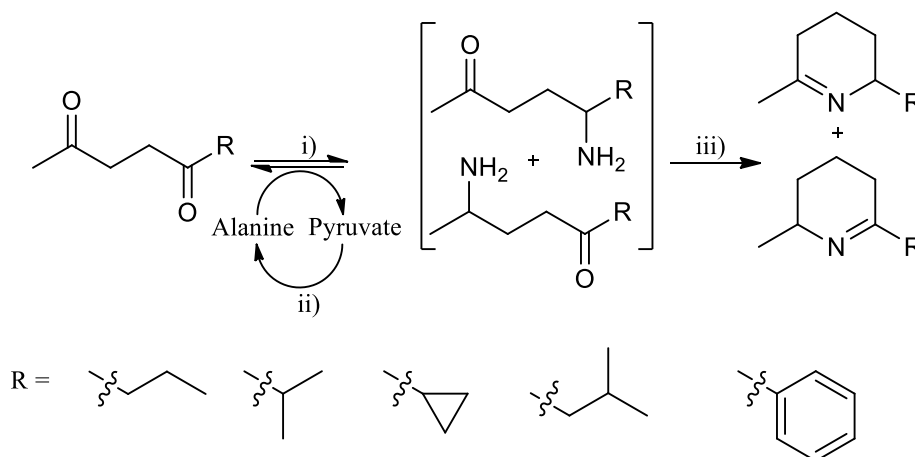
R	R'	TA- <i>e.e.</i>	MAO- <i>d.e.</i> ¹
Et	Ph	> 99% (<i>S</i>)	D9 94 % - (<i>2S,5R</i>).
Me	Bn	> 99% (<i>S</i>) > 99% (<i>R</i>)	D9 80 % (<i>2S,5R</i>). D9 99 % (<i>2R,5R</i>).
Me	Ph	> 99% (<i>R</i>) > 99% (<i>S</i>)	D9 90 % (<i>2R,5R</i>). D9 98 % (<i>2S,5R</i>).
Ph	Ph	-	-
Me	Me	> 99% (<i>R</i>) > 99% (<i>S</i>)	-

¹ Configurations assigned based on previous MAO-N oxidation reactions with similar substrates and the selectivity of the transaminase in the previous step.

The transaminase reactions at 5 mM concentrations proceeded to greater than 70% conversion for all compounds except for 1,4-diphenylbutane-1,4-dione which showed no conversion from the ketone to the corresponding imine. This is because as described in Section 1 the transaminase active site has a small and a large pocket in which the substrate fits therefore having two phenyl groups does not allow the substrate to fit into the active site of the transaminase and therefore renders the enzyme inactive with this substrate.

Investigations were then carried out to try to improve the low conversions obtained for the transaminase reactions at higher substrate concentrations. As mentioned in Section 1, pyruvate is known to inhibit transaminase enzymes and therefore needs to be removed completely or recycled back to alanine. This can be achieved through the use of an alanine dehydrogenase system or a LDH/GDH system. When using the LDH/GDH system at 5 mM reaction concentrations high conversion were achieved, however, when reactions were scaled up to 100 mM conversions were reduced significantly. Simon *et al.*, reported similar findings when removing pyruvate by reduction to lactate through the use of a LDH/GDH system, the conversions varied from 56–98%.¹⁰² They solved this problem by utilising an alanine dehydrogenase to recycle pyruvate back to alanine alongside a formate dehydrogenase to recycle the cofactor

NAD⁺ which is required by the alanine dehydrogenase (Scheme 43). Experiments were performed with 1-phenylpentane-1,4-dione at 50 mM concentrations using the LDH/GDH recycle system and the alanine dehydrogenase system used by Simon *et al.* Both systems showed high levels of conversion at 50 mM substrate concentrations, however the alanine dehydrogenase system resulted in a higher conversion of 94% compared to the LDH/GDH system which had a conversion of 86%. Reaction scale-up should therefore be performed using the alanine dehydrogenase system to achieve optimal results.



Reagents and conditions: i) ω -Transaminase ii) Alanine dehydrogenase, spontaneous cyclisation. Formate buffer, formate dehydrogenase, NAD⁺, 30 °C for 24 hours.

Scheme 43: Biotransformation by Simon *et al* for the regio- and stereoselective monoamination of diketones.

Different chemical reduction conditions were performed on (*S*)-2-methyl-5-phenyl-3,4-dihydro-2*H*-pyrrole to enable a comparison with the MAO-N catalysed reactions and to achieve the best reaction conditions for the synthesis of the corresponding pyrrolidine. Initially a reaction with NaBH₄ was investigated and after an hour at room temperature a *d.e.* of 10% was achieved (essentially a 50:50 mixture of both diastereomers). Secondly hydrogenation with Pd/C was investigated overnight at room temperature. Full consumption of the imine was observed but poor conversions to the corresponding pyrrolidines were achieved (< 10%) in poor *d.e.* (5%). The major product was unidentified however it was assumed to be the ring opened amine **72** (Figure 45). These results show the MAO-N reaction is the best of the methods investigated for the stereoselective synthesis of substituted pyrrolidines.

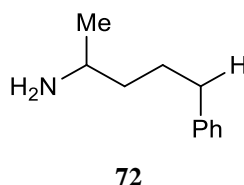


Figure 45: Structure of the ring opened amine **72** thought to be produced from the hydrogenation reaction.

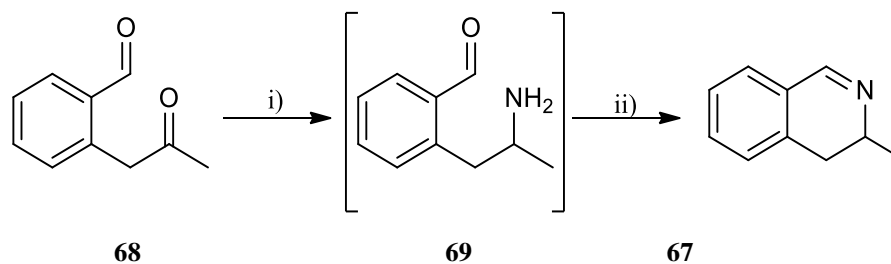
Next a one pot, two step, synthesis was attempted with the (*S*)-transaminase Cv TA2 and MAO-N/ammonia borane using 1-phenylpentane-1,4-dione as the substrate to see if the production of 2-methyl-5-methylpyrrolidine could be detected under these conditions. Chemo-enzymatic one pot reactions are desirable due to the avoidance of extractions between steps and in this instance no protection/deprotection steps would be required. Reactions were run for 24 h at 15 mM substrate concentration, 30 °C using the alanine dehydrogenase system and monitored *via* GC-FID and chiral HPLC. The transamination reaction went to completion after 24 h in > 99% *e.e.* MAO-N and ammonia borane were then added to the reaction mixture and the reaction was left for a further 24 h after which (2*S*,5*R*)-2-methyl-5-phenylpyrrolidine was generated in 99% *d.e.*

This one-pot two-step dual enzyme cascade reaction provides an attractive approach for the regio/stereoselective synthesis of enantiomerically pure 2,5-di-substituted pyrrolidines in high *d.e.* and *e.e.*

4.33 Methyl-3,4-dihydroisoquinoline

3-Methyl-3,4-dihydroisoquinoline **67** has attracted interest as a building block for the synthesis of antithrombotic agents, platelet aggregation inhibitors¹⁰³ and quinolone anti-infective agents.¹⁰⁴ We envisaged developing a new approach to this compound by utilising a transaminase enzyme for initial asymmetric amination of 2-(2-oxopropyl)benzaldehyde **68** followed by cyclisation (Scheme 44). Previous experiments within the Turner group have shown that ω -transaminase enzymes have little/no activity with aldehydes when compared to ketones, therefore a transaminase should selectively aminate the ketone in the presence of the aldehyde group to afford 2-(2-aminopropyl)benzaldehyde **69** which upon spontaneous cyclisation would yield 3-methyl-3,4-dihydroisoquinoline **67**. Either enantiomer of the dihydroisoquinoline could be obtained by using the commercially available (*R*)-selective Codexis transaminase

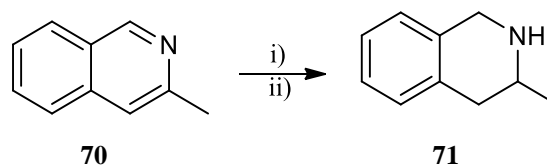
enzyme, ATA-117 and the over-produced recombinant (*S*)-selective transaminase, Cv TA2.



Reagents and conditions: i) Transaminase, LDH, GDH, glucose, L-alanine 30 °C, 100 mM HEPES pH 7.5, 20% DMSO. ii) Spontaneous cyclisation.

Scheme 44: Biotransformation employing (*S*)-transaminase Cv TA2 for the production of (*S*)-3-methyl-3,4-dihydroisoquinoline **67**.

Firstly, 2-(2-oxopropyl)benzaldehyde **68** was synthesised chemically following a previously reported method by *Lara et al.*¹⁰⁵ 2-Methylindene (Aldrich 449431) was oxidised using 3-chloroperbenzoic acid (Aldrich 273031) and sodium hydrogen carbonate to afford the corresponding epoxide in 32% yield. Treatment of the epoxide with ammonium cerium (IV) nitrate afforded 2-(2-oxopropyl)benzaldehyde **68** in 41% yield after flash chromatography.



Reagents and conditions: i) Microwave irradiation ii) EtOH, NH₄Cl and In.

Scheme 45: Microwave synthesis of (*rac*)-3-methyl-1,2,3,4-tetrahydroisoquinoline **71**.

A racemic HPLC standard of **67** was required to detect the formation of 3-methyl-3,4-dihydroisoquinoline by the transaminase enzymes. As shown in Scheme 45 commercially available 3-methylisoquinoline **70** (Aldrich 129895) was subjected to microwave irradiation in the presence of EtOH, In and NH₄Cl as described by *Moreno et al.*¹⁰⁶ (except for replacing the 5 day reflux with a 4 hour microwave step). (*rac*)-3-Methyl-1,2,3,4-tetrahydroisoquinoline **71** was obtained in 53% yield and subjected to the MAO-N oxidation reaction to afford (*rac*)-3-methyl-3,4-dihydroisoquinoline.

Biotransformations at 5 mM concentrations were carried out at 30 °C using the (*R*) and (*S*)-selective transaminases, ATA 117 and Cv TA2 respectively. The GDH/LDH recycle system was utilised to recycle pyruvate back to alanine and reactions were monitored

for a period of 24 h by chiral HPLC. After 30 minutes some over oxidation of the imine to form 3-methylisoquinoline was observed and after 2 h full conversion to the aromatic product occurred. Different temperatures were investigated and the reactions were carried out under N₂ to try and slow down the rate of the oxidation. Reactions were carried out at 15, 20 and 25 °C but unfortunately 3-methylisoquinoline was still detected after 30 min.

A report published by *Bonamore et al.*,¹⁰⁷ stated that the use of the reductant L-ascorbic acid helped prevent the oxidation of dopamine during the reaction time course. It was envisaged that by the addition of L-ascorbic acid to the biotransformations, the rate of oxidation of the imine transaminase product may be slowed or even prevented. L-Ascorbic acid was incorporated into the transaminase biotransformations and the reaction was monitored every 15 minutes by chiral HPLC. Although conversion to 3-methylisoquinoline was not completely eliminated the rate of oxidation was slowed such that formation of the isoquinoline was not observed until after 45 minutes. L-Ascorbic acid was thus incorporated into the biotransformations and the reactions were monitored by chiral HPLC. Full consumption of 2-(2-oxopropyl)benzaldehyde was observed after 1 hour and 3-methyl-3,4-dihydroisoquinoline was synthesised in > 99% *e.e.* for both enantiomers. (*R*) and (*S*) configurations were assigned based on previous transaminase catalysed reactions with similar substrates.

4.4 Conclusion

The aim of this work was to investigate the synthesis of a range of enantiomerically pure chiral amines utilising three different transaminase enzymes, the commercially available Codexis enzymes ATA-117 and ATA-113 (*R* and *S* selective) and the over-produced recombinant (*S*)-selective transaminase Cv TA2. Firstly, biotransformations were investigated utilising 4-bromo-acetophenone as a substrate. Reactions at 5 mM substrate concentration went to over 80% conversion in > 99% *e.e.* when using purified protein enzyme preparations. Reactions were scaled up although 4-bromo-acetophenone was insoluble at 10 mM even in the presence of 20% DMSO. Feeding the substrate as an 18 mM solution in DMSO together with shaking in an orbital shaker gave better retention of enzyme activity compared with paddle stirring which denatured the enzyme. A substrate inhibition curve was produced when the solution phase assay (developed in Section 2) was used to screen the transaminase reaction in the

deamination mode. 4-Bromo-1-phenyl-ethylamine causes inhibition of the transaminase at a concentration of 17 mM, therefore when operating in the forward transaminase direction product removal methods need to be employed in order to optimise the biotransformation. Additional work is required to determine whether 4-bromo-acetophenone causes substrate inhibition to the transaminase.

Cascade reactions were investigated using transaminase, GOase and MAO-N enzymes to examine whether the synthesis of chiral amines could be carried out in one pot by addition of multiple enzymes to the reaction flask. Initially GOase/transaminase cascades were investigated and it was observed that the LDH in the transaminase recycle system inactivated GOase. Subsequently, the reaction was carried out in one pot but in two steps. The GOase kinetic resolution went to completion with an *e.e.* of 96%. A solution of transaminase plus recycle system was added to the pot and both (*S*) and (*R*)-1-phenylethylamine was synthesised (utilising Cv TA2 and ATA-117 respectively) in over 70% conversion and > 99% *e.e.*

The transaminase/MAO-N cascade reactions were investigated starting from a series of diketones which were subjected to the (*R*) and (*S*)-selective transaminases, ATA-117 and Cv TA2. 5 mM transaminase reactions proceeded to greater than 80% conversion after 24 hours in > 99% (stereochemistry was inferred based on previous transaminase reactions carried out with both enzymes). The resulting imines, which had a defined stereocentre (either methyl or ethyl substitution) generated by the transaminase, were subjected to ammonia borane reduction to yield two amine diastereomers which could be interconverted by MAO-N. A range of chiral secondary amines, containing two stereogenic centres, were produced in high *d.e.*, the first being either an ethyl or methyl group which could be *R* or *S* depending of the selectivity of the transaminase and the second larger substituent (phenyl or benzyl) assumed to be (*R*) based on a (*S*)-selective MAO-N being used. Large scale transaminase reactions were found to have higher conversions when utilising the alanine dehydrogenase system instead of the LDH/GDH recycle system. The MAO-N reactions were found to be superior to standard chemical reduction techniques and gave the highest *d.e.* values. A one-pot, two-step, reaction was carried using the (*S*)-selective transaminase Cv TA2 and MAO-N resulting in (*2S,5R*)-2-methyl-5-phenylpyrrolidine in 99% *d.e.* after 48h.

Finally the synthesis of 3-methyl-3,4-dihydroisoquinoline was investigated by employing transaminase catalysed amination starting from the diacarbonyl compound,

2-(2-oxopropyl)benzaldehyde. HPLC standards were synthesised chemically and 5 mM reactions were carried out using the (*R*) and (*S*)-selective transaminases. It was noted that cyclisation occurred even without the presence of DMSO, however, over oxidation to the fully aromatic 3-methylisoquinoline was observed after half an hour and after 2 hours only the fully aromatic product could be seen. Addition of the reductant L-ascorbic acid reduced the rate of oxidation and after 1 h both enantiomers of 3-methyl-3,4-dihydroisoquinoline were present in > 99% *e.e.* with minimal 2-methylisoquinoline present. Larger scale biotransformations and product isolation is required to fully characterise the reaction and products.

5. Summary, conclusion and future work

5.1 Summary and conclusion

Cloning and expression in *E.coli* of three transaminase enzymes from *Chromobacterium violaceum* transaminase (Cv TA2), an *Ochrobactrum antropi* transaminase (Oa TA1) and a previously published a *Chromobacterium violaceum* transaminase (Cv TA1) was successfully carried out. These enzymes were characterised using a multi-enzyme solution phase assay also developed during the course of this research.

The purified transaminase Cv TA2 was subjected to the solution phase assay described in Section 2.1, the results were compared to substrate scope obtained for a previously published *C. violaceum* transaminase Cv TA1. Cv TA2 showed higher activity with 4-bromo-1-phenylethylamine but lower activity with (*S*)-1-phenylethylamine when compared to Cv TA1. Interestingly, Cv TA1 was less selective for alanine but also showed activity with some of the (*R*)-enantiomers of the amines screened when utilising L-AAO. Oa TA1 did not show any significant activity to any of the 35 different amines screened even when the keto acceptor pyruvate was exchanged for α -keto glutarate. Dynamic simulations did not reveal any significant differences between the two *C. violaceum* enzymes to identify where the differences in activity originated from.

Finally a commercially available (*R*)-selective transaminase (ATA-117) alongside the (*S*)-selective transaminase identified in this project were used in dual enzyme cascade reactions utilising either a galactose oxidase from *Fusarium* sp. or monoamine oxidase from *Aspergillus niger* to produce a number of primary and secondary amines in high *e.e.*, *d.e.* and conversion.

5.2 Future work

This project has provided an ideal starting point for further research into transaminases for chiral amine synthesis. Firstly, large scale preparative biotransformations for the formation of 3-methylisoquinoline (a pharmaceutical intermediate of interest to industry) should be investigated to see if this process can be achieved at industrially applicable substrate loadings.

However, the main focus for future work should be the development of new transaminase libraries. Dr Simon Willies within the Turner group is currently developing a solid phase screen based on the solution phase assay mentioned in this project. The use of alanine and hence the GDH/LDH recycle system can become problematic at an industrial scale due to costing. A possible solution to this problem would be to replace alanine as the amine donor with isopropylamine, but this would require developing enzymes that tolerate isopropylamine at high concentrations (to help drive the equilibrium to product formation).

The difference in activity of the two *Chromobacterium violaceum* transaminases should be investigated by carrying out the three mutations Gly225Ala, Cys424Ser and Ser425Ala (suggested in Section 2 of this project). Mutations at these positions should be generated both singly and combinatorially to revert Cv TA2 back to the original sequence of Cv TA1 and a comparison of activity of each mutant investigated. Another interesting mutation to perform would be to switch Ala231 for glycine and see if this alters the active site cleft and substrate preference and/or activity. These mutants (alongside the previously published crystal structure) could provide greater insight in to creating a protein variant with increased activity.

Expansion of this project using a high through-put screen will allow rapid development of transaminases that can be utilised on larger compounds, higher substrate loadings with greater stability under industrial process conditions (mimicking the methodology applied to Sitagliptin).

The ideal multistep one pot synthesis using various enzymes for amine production is attractive to a chemist but investigations into product removal techniques (such as resins and the use of biphasic systems) is required to overcome product inhibition of the transaminase enzyme.

6. Experimental

6.1 Materials

6.1.1 Chemicals, reagents and kits.

Commercially available reagents and chemicals were either purchased from Sigma-Aldrich Company Ltd, Acros organics or Fisher Scientific UK Ltd unless otherwise stated. Molecular biology reagents/kits were either purchased from Invitrogen, New England Biolabs, Stratagene or Qiagen.

6.1.2 Enzymes

The three enzymes peroxidase, type VI-A from horseradish (P6782, HRP), D-amino acid oxidase from porcine kidney (A5222, D-AAO) and L-amino acid oxidase from *Crotalusadamanteus* (A9378, L-AAO) were purchased from Sigma-Aldrich Company Ltd. The transaminase enzymes 117 and 113 (ATA), glucose dehydrogenase (GDH) and lactate dehydrogenase (LDH) were supplied free of charge by Codexis.

6.1.3 Strains

The strains of *E. coli* and their genotypes which were used in this research;

Strain	Genotype
BL21 (DE3)	$F^-ompThsdSB(rB^-, mB^-) gal dcm(DE3)$
XL1 Blue	<i>recA1 endA1 gyrA96 thi-1 hsdR17 supE44 relA1 lac</i> [F' <i>proAB lacIqZAM15 Tn10</i> (Tetr)]

Chromobacterium violaceum was purchased from LG standards (ATCC 12472, NCIMB 9178).

Strains were stored at -80 °C.

6.1.4 Plasmids

All genes were initially cloned into the cloning vector Zero Blunt TOPO PCR (Invitrogen part number 45-0245) and then sub-cloned into pET-16b (Novagen 69662-3). All constructs were stored at -20 °C.

6.1.5 Buffer solutions

Phosphate buffer

100 mM phosphate buffer (pH 8) was prepared by dissolving 174.18 g/L of K_2HPO_4 in 100 mL of dH_2O followed by the preparation of 136.09 g/L of KH_2PO_4 in 100 mL of dH_2O . 94.0 mL of K_2HPO_4 and 6.0 mL KH_2PO_4 were diluted with 900 mL of dH_2O .

HEPES

100 mM HEPES buffer was prepared by dissolving 23.83 g/L in 900 mL of dH_2O and the pH adjusted to 8 by the addition of 5 M NaOH. The volume of the solution was made up to 1000 mL with dH_2O .

50 × TAE buffer

TAE buffer consists of 242 g Tris base, 57.1 mL glacial acetic acid and 10 mL 0.5 M EDTA (pH 8.0) diluted with dH_2O to a final volume of 1 L.

TOWBIN buffer

TOWBIN buffer consists of 3 g Tris base, 4.08 g bicine and 100 mL of MeOH which was made to a final volume of 1 L using dH_2O .

Phosphate buffered saline (PBS)

2 g of K_2HPO_4 , 11.3 g of Na_2HPO_4 and 8 g of NaCl were added to 900 mL of dH_2O and the pH adjusted to 7.5. The volume of the solution was made up to 1000 mL with dH_2O .

Binding buffer for purification of His-tagged proteins

The binding buffer was prepared by dissolving 100 mM potassium phosphate, 40 mM imidazole and 300 mM NaCl in 1 L of dH₂O and the pH adjusted to 7.4. The resulting solution was degassed and filtered through a 0.45 µm pore filter.

Elution buffer for purification of His-tagged proteins

The Elution buffer was prepared by dissolving, 68 g of imidazole and 17 g NaCl in 900 mL of 100 mM potassium phosphate buffer and the pH adjusted to 7.4. The resulting solution was diluted to 1000 mL using 100 mM potassium phosphate buffer, degassed and filtered through a 0.45 µm pore filter.

Binding buffer for purification using anion exchange columns

The binding buffer was prepared by dissolving 20mM potassium phosphate and 2 M potassium chloride in 900 mL of dH₂O. The pH was adjusted to 8 and the solution was made to a final volume of 1L using dH₂O.

Elution buffer for purification using anion exchange columns

The elution buffer was prepared by dissolving 20mM potassium phosphate in 900 mL of dH₂O. The pH was adjusted to 8 and the solution was made to a final volume of 1L using dH₂O.

6.1.6 Growth media

LB:

To dH₂O (1 L) 10 g of tryptone, 10 g of NaCl and 5 g of yeast extract was added and stirred till dissolved, then sterilised by autoclaving.

LB Agar:

LB medium with the addition of 15g of bactoagar dissolved in 1 L of dH₂O. The mixture was then sterilised by autoclaving.

Nutrient broth:

To dH₂O (1 L) 13 g of Nutrient broth was added and stirred till dissolved, then sterilised by autoclaving.

Nutrient agar:

Nutrient broth and 15g of bactoagar were dissolved in 1 L of dH₂O. The mixture was then sterilised by autoclaving.

Minimal media:

Media A:

Trace element	Actual Concentration	Stock Concentration (Stock solution 1)
MgSO ₄ .7H ₂ O	1 g/L	10 × (10 g/L)
CaCl ₂	0.2 mM	10 × (2 mM)

Trace element	Actual Concentration	Stock Concentration (Stock solution 2)
ZnSO ₄ .H ₂ O	0.13 mg/L	1000 × (130 mg/L)
MnCl ₂ .4H ₂ O	0.089 mg/L	1000 × (88.7 mg/L)
H ₃ BO ₃ (Boric acid)	0.02 mg/L	1000 × (20 mg/L)
CuSO ₄ .5H ₂ O	0.14 mg/L	1000 × (140 mg/L)
CoCl ₂ .6H ₂ O	0.09 mg/L	1000 × (90 mg/L)
NiSO ₄ .6H ₂ O	0.1 mg/L	1000 × (100 mg/L)
(Na) ₂ MoO ₄	1.90 mg/L	1000 × (1903 mg/L)
FeCl ₃ .6H ₂ O	3.89 mg/L	1000 × (3800 mg/L)

The trace elements were combined to make stock solutions 1 and 2 then Autoclaved. 50 mM potassium phosphate buffer, 50 mM (*S*)- α -MBA, 100 mM glycerol or 100 mM sodium pyruvate or a combination of both (50 mM glycerol and 50 mM sodium pyruvate) were added to the appropriate volumes of stock solutions 1 and 2 and diluted to a litre with dH₂O then pH was then adjusted to 8 with concentrated HCl. The solution was filter sterilised through a 0.22 μ M filter.

Minimal media plates

- Media A
- 1% Agar

6.1.7 Antibiotics

Ampicillin

A 1000× stock solution of ampicillin was made by dissolving 100 mg/mL of ampicillin in dH₂O followed by sterilisation using a 0.22 µm pore filter.

Kanamycin

A 1000× stock solution of kanamycin was made by dissolving 50 mg/mL of kanamycin in dH₂O followed by sterilisation using a 0.22 µm pore filter.

Chloramphenicol

A 1000× stock solution of chloramphenicol was made by dissolving 30 mg/mL of chloramphenicol in EtOH.

Solutions were stored in 1 mL aliquots at -20 °C.

6.1.8 IPTG

0.47 g of IPTG was dissolved in 10 mL dH₂O, followed by sterilisation using a 0.22 µm pore filter creating a stock solution with a final concentration of 200 mM.

6.1.9 Enzyme stocks for solution phase assay

HRP stock: 10 mL of 1 g/L (1550 U/mg) of HRP was prepared in dH₂O.

ATA-117 stock: 10 mL of 5 g/L ATA-117 was prepared in dH₂O which was then diluted to a final stock concentration of 0.6 g/L.

ATA-113 stock: 10 mL of 5 g/L ATA-113 was prepared in dH₂O which was then diluted to a final stock concentration of 0.6 g/L for use in the optimised assay.

D-AAO stock: 10 mL of 60 U D-AAO was prepared in dH₂O.

6.1.10 Sample preparation for colony PCR

To 20 µL of sterile dH₂O suspend one or two colonies from a pure culture. Use 2 µL of the resulting solution as a template for PCR reactions.

6.1.11 DNA and protein gel markers

1 kb DNA Ladder (N3232S) were purchased from New England Biolabs UK and the pre-stained protein ladder plus (SM18115) was purchased from Fermentas.

6.2 Methods

6.2.1 Colourimetric transaminase assay with PGR

Substrate mixture:

0.1 g/L of PGR, 0.2 g/L of sodium pyruvate, and 0.05 g/L of PLP were added to 1 L of 100 mM phosphate buffer pH 8.

Solution 1:

5 mM of amine donor and 50 mL of the substrate mixture was added to a falcon tube and pH adjusted to 8.

Solution 2:

10 μ L of HRP (1 g/L), 20 μ L of D-AAO (30 U) and 100 μ L of the Solution 1.

Solution 3:

10 μ L of HRP (1 g/L), 20 μ L of D-AAO (60 U) and 100 μ L of the Solution 1.

Solution 4:

10 μ L of HRP (1 g/L), 10 μ L of L-AAO (4.2 U) and 100 μ L of the Solution 1.

Standard assay conditions for use with ATA 117:

In a 96-well MTP 100 μ L aliquots of solution 2 was dispensed into individual wells and assays were initiated by the addition of 2.5 μ L of ATA-117 (5 g/L). Experiments were run on a spectrophotometer at 30 °C with a wavelength of 540 nm and absorbance readings taken every 30 seconds.

Optimised assay conditions for use with ATA 117:

In a 96-well MTP 100 μ L aliquots of solution 3 was dispensed into individual wells and assays were initiated by the addition of 2.5 μ L of ATA-117 (0.6 g/L). Experiments were run on a spectrophotometer at 30 °C with a wavelength of 540 nm and absorbance readings taken every 30 seconds.

Optimised assay conditions for use with ATA 113:

In a 96-well MTP 100 μ L aliquots of solution 4 was dispensed into individual wells and assays were initiated by the addition of 2.5 μ L of ATA-113 (0.6 g/L). Experiments were

run on a spectrophotometer at 30 °C with a wavelength of 540 nm and absorbance readings taken every 30 seconds.

6.2.2 Colourimetric transaminase assay with TBHBA 4-AAP

In two separate 1 mL tubes a solution of TBHBA (20 mg/mL in DMSO, Sigma 439533) was made alongside a 1 mL solution of 4-AAP (100 mg/mL in 100mM HEPES buffer pH 8, Sigma 06800).

A stock solution (Stock A) of 15 mM amine donor (10 mL) was made in a 15 mL falcon tube with 100 mM phosphate buffer, the pH was adjusted to 8 after addition of the amine with 1 M HCl.

A stock solution (Stock B) was then made in a 15 mL falcon tube containing 5 mL of 100mM HEPES pH 8.0, 200 μ L of the 20 mg/mL TBHBA solution, 30 μ L of the 100 mg/mL 4-AAP solution, 20U AAO, HRP (1 mg, Sigma P8375) and sodium pyruvate (0.2 mg/mL). Adjust pH to 8 and make to a final volume of 10 mL with 100mM HEPES buffer pH 8.

In a 96 well plate 50 μ L of Stock A was added to each well, 50 μ L Stock B and 50 μ L of purified enzyme solution (concentration 1 mg/mL) to start assay.). Experiments were run on a spectrophotometer at 30 °C with a wavelength of 510 nm and absorbance readings taken every 30 seconds.

6.2.3 Path length determination

The path length of a series of volumes (200 μ L, 132.5 μ L, 122.5 μ L and 100 μ L) was determined in a flat-bottomed 96 well MTP. A FAD solution (18 mM) was prepared in 100 mM phosphate buffer 7.7. Using the Beer-Lambert law $A = \epsilon \times c \times L$ the path length for each volume was experimentally determined.⁷⁵

A = absorbance

ϵ =extinction coefficient ($\text{mM}^{-1}\text{cm}^{-1}$)

c = concentration (mM)

L = path length (cm)

6.2.4 Extinction coefficient of pyrogallol red

A standard curve of PGR was prepared over a concentration range of 3.05×10^{-5} to 1 mM in 100 mM phosphate buffer (pH 8). 100 μ L was placed into 96-well MTP and analysed on a Molecular Devices SpectraMax M2 Photometer over three different wavelengths (540, 550 and 560 nm). The linear range of 540 nm from a standard curve produced was used to calculate the extinction coefficient (gradient is equal to $\epsilon \times L$ according to the Beer-Lambert law). For a 100 μ L solution the path length was previously calculated to be 0.31 cm.

6.2.5 Genomic DNA purification

5 mL of overnight bacterial culture was harvested by centrifuging at $8000 \times g$ for 10 mins. The genomic DNA was extracted and purified using a DNeasy blood and tissue kit from QIAGEN (69504). The procedure provided was followed and the eluted genomic DNA was stored at -20°C .

6.2.6 16S rRNA sequencing PCR recipe

Primer	Sequence
27F	5'-GTGCTGCAGAGAGTTTGATCCTGGCTCAG-3'
1492R	5'-CACGGATCCTACGGGTACCTTGTTACGACTT-3'

PCR Solution	
Solution	Volume (μ L)
Primers (F/R)	2 (100 μ M)
Template	2
Sterile H ₂ O	39
Taq polymerase*	1
dNTP's	1
Buffer (10 \times)	5

* Taq polymerase was purchased from New England Biolabs (M02735).

Cycle	Temperature $^{\circ}$ C	Time	30 cycles
1	94	2 mins	
2	94	15 Sec	
3	60	30 Sec	
4	72	90 Sec	
5	72	10 mins	

PCR product size = 1400 bp

6.2.7 Plasmid DNA purification

5 mL of overnight bacterial culture was harvested by centrifuging at $8000 \times g$ for 10 mins. The plasmid DNA was purified using a QIAGEN DNA mini prep kit (27104). The procedure provided was followed and the eluted plasmid DNA was stored at -20° C.

6.2.8 PCR of *C. violaceum*

The PCR of *C. violaceum* was repeated as described by the John Ward group at UCL⁶³ using the primers below.

Primer	Sequence
CV1-R	5'-CTCGAGCTAAGCCAGCCCGCGCGCCTTCAG-3'
CV1-F	5'-CAT-ATGCAGAAGCAACGTACGACCAGCC-3'

PCR Solution	
Solution	Volume (μ L)
Primers (F/R)	3 (100 μ M)
Template	2
dNTP's*	1
PFU polymerase*	1
Buffer (10 \times)	5
Sterile dH ₂ O	38

*PFU polymerase was purchased from Stratagene (600136-81) and the dNTP's were purchased from Fermentas (R0181).

Cycle	Temperature $^{\circ}$ C	Time	30 cycles
1	95	2 mins	
2	94	15 Sec	
3	62	30 Sec	
4	68	90 Sec	

PCR product size = 1500 bp

6.2.9 PCR of *Ochrobactrum sp* genomic DNA.

<i>Primer</i>	<i>Sequence</i>
XhoI F	5' GCACTCGAGATGCAGTTTATTGATCTTGGAGCGCA 3'
BamH1R	5' TGGTTTTACGGAAGAAGGCCTGAGGATCCACG 3'

PCR Solution	
Solution	Volume (μ L)
Primers (F/R)	3 (100 μ M)
Template	2
dNTP's	1
PFU polymerase	1
Buffer (10 \times)	5
Sterile dH ₂ O	38

Cycle	Temperature $^{\circ}$ C	Time	30 cycles
1	95	2 mins	
2	94	15 Sec	
3	51.4	30 Sec	
4	68	90 Sec	

PCR product size = 1400 bp

6.2.10 Gel extraction

The appropriate bands were extracted from agarose gels and purified using a gel extraction kit from QIAGEN (28604) following the manufactures protocol.

6.2.11 DNA quantification

DNA quantification was carried out using a NanoDrop 1000 spectrophotometer from Thermo Scientific. Measurements were taken following the manufactures protocol using 2 μ L of sample.

6.2.12 Cloning (Zero blunt TOPO)

Cloning of the PCR product was carried out using a ZERO Blunt TOPO PCR cloning kit from Invitrogen (K2830-20) following the manufactures protocol.

6.2.13 Restriction Enzyme digests

All restrictions enzymes were purchased from New England Biolabs and used with the 10 x buffers supplied.

The volumes of each constituent are:

EcoR1 (1 μ L)

5 μ L 10x buffer

1 μ L BSA (if required)

~400ng of DNA

dH₂O to a total volume of 50 μ L.

Restrict at 37 °C for 1 hour.

BamH1 (1 μ L)

Nde1 (1 μ L)

5 μ L 10x buffer

1 μ L BSA (if required)

~400ng of DNA

dH₂O to a total volume of 50 μ L.

Restrict at 37 °C for 1 hour.

Xho1 (1 μ L)

Nde1 (1 μ L)

5 μ L 10x buffer

1 μ L BSA (if required)

~400ng of DNA

dH₂O to a total volume of 50 μ L.

Restrict at 37 °C for 1 hour.

6.2.14 Transformation of *E. coli*

Chemically competent cells, strains BL21 (DE3), BL21 STAR and XL-1 Blue, were transformed according to the manufacturer's protocol.

6.2.15 Expression of PJH2 in BL21 (DE3)

A single colony of BL21 (DE3) transformed with PJH2 was picked and grown overnight in a 5 mL culture. 500 μ L was used to inoculate a 500 mL culture and was grown in a shaking incubator at 37 °C until an OD₆₀₀ of 0.5-0.6 was reached. Protein production was then induced by the addition of 2 mM IPTG. The induced culture was left for 5 hours at 37 °C and the protein then analysed by SDS-PAGE.

6.2.16 Expression of PJH3 in BL21 (DE3)

A single colony of BL21 (DE3) transformed with PJH3 was picked and grown overnight in a 5 mL culture. 500 μ L was used to inoculate a 500 mL culture and was grown in a shaking incubator at 37 °C until an OD₆₀₀ of 0.5-0.6 was reached. Protein production was then induced by the addition of 2 mM IPTG. The induced culture was left overnight at 30 °C and the protein then analysed by SDS-PAGE.

6.2.17 MAO-N transformation and expression

Chemically competent cells, *E. coli* strains C43 (DE3), were transformed according to the manufacturer's protocol. 5 mL of LB medium (containing 100 μ g/mL of ampicillin) was inoculated from a single colony of *E. coli* C43 (DE3) harbouring the [pET16b MAO-N (D(X))] plasmid and the culture was grown to saturation at 30 °C and 120 rpm. This culture was used to inoculate 600 mL of autoinduction medium (4ZY-LAC-SUC; containing 100 μ g/mL of ampicillin) and the new culture was grown at 25 °C and 150 rpm for 72 h. The cells were harvested by centrifugation (8000 rpm, 20 min), resuspended in phosphate buffer (100 mM K-Pi, pH 7.7) and centrifuged again (4000 rpm, 20 min). The cell pellets were stored at -20 °C until use.

6.2.18 GOase expression

A falcon tube containing 5 ml of LB medium, supplemented with ampicillin, was inoculated with a single colony and incubated at 37 °C, 250 rpm until an OD₆₀₀ of 0.6

was reached. Once the OD₆₀₀ was reached the falcon tube was immediately placed on ice. This culture was used to inoculate fresh LB medium (600 ml), supplemented with ampicillin, and incubated overnight at 26 °C. The next day, the culture was transferred into falcon tubes and the cells were harvested by centrifugation at 4000 rpm for 30 min at 4 °C (Eppendorff bench top centrifuge). The supernatant was discarded and the cells were lysed as follows: Initially each pellet was resuspended in 15 ml buffer NaPi 20 mM, NaCl 500 mM, PMSF 1 mM pH 7.4. Fresh lysozyme solution (10 mg/ml) was added to each falcon tube, which was then incubated at 37 °C for 15 min. The cells were lysed by 10 bursts of sonication of 30 sec each. Lysis suspension was centrifuged at 4000 rpm for 30 min at 4 °C and the supernatant was collected (cell free extract). The process was repeated and the two cell free extracts and pellet were stored at 4 °C.

6.2.19 Purification of proteins on anion exchange column

Sample preparation

To the Cell Free Extract obtained from cell lysis add the same volume of binding buffer pH 7.4. Filter the sample through a 0.45 µm filter followed by a 0.22 µm before applying it to the column.

Purification

Protein purification was carried out on a HiTrap Butyl Q FF 1 mL column (GE healthcare 17-5053-01) following the manufactures protocol.

6.2.20 Purification of His-tagged proteins

Sample preparation

To the Cell Free Extract obtained from cell lysis add the same volume of binding buffer pH 7.4. Filter the sample through a 0.45 µm filter followed by a 0.22 µm before applying it to the column.

Purification

Protein purification was carried out on a HisTrap HP 1 mL or 5 mL column (GE healthcare 17-5247-01) following the manufactures protocol.

6.2.21 Chemistry and biotransformations

Starting materials were purchased from Acros and Sigma-Aldrich and used as received. 1,4-Disubstituted ketones were prepared by published procedures by Diego Ghislieri. Solvents were analytical or HPLC grade or were purchased dried over molecular sieves where necessary. Column chromatography was performed on silica gel (Sigma, 220-440 mesh). ^1H and ^{13}C NMR spectra were recorded on a BrukerAvance 400 (400 MHz for ^1H and 100.6 MHz for ^{13}C) in CDCl_3 without additional standard. Chemical shifts are reported in δ values (ppm) and are relative to the standard ($\text{RSi}(\text{CH}_3)_3$, $^{13}\text{C} = 0.0$) or the solvent signal (CHCl_3 , $^1\text{H} = 7.26$; CDCl_3 , $^{13}\text{C} = 77.0$).

GC-MS spectra were recorded on a Hewlett Packard HP 6890 equipped with a HP-1MS column, a HP 5973 Mass Selective Detector and an ATLAS GL FOCUS sampling robot. GC analysis was performed on Agilent 6850 GCs equipped with a GerstelMultipurposesampler MPS2L and the columns indicated for each compound separately. Normal phase HPLC was performed on an Agilent system equipped with a G1379A degasser, G1312A binary pump, a G1329 autosampler unit, a G1315B diode array detector and a G1316A temperature controlled column compartment; column and conditions are indicated for each compound separately.

6.2.22 Biotransformation's for the synthesis of chiral amines

Utilising the LDH/GDH recycle system⁶⁹

The below biotransformation's used the LDH/GDH recycle system unless otherwise stated in the text.

2 × stock solution of the GDH recycling system

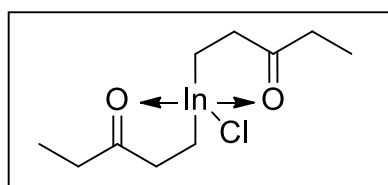
Glucose 20g/L (0.11 mol), NAD^+ 2g/L, PLP 1g/L (4.04 mmol) and L-alanine 90g/L (1.01 mol) were added to a 50mL Falcon tube and 5 mL of 100 mM HEPES buffer was added and the pH of the solution was adjusted to 8. To 500 μL of the resulting solution, 200 μL 25 mM solution of ketone (in DMSO), 200 μL of enzyme solution in 100 mM HEPES buffer and 100 μL of 100 mM HEPES buffer was added to make a final volume of 1 mL, 24 h, 30 °C. The reactions were monitored by GC-MS and, when the enzyme didn't show turnover, stopped by acidification with 1 M HCl. The solution was then centrifuged at 8000 g for 10 minutes and the supernatant extracted with dichloromethane (3 x 5 mL). The aqueous phase was then basified with 10 M NaOH

and extracted with CH_2Cl_2 (3 x 5 mL). The combined organic phases were washed with water (3 x 5 mL), dried over MgSO_4 and concentrated under vacuum.

Using the alanine dehydrogenase system¹⁰²

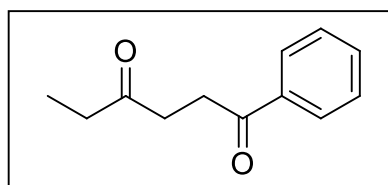
5 mM ketone, ATA-117 (5 g/L in 150 mM ammonium formate) or purified Cv TA2 (5 g/L), 1 mM PLP, 1 mM NAD^+ , 5 equiv D- or L-alanine, 12 U alanine dehydrogenase, 11 U formate dehydrogenase, 150 mM ammonium formate, 24 h, 30 °C. The same work-up was used as in the LDH/GDH system.

Synthesis of racemic intermediates and standards



The indium complex was synthesised following a previous published protocol by Z. Shen *et al.*¹⁰⁸ Under vigorously stirring, to a solution of 1-penten-3-one (1.7 g, 20 mmol) in a mixture 1:1 $\text{CH}_3\text{CN}:\text{H}_2\text{O}$ (100 mL)

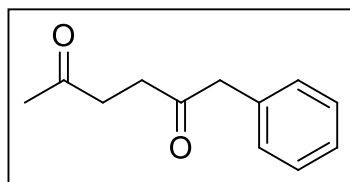
was added indium (1.84 g, 16 mmol) and InCl_3 (1.8 g, 8.0 mmol). After 24 hours, the mixture was extracted with CH_2Cl_2 (3 x 20 mL) and dried over MgSO_4 . The organic phase was then concentrated under vacuum to give 2.85 g of the indium complex in 89% yield.



1-Phenylhexan-1,4-dione 73.

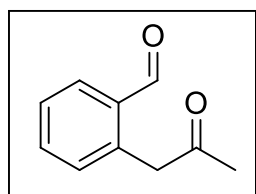
1-Phenylhexan-1,4-dione was synthesised following a previous published protocol by Z. Shen *et al.*¹⁰⁸ Under nitrogen atmosphere, to a solution of indium

homoenolate (960 mg, 3.00 mmol) in anhydrous THF (30 mL) was added benzoyl chloride (700 mg, 5.00 mmol) and $\text{PdCl}_2(\text{PPh}_3)_2$ (180 mg, 0.25 mmol). The reaction mixture was stirred at reflux for 6 hours. Solvent was removed under vacuum and the residue was purified by silica gel column chromatography using Cyclohexane/EtOAc 9:1 as eluent giving 1-phenylhexane-1,4-dione in 84% isolated yield (0.079 g, 4.200 mmol). ^1H NMR (400 MHz, CDCl_3): δ 8.03-7.99 (m, 2H, Ar), 7.61-7.55 (m, 1H, Ar), 7.51-7.45 (m, 2H, Ar), 3.32 (t, $J = 6.3$ Hz, CH_2), 2.88 (t, $J = 6.3$ Hz, CH_2), 2.59 (q, $J = 7.3$ Hz, CH_2), 1.12 (t, $J = 7.3$ Hz, CH_3). ^{13}C NMR (100 MHz, CDCl_3): δ ppm 210.2, 198.8, 136.6, 133.3, 128.6, 128.1, 36.0, 35.8, 32.5, 7.9.

**1-Phenylhexan-2,5-dione 74.**

1-Phenylhexan-2,5-dione was synthesised following a previous published protocol by H. Stetter *et al.*¹⁰⁹ Under nitrogen atmosphere, to a solution of phenylpyruvic acid (1.0 g, 6.1 mmol) in EtOH (10 mL) was added triethylamine (1.2 mL, 9.7 mmol), 1-buten-3-one (0.7 mL, 9.1 mmol) and 3-benzyl-5-(2-hydroxyethyl)-4-methylthiazolium chloride (165 mg, 0.61 mmol). The mixture was stirred at reflux for 4 hours. The solvent was removed under vacuum, then CH₂Cl₂ (50 mL) was added and the organic phase washed with 10% H₂SO₄ (2 x 50 mL). Solvent was removed under vacuum to give 980 mg of crude 1-phenylhexane-2,5-dione in 85% isolated yield.

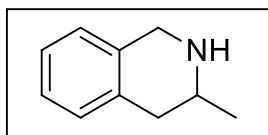
¹H NMR (400 MHz, CDCl₃): δ 7.35-7.27 (m, 3H, Ar), 7.21-7.18 (m, 2H, Ar), 3.75 (s, CH₂), 2.75-2.66 (m, 4H, CH₂, CH₂), 2.17 (s, CH₃). ¹³C NMR (100 MHz, CDCl₃): δ 207.2, 207.0, 134.2, 129.5, 128.7, 127.0, 50.1, 37.0, 35.5, 29.9.

**2-(2-Oxopropyl)benzaldehyde 75.**¹⁰⁵

Powdered m-CPBA (2.0 g, 9.0 mmol, 77%, 1.2 eq) was added to a stirred heterogeneous mixture of aqueous NaHCO₃ (150 mL, 0.30 M) and 2-methylindene (1.0 mL, 7.5 mmol) on ice over 15 minutes. The suspension was vigorously stirred at room temperature overnight and then extracted with diethyl ether (3 x 100 mL). The organic phase was washed with brine (10 mL), dried over MgSO₄ and concentrated under vacuum. Flash chromatography using petroleum ether/EtOAc 1:10 as eluent afforded 350 mg of 2-methylindene oxide in 32% yield as colourless oil. ¹H NMR (400 MHz, CDCl₃): δ 7.54 (d, *J* = 7.2, 1H, Ar), 7.32-7.19 (m, 3H, Ar), 4.09 (s, 1H, CH), 3.21 (d, *J* = 17.7 Hz, CH), 2.95 (d, *J* = 17.7 Hz, CH), 1.75 (s, CH₃). ¹³C-NMR (100 MHz, CDCl₃): 34.6, 57.6, 59.1, 125.1, 126.0, 126.2, 128.5, 140.8, 143.5.

A solution of the 2-methylindene oxide (294 mg, 2.0 mmol) and ammonium ceric nitrate (983 mg, 2.1 mmol) in a mixture 3:1 CH₃CN/H₂O (150 mL) was stirred overnight at room temperature. The solution was diluted with water (200 mL) and extracted with CHCl₃ (3 x 150 mL). The organic phase was dried over MgSO₄ and concentrated under vacuum. Flash chromatography using petroleum ether/EtOAc 2:1 as eluent afforded 160 mg of pure dicarbonyl compound 2-(2-oxo-propyl)-benzaldehyde in 41% yield as yellow oil. ¹H NMR (400 MHz, CDCl₃): δ 10.01 (s, CH), 7.82 (dd, *J* =

7.4, 1.6 Hz, 1H, Ar), 7.60-7.47 (m, 2H, Ar), 7.22 (m, br, 1H, Ar), 4.13 (s, CH₂), 2.33 (s, CH₃).

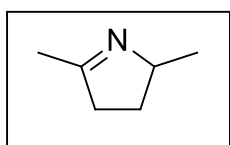


3-Methyl-1,2,3,4-tetrahydroisoquinoline 71.¹⁰⁵

3-Methylisoquinoline (28 mg, 0.2 mmol) was dissolved in ethanol (1 mL). Aqueous saturated ammonium chloride (300 μ L) and indium powder (Avocado Research Chemicals Ltd, L18757.06) (200 mg) were added to the mixture. The mixture was stirred in a microwave tube and heated to 160 °C for 1 hour (microwave irradiation, 300 W, 2 min ramp time). The solution was cooled to room temperature and water (5 mL) was added. The pH was then adjusted to 9 and the mixture was filtered through a celite plug. The aqueous layer was extracted with CH₂Cl₂ (3 x 20 mL). The combined organics phases were dried over MgSO₄ and concentrated under vacuum to give 17 mg of 3-methyl-1,2,3,4-tetrahydroisoquinoline in 60% yield as yellow oil. ¹H NMR (400 MHz, CDCl₃): δ 7.07 (m, 6H, Ar), 4.09 (q, J = 1.9 Hz, CH₂), 3.10 – 2.96 (m, 1H, CH), 2.79 (dd, J = 16.4, 3.6 Hz, CH), 2.53 (dd, J = 16.3, 10.7 Hz, CH), 1.91 (broad s, NH), 1.26 (d, J = 6.3 Hz, CH₃). ¹³C NMR (100 MHz, CDCl₃): δ 135.3, 134.9, 129.2, 126.2, 126.2, 125.9, 49.4, 48.6, 37.3, 22.5.

HPLC: Chiralpack IC 6.4 mm x 250 mm x 5 μ m, 90:10 (hexane/propan-2-ol)

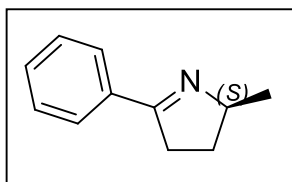
1 mL/min, 3-methylisoquinoline 8.89 mins, racemic amine 6.63 min and 8.0 min.



2,5-Dimethyl-3,4-dihydro-2H-pyrrole 61.

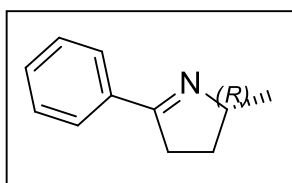
2,5-Hexanedione (1.1 mL, 9.7 mmol) was dissolved in DMSO (25 mL) was added to a solution containing Cv TA2 and the GDH recycling system (100 mL). The reaction was stopped after 72 hours. 221 mg of compound were obtained as yellow oil in 27% yield. ¹H NMR (400 MHz, CDCl₃): δ 4.06-3.92 (m, CH), 2.58-2.37 (m, CH₂), 2.14-2.03 (m, CH), 2.00 (s, CH₃), 1.37 (m, CH), 1.23 (d, J = 6.8 Hz, CH₃).

GC-MS EI (m/z): 97, imine 2.69 min, diketone MS EI (m/z) 114, 4.27 min.

**(S)-2-Methyl-5-phenyl-3,4-dihydro-2H-pyrrole 63.**

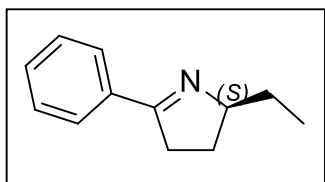
1-Phenylpentane-1,4-dione (1.2 g, 6.7 mmol) was dissolved in DMSO (25 mL) and added to a solution containing CvTA2 and the GDH recycling system (100 mL). The reaction was stopped after 72 hours. 262 mg of 2-methyl-5-phenyl-3,4-dihydro-2H-pyrrole were obtained as yellow oil in 21% yield. ^1H NMR (400 MHz, CDCl_3): δ 7.89-7.84 (m, 2H, Ar), 7.48-7.39 (m, 3H, Ar), 4.48-4.26 (m, CH), 3.09 (m, CH), 2.92 (m, CH), 2.28 (m, CH), 1.59 (m, CH), 1.39 (d, $J = 7.2$ Hz, CH_3). ^{13}C NMR (100 MHz, CDCl_3): δ 172.0, 134.5, 130.4, 128.4, 127.7, 68.3, 35.2, 29.5, 22.1. $[\alpha]_{24}^{\text{D}} - 110$ ($c = 2.0$, CHCl_3). NMR data was in good correlation of previously published data.¹¹⁰

GC-MS EI (m/z): 159, imine 7.42 mins, diketone MS EI (m/z) 176, 8.9 mins.

**(R)-2-Methyl-5-phenyl-3,4-dihydro-2H-pyrrole 63.**

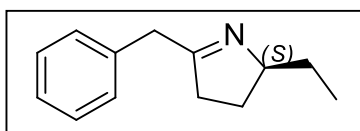
1-Phenylpentane-1,4-dione (1.2 g, 25 mmol) was dissolved in DMSO (6 mL) and added to a solution containing ATA-117 and the GDH recycling system (24 mL). The reaction was stopped after 72 hours. 262 mg of 2-methyl-5-phenyl-3,4-dihydro-2H-pyrrole were obtained as yellow oil in 21% yield. ^1H NMR (400 MHz, CDCl_3): δ 7.89-7.84 (m, 2H, Ar), 7.48-7.39 (m, 3H, Ar), 4.48-4.26 (m, CH), 3.09 (m, CH), 2.92 (m, CH), 2.28 (m, CH), 1.59 (m, CH), 1.39 (d, $J = 7.2$ Hz, CH_3). ^{13}C NMR (100 MHz, CDCl_3): δ 172.0, 134.5, 130.4, 128.4, 127.7, 68.3, 35.2, 29.5, 22.1. $[\alpha]_{24}^{\text{D}} + 106$ ($c = 1.5$, CHCl_3). NMR data was in good correlation of previously published data.¹¹⁰

GC-MS EI (m/z): 159, imine 7.42 mins, diketone MS EI (m/z) 176, 8.9 mins.

**(S)-2-Ethyl-5-phenyl-3,4-dihydro-2H-pyrrole 76.**

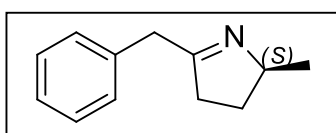
1-Phenylhexane-1,4-dione (10 mg, 0.1 mmol) was dissolved in DMSO (400 μ L) and added to a solution containing Cv TA2 and the GDH recycling system (1.6 mL). The reaction was stopped after 24 hours. ^1H NMR (400 MHz, CDCl_3): δ 7.87-7.83 (m, 2H, Ar), 7.43-7.37 (m, 3H, Ar), 4.18-4.09 (m, CH), 3.07-2.97 (m, CH), 2.94-2.84 (m, CH), 2.24-2.15 (m, CH), 1.93-1.83 (m, CH), 1.67-1.50 (m, CH_2), 1.04-1.00 (t, $J = 8$ Hz, CH_3). ^{13}C NMR (100 MHz, CDCl_3): δ 172.0, 134.4, 130.9, 129.0, 128.1, 74.5, 35.0, 29.9, 28.3, 11.4. $[\alpha]_{24}^{\text{D}}$ - 67.59 ($c = 2.0$, CHCl_3). NMRs were in good correlation to published data.¹¹¹

GC-MS EI (m/z): 173, imine 8.69 mins, diketone MS EI (m/z) 113, 10.04 mins.

**(S)-5-Benzyl-2-ethyl-3,4-dihydro-2H-pyrrole 77.**

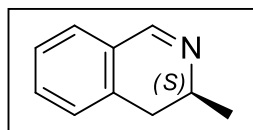
1-Phenylheptane-2,5-dione (10 mg, 0.1 mmol) was dissolved in DMSO (400 μ L) and added to a solution containing Cv TA2 and the GDH recycling system (1.6 mL). The reaction was stopped after 24 hours.

GC-MS EI (m/z): 187, imine 8.86 mins, diketone MS EI (m/z) 161, 9.80 mins.

**(S)-5-Benzyl-2-methyl-3,4-dihydro-2H-pyrrole 66.**

1-phenylhexane-2,5-dione (500 mg, 2.63 mmol) was dissolved in DMSO (25 mL) and added to a solution containing Cv TA2 and the GDH recycling system (100 mL). The reaction was stopped after 72 hours. 291 mg of compound 5-benzyl-2-methyl-3,4-dihydro-2H-pyrrole was obtained as yellow oil in 64% yield. $[\alpha]_{24}^{\text{D}}$ - 27.6 ($c = 2.0$, CHCl_3).

GC-MS EI (m/z): 173.2, imine 7.96 mins, diketone MS EI (m/z) 172.1, 9.67 mins

**(S)-3-Methyl-3,4-dihydroisoquinoline 67.**¹⁰⁵

2-(2-oxopropyl)benzaldehyde (150 mg, 0.93 mmol) was dissolved in DMSO (25 mL) and added to a solution containing Cv TA2, 5 mM L-ascorbic acid (Sigma A5960) and the GDH recycling system (50 mL). The reaction was stopped after 72 hours. 102 mg of 3-methyl-3,4-dihydroisoquinoline were obtained as yellow oil in 76% yield. ¹H NMR (400MHz, CDCl₃): δ 8.33 (s, 1H, CH), 7.40-7.32 (m, 1H, Ar), 7.29 (m, 1H, Ar), 7.20-7.12 (m, 2H, Ar), 3.81-3.63 (m, CH), 2.81 (dd, *J* = 16.3 Hz, CH), 2.62-2.49 (m, CH), 1.41 (d, *J* = 20 Hz, CH₃). ¹³C NMR (100 MHz, CDCl₃) δ ppm, 135.3, 134.9, 129.2, 126.21, 126.2, 125.9, 49.4, 48.6, 37.3, 22.6.

GC-MS EI (m/z): 143.1, imine 7.78 mins

HPLC: Chiralpack IC 6.4 mm x 250 mm x 5 μm, 90:10 (hexane/propan-2-ol)

1 mL/min, racemic imine 9.40 mins and 9.73 mins.

6.2.23 MAO-N stereoselective conversion general procedure

In a 2 mL Eppendorf tube, the 2-5 disubstitutedpyrrolines (4.5 μL of 1 M solution in DMF), NH₃BH₃ (18 μL of 1 M solution in 1 M KPO₄-buffer, pH = 7.8) and cell pellet of MAO-N D9 or D11 from *E. coli* cultures (280 μL of a solution 100 mg/mL in 1 M KPO₄-buffer, pH = 7.8) were mixed. If necessary, the pH of the solution was adjusted to 7.8 by addition of HCl. The tube was placed in a shaking incubator and shaken at 37 °C and 250 rpm. In total 5 reactions were set up for each pyrroline. The reaction was monitored by GC taking a reaction and working it up every 1, 3, 6, 24 and 48 hours. GC samples were prepared as follows: aqueous NaOH solution (10 μL, 10 M) was added to the reaction mixture in the Eppendorf tube, followed by 1 mL of CH₂Cl₂. After vigorous mixing, by means of a vortex mixer, the sample was centrifuged at 13200 rpm for 1 minute. The organic phase was separated, dried with MgSO₄ and analysed by GC.

7. References

1. Straathof, A. J., Panke, S. & Schmid, A. The production of fine chemicals by biotransformation. *Current opinion in biotechnology* **13**, 548–556 (2002).
2. Yazbeck, D. R., Martinez, C. a., Hu, S. & Tao, J. Challenges in the development of an efficient enzymatic process in the pharmaceutical industry. *Tetrahedron: Asymmetry* **15**, 2757–2763 (2004).
3. Akhurst, R. J. Taking thalidomide out of rehab. *Nature Medicine* **16**, 370–372 (2010).
4. Food and drug Administration. *FDA's policy statement for the new development of new stereoisomeric drugs*. 57 Fed.Reg. 22 249 (1992).
5. Facultatis, A. & Universitatis, P. The Chiral Switch : The Development of Single Enantiomer Drugs. *Acta Facultatis Pharmaceuticae Universitatis Comenianae* 7–23 (2003).
6. McConathy, J. & Owens, M. J. Stereochemistry in Drug Action. *Primary care companion to the Journal of clinical psychiatry* **5**, 70–73 (2003).
7. Pollard, D. J. & Woodley, J. M. Biocatalysis for pharmaceutical intermediates: the future is now. *Trends in biotechnology* **25**, 66–73 (2007).
8. Woodley, J. M. New opportunities for biocatalysis: making pharmaceutical processes greener. *Trends in biotechnology* **26**, 321–7 (2008).
9. Villain, G. & Gaset, A. A Regioselective Hydration of Acrylonitrile to Give Acrylamide Catalysed by (Pd(OH)₂(bipyridine)(H₂O)). *Tetrahedron Letters* **21**, 2901 – 2904 (1980).
10. Patel, R. N. Biocatalysis : Synthesis of chiral intermediates for drugs. *Current opinion in drug discovery and development* 741–764 (2006).
11. Rasor, J. P. & Voss, E. Enzyme-catalyzed processes in pharmaceutical industry. *Drug Discovery Today* **221**, 145–158 (2001).
12. Turner, N. J. Directed evolution drives the next generation of biocatalysts. *Nature chemical biology* **5**, 567–73 (2009).
13. Turner, N. Directed evolution of enzymes for applied biocatalysis. *Trends in Biotechnology* **21**, 474–478 (2003).
14. Whittall, John and Sutton, P. W. *Practical methods for Biocatalysis and Biotransformations*. (John Wiley and sons Ltd: 2010).doi:978-0-470-51927-1
15. Ward, R. S. Dynamic Kinetic Resolution. *Tetrahedron: Asymmetry* **6**, 1475–1490 (1995).

16. Schnell, B., Faber, K. & Kroutil, W. Enzymatic Racemisation and its Application to Synthetic Biotransformations. *Advanced Synthesis & Catalysis* **345**, 653–666 (2003).
17. Hasan, F., Shah, A. A. & Hameed, A. Industrial applications of microbial lipases. *Enzyme and Microbial Technology* **39**, 235–251 (2006).
18. Maurer, K.-H. Detergent proteases. *Current opinion in biotechnology* **15**, 330–4 (2004).
19. Panda, T. & Gowrishankar, B. S. Production and applications of esterases. *Applied microbiology and biotechnology* **67**, 160–9 (2005).
20. Turner, N. J. & Carr, R. Biocatalysis in the pharmaceutical and biotechnology industries. 743–755 (2007).
21. Rajan, S. Dr Reddy's Laboratoires Ltd. (2011).
<http://www.drreddys.com/media/popups/sep22_2011.html>
22. Breuer, M. *et al.* Industrial methods for the production of optically active intermediates. *Angewandte Chemie (International ed. in English)* **43**, 788–824 (2004).
23. Nugent, T. C. & El-Shazly, M. Chiral Amine Synthesis - Recent Developments and Trends for Enamide Reduction, Reductive Amination, and Imine Reduction. *Advanced Synthesis & Catalysis* **352**, 753–819 (2010).
24. Truppo, Matthew D and Turner, N. J. Biocatalytic Routes to Nonracemic Chiral Amines. *Chiral Amine Synthesis* 431–459 (2010).
25. Klibanov, A. M. Asymmetric transformations catalyzed by enzymes in organic solvents. *Ace. Chem. Res.* **23**, 114–120 (1990).
26. Chen, C. & Sih, C. J. General Aspects and Optimization of Enantioselective Biocatalysis in Organic Solvents : The Use of Lipases New Synthetic. *Angew. Chem. Inr. Ed. Engl* **28**, 695–707 (1989).
27. Kitaguchi, H., Fitzpatrick, P. A., Huber, J. E. & Klibanov, A. M. Enzymatic resolution of racemic amines: Crucial role of solvent. *American Chemical Society* 3094–3095 (1989).
28. Shin, J.-S. & Kim, B.-G. Kinetic Modeling of omega-Transamination for Enzymatic Kinetic Resolution of α -Methylbenzylamine. *Biotechnology and bioengineering* **60**, 534–541 (1998).
29. Shin, J. S. & Kim, B. G. Kinetic resolution of alpha-methylbenzylamine with omicron-transaminase screened from soil microorganisms: application of a biphasic system to overcome product inhibition. *Biotechnology and bioengineering* **55**, 348–58 (1997).

30. Shin, J. S., Kim, B. G., Liese, a & Wandrey, C. Kinetic resolution of chiral amines with omega-transaminase using an enzyme-membrane reactor. *Biotechnology and bioengineering* **73**, 179–87 (2001).
31. Truppo, M. D., Turner, N. J. & Rozzell, J. D. Efficient kinetic resolution of racemic amines using a transaminase in combination with an amino acid oxidase. *Chemical communications (Cambridge, England)* 2127–9 (2009).doi:10.1039/b902995h
32. Reetz, M. T. & Schimossek, K. Lipase-Catalyzed Dynamic Kinetic Resolution of Chiral Amines: Use of Palladium as the Racemization Catalyst. *Chimia* **50**, 668–669 (1996).
33. Parvulescu, A., De Vos, D. & Jacobs, P. Efficient dynamic kinetic resolution of secondary amines with Pd on alkaline earth salts and a lipase. *Chemical communications* 5307–9 (2005).doi:10.1039/b509747a
34. Kim, M.-J., Kim, W.-H., Han, K., Choi, Y. K. & Park, J. Dynamic kinetic resolution of primary amines with a recyclable Pd nanocatalyst for racemization. *Organic letters* **9**, 1157–9 (2007).
35. Kim, Y., Park, J. & Kim, M.-J. Fast racemization and dynamic kinetic resolution of primary benzyl amines. *Tetrahedron Letters* **51**, 5581–5584 (2010).
36. Samec, J. S. M., Hermanns, N., Ba, J. & Alida, H. E. An efficient and mild ruthenium-catalyzed racemization of amines : application to the synthesis of enantiomerically pure amines. *Tetrahedron Letters* **43**, 4699–4702 (2002).
37. Paetzold, J. & Bäckvall, J. E. Chemoenzymatic Dynamic Kinetic Resolution of Primary Amines. *Journal of the American Chemical Society* **127**, 17620 (2005).
38. Hoben, C. E., Kanupp, L. & Bäckvall, J.-E. Practical chemoenzymatic dynamic kinetic resolution of primary amines via transfer of a readily removable benzyloxycarbonyl group. *Tetrahedron Letters* **49**, 977–979 (2008).
39. Kim, Y., Park, J. & Kim, M.-J. Dynamic Kinetic Resolution of Amines and Amino Acids by Enzyme-Metal Cocatalysis. *ChemCatChem* **3**, 271–277 (2011).
40. Parvulescu, A. N., Jacobs, P. A. & De Vos, D. E. Heterogeneous Raney Nickel and Cobalt Catalysts for Racemization and Dynamic Kinetic Resolution of Amines. *Advanced Synthesis & Catalysis* **350**, 113–121 (2008).
41. Poulhès, F., Vanthuylne, N., Bertrand, M. P., Gastaldi, S. & Gil, G. Chemoenzymatic dynamic kinetic resolution of primary amines catalyzed by CAL-B at 38–40 °C. *The Journal of organic chemistry* **76**, 7281–6 (2011).
42. Koszelewski, D., Grischek, B., Glueck, S. M., Kroutil, W. & Faber, K. Enzymatic racemization of amines catalyzed by enantiocomplementary ω -transaminases. *Chemistry (Weinheiman der Bergstrasse, Germany)* **17**, 378–83 (2011).

43. Martínez-Rodríguez, S., Martínez-Gómez, A. I., Rodríguez-Vico, F., Clemente-Jiménez, J. M. & Las Heras-Vázquez, F. J. Carbamoylases: characteristics and applications in biotechnological processes. *Applied microbiology and biotechnology* **85**, 441–58 (2010).
44. Lerch K, S. B. Cloning, sequencing and heterologous expression of the monoamine oxidase gene from *Aspergillus niger*. *Mol. Gen. Genet.* **247**, 430–438 (1995).
45. Schilling, B. & Lerch, K. Amine oxidases from *Aspergillus niger*: identification of a novel flavin-dependent enzyme. *Biochimica et Biophysica Acta* **1243**, 529–37 (1995).
46. Alexeeva, M., Enright, A., Dawson, M. J., Mahmoudian, M. & Turner, N. J. Deracemization of alpha-methylbenzylamine using an enzyme obtained by in vitro evolution. *Angewandte Chemie (International ed. in English)* **41**, 3177–80 (2002).
47. Atkin, K. E. *et al.* The structure of monoamine oxidase from *Aspergillus niger* provides a molecular context for improvements in activity obtained by directed evolution. *Journal of molecular biology* **384**, 1218–31 (2008).
48. Carr, R. *et al.* Directed evolution of an amine oxidase for the preparative deracemisation of cyclic secondary amines. *ChemBioChem* **6**, 637–9 (2005).
49. Köhler, V. *et al.* Enantioselective biocatalytic oxidative desymmetrization of substituted pyrrolidines. *Angewandte Chemie* **49**, 2182–4 (2010).
50. Koszelewski, D., Pressnitz, D., Clay, D. & Kroutil, W. Deracemization of mexiletine biocatalyzed by omega-transaminases. *Organic letters* **11**, 4810–2 (2009).
51. Kim, K. Purification and Properties of a amine alpha-ketoglutarate Transaminase from *Escherichia coli*. *Journal of Biological Chemistry* **239**, 2–5 (1964).
52. Stirling, D. I., Zeitlin, A., Matcham, G. & Rozzell, J. D. Enantiomeric enrichment and stereoselective synthesis of chiral amines. (1992).
53. Stirling, D. I., Zeitlin, A. & Matcham, G. Enantiomeric enrichment and stereoselective synthesis of chiral amines. (1990).
54. Stirling, D. I., Matcham, G. & Zeitlin, A. Enantiomeric enrichment and stereoselective synthesis of chiral amines. (1992).
55. Savile, C. K. *et al.* Biocatalytic asymmetric synthesis of chiral amines from ketones applied to sitagliptin manufacture. *Science* **329**, 305–9 (2010).
56. Christen, P. & Metzler, D. E. *Transaminases*. (John Wiley & sons: New York, 1985).
57. Jansonius, J. N. Structure, evolution and action of vitamin Bs-dependent enzymes Johan N Jansonius. *Current Opinion in Structural Biology* 759–769 (1998).

58. Hayashi, H., Mizuguchi, H. & Kagamiyama, H. The imine-pyridine torsion of the pyridoxal 5'-phosphate Schiff base of aspartate aminotransferase lowers its pKa in the unliganded enzyme and is crucial for the successive increase in the pKa during catalysis. *Biochemistry* **37**, 15076–85 (1998).
59. Humble, M. S. *et al.* Crystal structures of the *Chromobacterium violaceum* ω -transaminase reveal major structural rearrangements upon binding of coenzyme PLP. *The FEBS journal* **279**, 779–92 (2012).
60. Shin, J.-S. & Kim, B.-G. Exploring the active site of amine:pyruvate aminotransferase on the basis of the substrate structure-reactivity relationship: how the enzyme controls substrate specificity and stereoselectivity. *The Journal of organic chemistry* **67**, 2848–53 (2002).
61. Haring, D., Kuang, H., Qi, D. & Distefano, M. D. Converting a fatty acid binding protein to an artificial transaminase : novel catalysts by chemical and genetic modification of a protein cavity. *Journal of Molecular Catalysis* 5–8 (2001).
62. Häring, D., Lees, M. R., Banaszak, L. J. & Distefano, M. D. Exploring routes to stabilize a cationic pyridoxamine in an artificial transaminase: site-directed mutagenesis versus synthetic cofactors. *Protein Engineering* **15**, 603–10 (2002).
63. Karpeisky, M. Y. & Ivanov, V. I. A molecular mechanism for enzymatic transamination. *Nature* **210**, 493–496 (1966).
64. Kirsch, J. F. *et al.* Mechanism of action of aspartate aminotransferase proposed on the basis of its spatial structure. *Journal of Molecular Biology* **174**, 497–525 (1984).
65. Koszelewski, D., Lavandera, I., Clay, D., Rozzell, D. & Kroutil, W. Asymmetric Synthesis of Optically Pure Pharmacologically Relevant Amines Employing ω -Transaminases. *Advanced Synthesis & Catalysis* **350**, 2761–2766 (2008).
66. Nestl, B. M., Nebel, B. a & Hauer, B. Recent progress in industrial biocatalysis. *Current Opinion in Chemical Biology* **15**, 187–93 (2011).
67. Tufvesson, P. *et al.* Process considerations for the asymmetric synthesis of chiral amines using transaminases. *Biotechnology and Bioengineering* **108**, 1479–93 (2011).
68. John, W. & Peter, S. *Practical Methods for Biocatalysis and Biotransformations* 2. (Wiley: 2012).
69. Truppo, M. D., Rozzell, J. D., Moore, J. C. & Turner, N. J. Rapid screening and scale-up of transaminase catalysed reactions. *Organic & Biomolecular Chemistry* **7**, 395–8 (2009).
70. Truppo, M. D., Rozzell, J. D. & Turner, N. J. Efficient Production of Enantiomerically Pure Chiral Amines at Concentrations of 50 g / L Using Transaminases Abstract : *Organic Process Research & Development* **14**, 234–237 (2010).

71. Li, T., Kootstra, A. B. & Fotheringham, I. G. Nonproteinogenic α -Amino Acid Preparation Using Equilibrium Shifted Transamination Abstract : *Amino Acids* 533–538 (2002).
72. Höhne, M., Kühl, S., Robins, K. & Bornscheuer, U. T. Efficient asymmetric synthesis of chiral amines by combining transaminase and pyruvate decarboxylase. *ChemBioChem* **9**, 363–5 (2008).
73. Hwang, B. High-throughput screening method for the identification of active and enantioselective ω -transaminases. *Enzyme and Microbial Technology* **34**, 429–436 (2004).
74. Schätzle, S., Höhne, M., Redestad, E., Robins, K. & Bornscheuer, U. T. Rapid and sensitive kinetic assay for characterization of omega-transaminases. *Analytical chemistry* **81**, 8244–8 (2009).
75. Schätzle, S., Höhne, M., Robins, K. & Bornscheuer, U. T. Conductometric method for the rapid characterization of the substrate specificity of amine-transaminases. *Analytical chemistry* **82**, 2082–6 (2010).
76. Sehl, T. *et al.* TTC-based screening assay for ω -transaminases: A rapid method to detect reduction of 2-hydroxy ketones. *Journal of Biotechnology* **159**, 188–194 (2012).
77. Fotheringham, I. G. & Oswald, N. Method to increase the yield and improve purification of products from transaminase reactions. (2007).at <<http://www.freshpatents.com/Method-to-increase-the-yield-and-improve-purification-of-products-from-transaminase-reactions-dt20080904ptan20080213845.php?type=description>>
78. Leng, Y., Zheng, P. & Sun, Z.-H. Continuous production of l-phenylalanine from phenylpyruvic acid and l-aspartic acid by immobilized recombinant Escherichia coli SW0209-52. *Process Biochemistry* **41**, 1669–1672 (2006).
79. Meiwes, J., Schudok, M. & Kretzschmar, G. Asymmetric synthesis of l-thienylalanines. *Tetrahedron: Asymmetry* **8**, 527–536 (1997).
80. Cho, B.-K., Cho, H. J., Park, S.-H., Yun, H. & Kim, B.-G. Simultaneous synthesis of enantiomerically pure (S)-amino acids and (R)-amines using coupled transaminase reactions. *Biotechnology and Bioengineering* **81**, 783–9 (2003).
81. Seebach, D., Gardiner, J. & Zu, C.- Beta-Peptidic Peptidomimetics. *Accounts of chemical research* **41**, (2008).
82. Cheng, R. P., Gellman, S. H. & DeGrado, W. F. Beta-Peptides: From structure to function. *Chemical reviews* **101**, 3219–32 (2001).
83. Kim, J. *et al.* Cloning and Characterization of a Novel Transaminase from Mesorhizobium sp . Strain LUK : a New Biocatalyst for the Synthesis of Enantiomerically Pure Amino Acids. *Society* **73**, 1772–1782 (2007).

84. Escalettes, F. & Turner, N. J. Directed evolution of galactose oxidase: generation of enantioselective secondary alcohol oxidases. *Chembiochem : a European journal of chemical biology* **9**, 857–60 (2008).
85. Truppo, M. D. Rapid Screening and Process Development of Biocatalytic Reactions. *Reactions* (2009).
86. Kaulmann, U., Smithies, K., Smith, M., Hailes, H. & Ward, J. Substrate spectrum of ω -transaminase from *Chromobacterium violaceum* DSM30191 and its potential for biocatalysis. *Enzyme and Microbial Technology* **41**, 628–637 (2007).
87. Rowles, I. Development of Novel Ammonia-Lyase Biocatalysts for the Production of Unnatural Amino Acids for Industry. (2009).
88. Ismail, H., Lau, R. M., van Rantwijk, F. & Sheldon, R. A. Fully Enzymatic Resolution of Chiral Amines: Acylation and Deacylation in the Presence of *Candida antarctica* Lipase B. *Advanced Synthesis & Catalysis* **350**, 1511–1516 (2008).
89. Shin, J.-S., Yun, H., Jang, J.-W., Park, I. & Kim, B.-G. Purification, characterization, and molecular cloning of a novel amine:pyruvate transaminase from *Vibrio fluvialis* JS17. *Applied Microbiology and Biotechnology* **61**, 463–71 (2003).
90. Yun, H., Lim, S., Cho, B. & Kim, B. ω -Amino Acid : Pyruvate Transaminase from *Alcaligenes denitrificans* Y2k-2 : a New Catalyst for Kinetic Resolution of β -Amino Acids and Amines. *Applied and Environmental Microbiology* **70**, 2529–2534 (2004).
91. Iwasaki, a, Yamada, Y., Kizaki, N., Ikenaka, Y. & Hasegawa, J. Microbial synthesis of chiral amines by (R)-specific transamination with *Arthrobacter* sp. KNK168. *Applied Microbiology and Biotechnology* **69**, 499–505 (2006).
92. Ito, N., Kawano, S., Hasegawa, J. & Yasohara, Y. Purification and Characterization of a Novel (S)-Enantioselective Transaminase from *Pseudomonas fluorescens* KNK08-18 for the Synthesis of Optically Active Amines. *Bioscience, Biotechnology, and Biochemistry* **75**, 2093–2098 (2011).
93. Hanson, R. L. *et al.* Preparation of (R)-Amines from Racemic Amines with an (S)-Amine Transaminase from *Bacillus megaterium*. *Advanced Synthesis & Catalysis* **350**, 1367–1375 (2008).
94. Sayer, C., Isupov, M. N. & Littlechild, J. a Crystallization and preliminary X-ray diffraction analysis of omega-amino acid:pyruvate transaminase from *Chromobacterium violaceum*. *Acta Crystallographica*. **63**, 117–9 (2007).
95. Sayer, C. Structural studies on ω -amine : pyruvate and serine: pyruvate aminotransferase enzymes. 232 (2009).

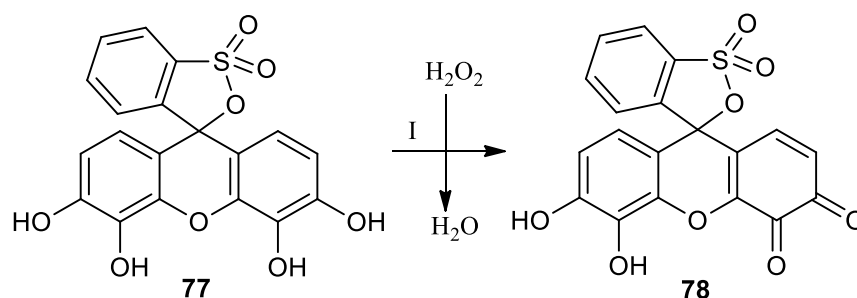
96. Committee for Proprietary Medical products. *Working parties on quality, safety and efficacy of medical products. Notes for guidance: investigation of chiral active substances*. III/3501/91 (1993).
97. Caner Hava ,GronerEfrat, L. L. and A. I. . Trends in the development of chiral drugs.*Drug Discovery Today* **9**, 105–110 (2004).
98. Tokushige, H. *et al.* Effects of topical administration of y-39983, a selective rho-associated protein kinase inhibitor, on ocular tissues in rabbits and monkeys. *Investigative ophthalmology & visual science* **48**, 3216–22 (2007).
99. Pascal, A. Ccombinations Comprising Alpha-2-Delta Ligands. (2005).at <http://worldwide.espacenet.com/publicationDetails/biblio?CC=WO&NR=2005102389A2&KC=A2&FT=D&ND=3&date=20051103&DB=EPODOC&locale=en_EP>
100. Yamagishi Tatsuya; Okumura Yoshijuki; Nukui Seiji; NakaoKazunan Phenyl or Pyridyl Amide Compounds as Prostaglandin E2 Antagonists. (2005).at <http://worldwide.espacenet.com/publicationDetails/biblio?CC=WO&NR=2005021508A1&KC=A1&FT=D&ND=3&date=20050310&DB=EPODOC&locale=en_EP>
101. Ricca, E., Brucher, B. &Schrittwieser, J. H. Multi-Enzymatic Cascade Reactions: Overview and Perspectives. *Advanced Synthesis & Catalysis* **353**, 2239–2262 (2011).
102. Simon, R. C. *et al.* Regio- and Stereoselective Monoamination of Diketones Without Protecting Groups. *Angewandte Chemie* **51**, 1–5 (2012).
103. KohamaHiromasa; Nakata Nobbuyuki; Suzuki Masahiro; TerajimaYoukoTetrahydroisoquinoline Derivative and Medicinal Preparation Containing The Same. (1996).at <http://worldwide.espacenet.com/publicationDetails/biblio?CC=WO&NR=9613497A1&KC=A1&FT=D&ND=3&date=19960509&DB=EPODOC&locale=en_EP>
104. Fecik, R. *aet al.* Chiral DNA gyrase inhibitors. 3. Probing the chiral preference of the active site of DNA gyrase. Synthesis of 10-fluoro-6-methyl-6,7-dihydro-9-piperazinyl- 2H-benzo[a]quinolizin-20-one-3-carboxylic acid analogues. *Journal of medicinal chemistry* **48**, 1229–36 (2005).
105. Lara, M., Mutti, F. G., Glueck, S. M. &Kroutil, W. Oxidative enzymatic alkene cleavage: indications for a nonclassical enzyme mechanism. *Journal of the American Chemical Society* **131**, 5368–9 (2009).
106. Moreno, A. Y., Mayorov, A. V. &Janda, K. D. Impact of distinct chemical structures for the development of a methamphetamine vaccine. *Journal of the American Chemical Society* **133**, 6587–95 (2011).
107. Bonamore, A. *et al.* An enzymatic, stereoselective synthesis of (S)-norcoclaurine. *Green Chemistry* **12**, 1623 (2010).

108. Zhi-Liang Shen, Kelvin KauKiatGoh, Hao-Lun Cheong, Colin Hong An Wong, Yin-Chang Lai, Yong-Sheng Yang, T.-P. L. Synthesis of Water-Tolerant Indium Homoenate in Aqueous Media and Its Application in the Synthesis of 1,4-Dicarbonyl Compounds via Palladium-Catalyzed Coupling with Acid Chloride. *Journal of the American Chemical Society* **132**, 15852–15855 (2010).
109. Stetter, H., Lorenz, G. Ketosauenaquivalent fur aldehyde in der thiazoliumsalsz-katalysierten addition. *Chem. Ber.* **118**, 1115 – 1125 (1985).
110. Jaesook Yun and Stephen L. Buchwald. Kinetic Resolution and Isomerization of 2,5-Disubstituted Pyrrolines. *Chirality* **12**, 476–478 (2000).
111. Alberto Soldevilla, D. S. & Pedro J. Campos, and M. A. R. The N-Cyclopropylimine-1-pyrroline Photorearrangement as a Synthetic Tool: Scope and Limitations. *J. Org. Chem.* **70**, 6976–6979 (2005).
112. Reiss, R. Engineering Monoamine Oxidase-N for the Deracemisation of Racemic amines. (2008).

8. Appendix

8.1 Solution phase assay

8.1.1 Proposed mechanism for PGR oxidation



Reagents: I) Horseradish peroxidase

Scheme 46: Estimated pyrogallol red oxidation by horseradish peroxidase.

Scheme 44 shows the proposed mechanism by previous members of the Turner/Flitsch group, neither the mechanism or the structure for the oxidised product has been confirmed.¹¹²

8.1.2 PGR colour spectrum



Figure 46: Pyrogallol colour spectrum

Figure 46 shows the colour spectrum of PGR, the left hand side is at time zero and the right hand side is full consumption of PGR by HRP.

8.1.3 PGR Absorption spectrum

Figure 47 shows a PGR absorption spectrum carried out over the wavelengths 300nm to 700nm with a maximum at 540nm.

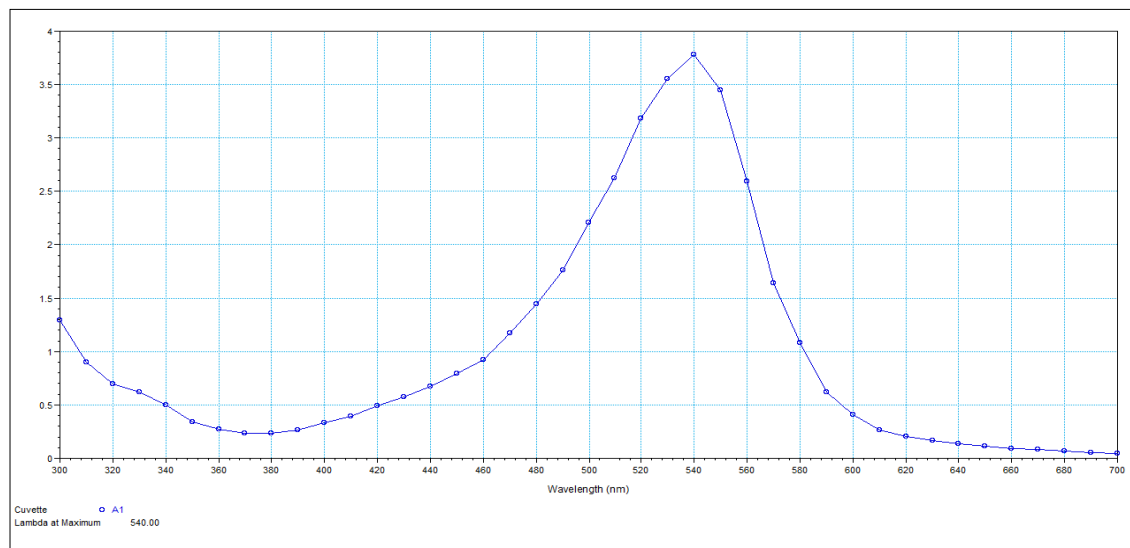


Figure 47: PGR absorbance spectrum.

8.1.4 Pyrogallol red standard curve

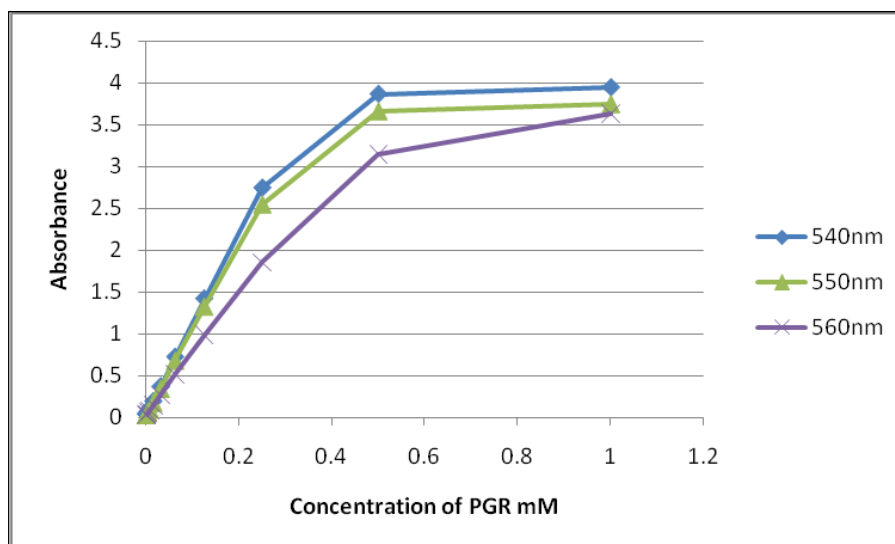


Figure 48: Standard curve of pyrogallol red at three different wavelengths.

Figure 48 shows a PGR standard curve over three different wavelengths (540, 550 and 560nm), maximum absorbance was observed to be 540nm.

8.2 pH and temperature profile of Cv TA2

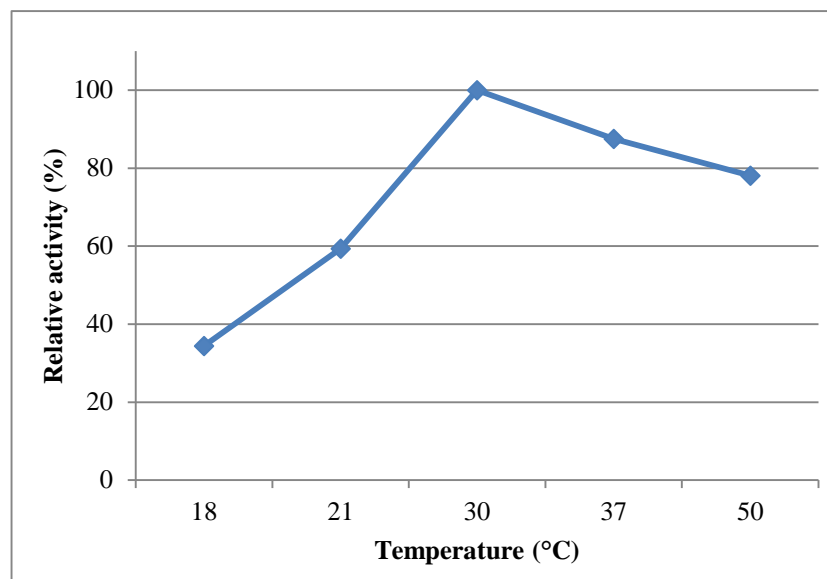


Figure 49: Temperature profile for Cv TA2.

Figure 49 shows the temperature profile for Cv TA2. The optimum temperature for the enzyme is 30 °C.

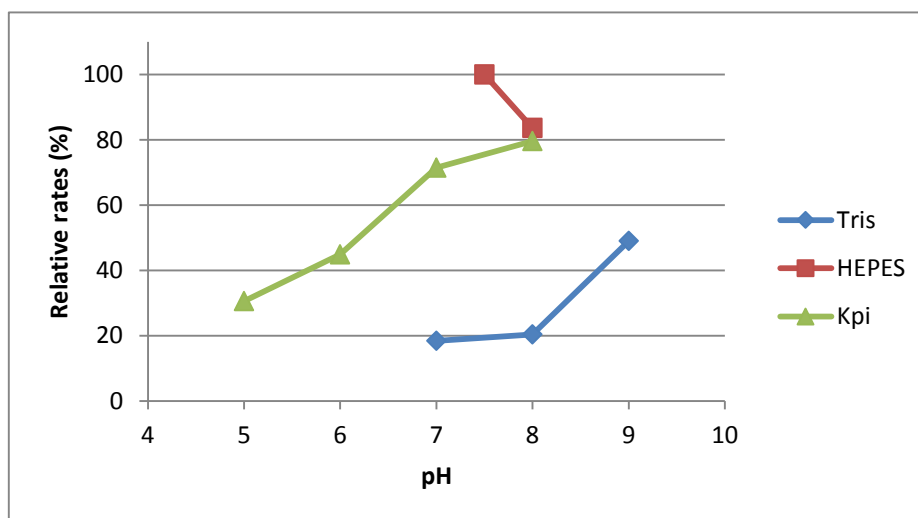


Figure 50: Effect of different buffers (100mM concentration)/pH on relative activity of Cv TA2.

Figure 50 shows a pH and buffer profile for Cv TA2. The optimum conditions are pH 7.5 in 100 mM HEPES.

8.3 Plasmids

8.3.1 PJH1 Vector map

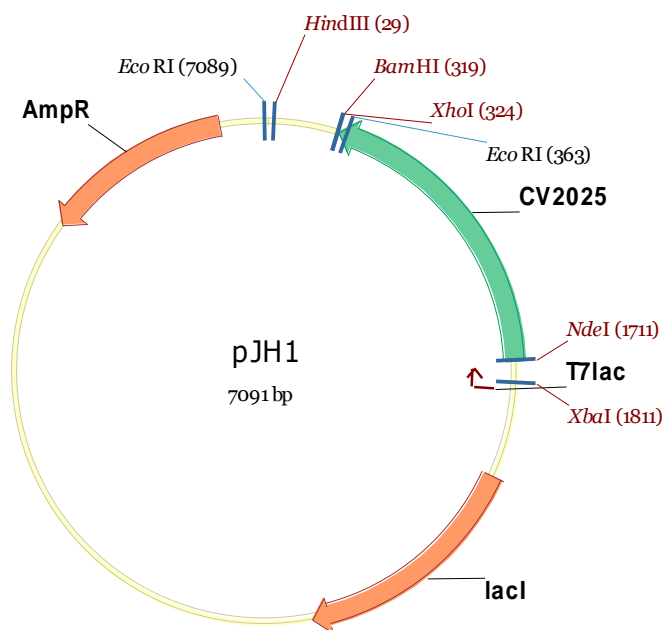


Figure 51: Vector map of a transaminase gene from *C. Violaceum* (2025) obtained from Prof. Helen Hailes, University College London, cloned into pET16b. Multiple cloning sites used in this study (*Nde*I and *Xho*I) and the plasmid carries an ampicillin resistance marker.

8.3.2 Vector map of PJH2

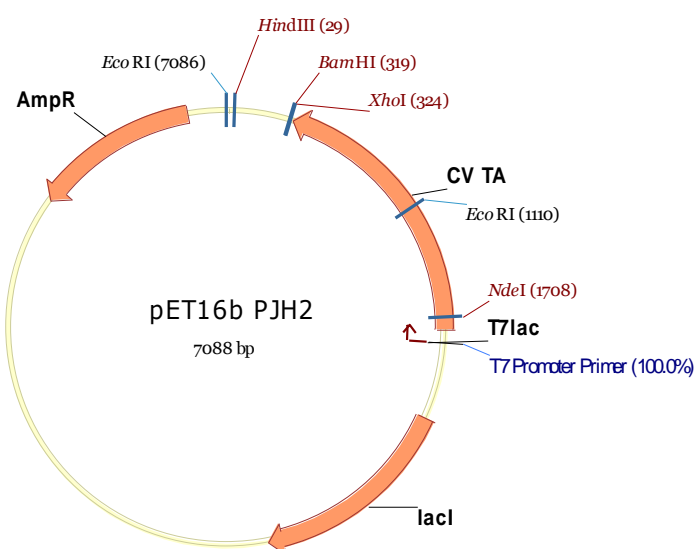


Figure 52: Vector map of a transaminase gene from *C. Violaceum* (CMC 104818) obtained from the Chirotech microbial culture collection, cloned into pET16b. Multiple cloning sites used in this study (*Nde*I and *Xho*I) and the plasmid carries an ampicillin resistance marker.

8.3.3 Vector map of PJH3

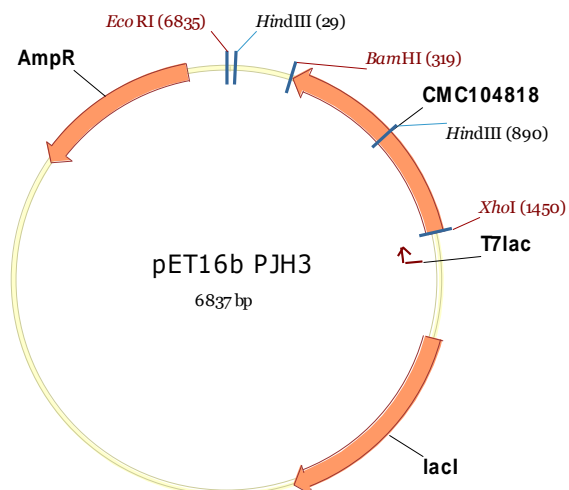


Figure 53: Vector map of a transaminase gene from *Ochrobactrum sp.* (CMC 104240) obtained from the Chirotech microbial culture collection, cloned into pET16b. Multiple cloning sites (*Bam* HI and *Xho* I) and the plasmid carries an ampicillin resistance marker.

8.3.5 Zero blunt topopCR vector map

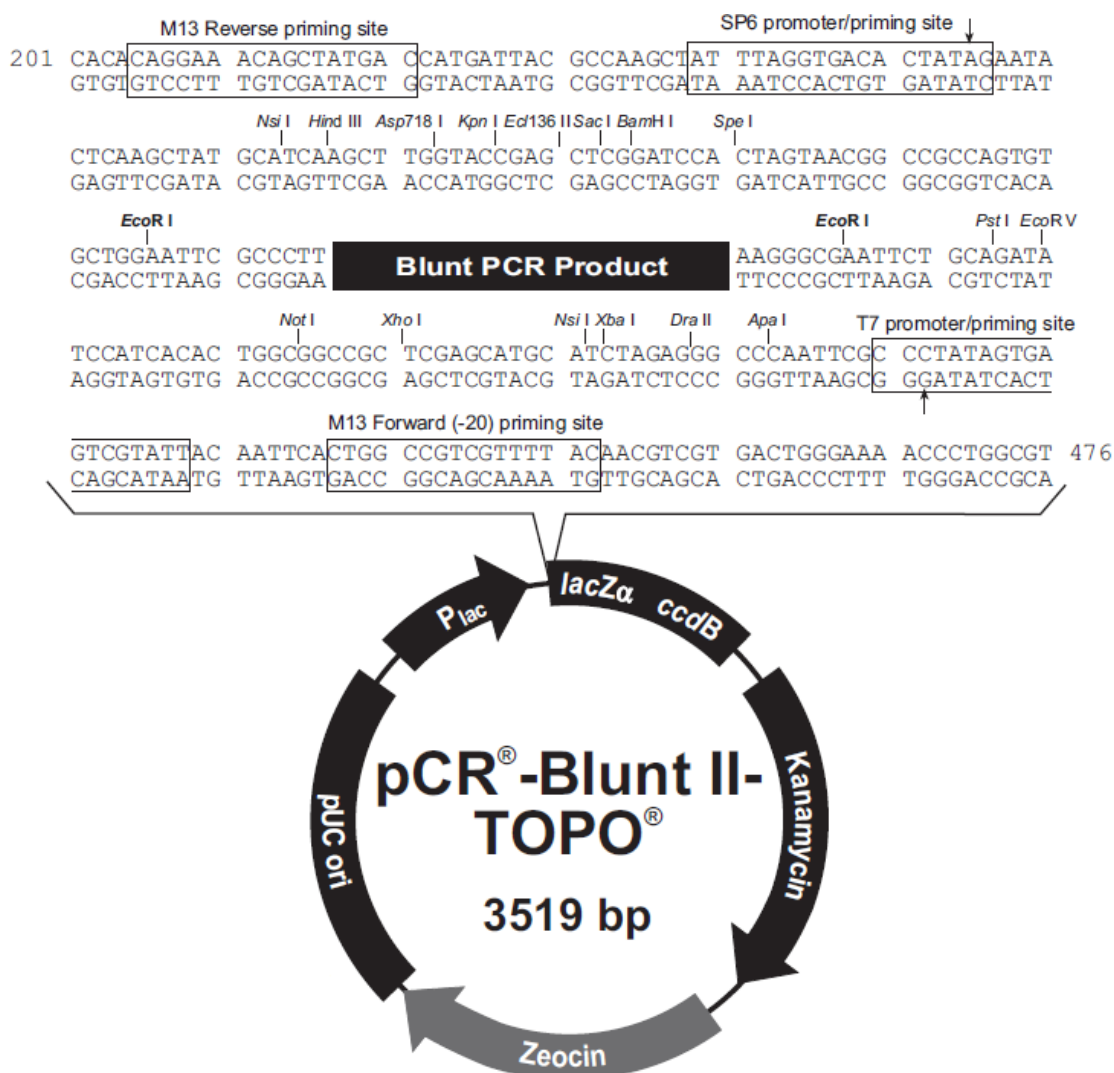


Figure 55: pCR-Blunt II-TOPO vector map. Multiple cloning sites used in this study (*Eco* RI, *Xho*I and *Bam* HI).

8.4 DNA sequences

8.4.1 *Chromobacterium violaceum* Cv TA2

ATGCAGAAGCAACGTACGACCAGCCAATGGCGCGAACTGGATGCCGCCATCACCTGCATC
 CGTTTACCGATAACCGCATCGCTGAACCAGGCGGGCGCGCGGTGATGACGCGCGGAGAAGG
 CATCTATCTGTGGGATTCGGACGGCAACAAGATCATCGACGGCATGGCCGGCCTATGGTGTG
 TGAACGTGGCTACGGCCGCAAGGATTTCCGCCGAGGTGGCGCGCCGCCAGATGGAAGAGCT
 GCCGTTCTACAACACCTTCTTCAAGACCACGCATCCGGCGGTGGTTCGAACTGTCCCGCCTGT
 TGGCCGAAGTGACGCCAGCCGGCTTCGACCACGTGTTTTACACCAACTCAGGCTCGGAGTCG
 GTGGACACCATGATCCGCATGGTGCGCCGCTACTGGGACGTGCAGGGCAAGCCGGAGAAGA
 AGACGTGATCGGCCGTTGGAACGGCTATCACGGCTCCACCATCGGCCGGCCAGTCTGGGC
 GGCATGAAGTACATGCATGAGCAGGGCGATCTGCCGATTCCGGGCATGGCCCATATCGAGC
 AGCCGTGGTGGTACAAGCACGCAAGGACATGACGCCGGACGAATTCGGCGTGGTGGCCGC
 GCGCTGGCTGGACGAGAAGATCCAGGAGATCGGCGCCGACAAGGTGGCGGCTTTTGTGCC
 GAACCCATCCAGGGCGCTGGCGGGGTGATCATAACGCCAGCCACCTACTGGCCGAAATCG
 AGCGCATCTGCCGCAAGCACGATGTGTTGATTGTGGCGGACGAAGTGATCTGCGGTTTCGGC
 CGCACCGGCGAATGGTTCGGCCATCAGCATTTCGGCTTCCAGCCTGACCTGTTACCCGCGGC
 TAAGGGCTTGTGTCGGGCTACTTGCCGATCGGCGCGGTGTTTCGTGGCAAGCGCGTGGCGG
 AAGGCCTGATCGCCGGCGGCGACTTCAACCACGGCTTACCTATTCGGCCATCCGGTCTGC
 GCCGCGGTGGCGCACGCCAATGTGGTGGCGCTGCGAGACGAGGGCATCGTCCAGCGCGTCA
 AGGACGACATCGGTCCTTACATGCAGAAGCGTTGGCGCGAGACCTTCAGTCAGTTCGAGCAC
 GTGGACGACGTGCGCGGCGTCGGCCTGATCCAAGCCTTACGCTGGTGAAGAACAAGGCGA
 AGCGCGAGCTGTTCCCGATTTCCGGCGAGGTCGGCACGCTATGCCGCGACATCTTCTCCGC
 AACAACCTGATCATGCGCGCTTTCGGCGACCATATCGTATGTTCCGCCCGCTGGTGTGAC
 GCGAGCCGAAGTGGATGAAATGCTGGGGGTGGCGGCGGCTTGCCTAGCCGAGTTCGAGCAG
 GCGCTGAAGGCGCGCGGGCTGGCTTAG

Figure 56: DNA sequence *Chromobacterium violaceum* transaminase Cv TA2.

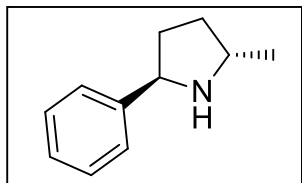
8.4.2 *Ochrobactrum antropi* Oa TA1

ATGCAGTTTATTGATCTTGGAGCGCAACGCGCGGTATCGAAGACCGTCTTAATGCCGCCGT
 TTCCAAGGTAGTTGCCGAAGGCCGTTATATTCTTGGTCTTGAAGTCGCTGAGTTCGAAAAGA
 AACTCGGTGAATATCTGGGCGTGAACATGTGATCGCCTGCGCCAACGGCACCGACGCTTTG
 CAGATGCCTTTGATGGCGCGCGGTATCGGCCCGGGTCATGCGGTGTTTCGTTTCTTCGTTACG
 TTCGCTGCAACCGCTGAAGTCGTTGCCCTTGTGGCGCAGAGCCGGTTCGTTGATGTCGAT
 GCCGACACCTACAACATGAATATTGAACAGCTTGAAGCCGCTATTGCGGCCATCCGCAAGG
 AAGGTGCTCTTGAGCCCAAGGCAATCATTCTGTGACCTGTTTCGGTCTTGCTGCCGATTACA
 ACCGCATCACTGCCGTTGCAGATCGCGAAGGTCTGTTTCGTGATTGAAGACGCGGCTCAGTCG
 ATTGGTGGCAAGCGCGACAACGTCATGTGCGGCGCTTTCGGCCATGTCCGGTGCACAAGCTT
 CTATACCCGGCCAAGCCGCTCGGCTGCTATGGCGACGGCGGTGCAATGTTACCAATGATGC
 TGAATCGCCGACACGTTGCGCTCTGTGCTTTTCCACGGCAAGGGTGAACACAGTACGACA
 ATGTTTCGATTGGGCTGAACTCGCGCCTCGATACAATTCAGGCTGCTATTCTTCTGAAAAAG
 TTAGCGATCCTTGAAGACGAAATGGAAGCGCGGACCCGATTGCCAAGCGATAACAATGAAT
 TGCTCAAGGATGTAGTCAAGGTTTCTGGTCTGCTGCTGGCAACCGTTCGGCCTGGGCACAG
 TATTCGATTGAAAGCGAAAACCGCGATGGTCTGAAGGCACATCTTCAGGCAGCCGGCATTCC
 ATCGGTTATCTACTATGTGAAGCCGCTGCATCTGCAGACAGCATAACAAGCATTATCCGATTG
 CACCGGGTGGTCTGCCTGTTTCGGAAGCGCTGCCTGCACGCATTCTCAGCCTGCCGATGCAT
 CCTTATCTTTCGGAAGAAGATCAGGACAAGATCATCGGCGCGATCCGTGGTTTTACGGAAA
 GAAGGCCTGA

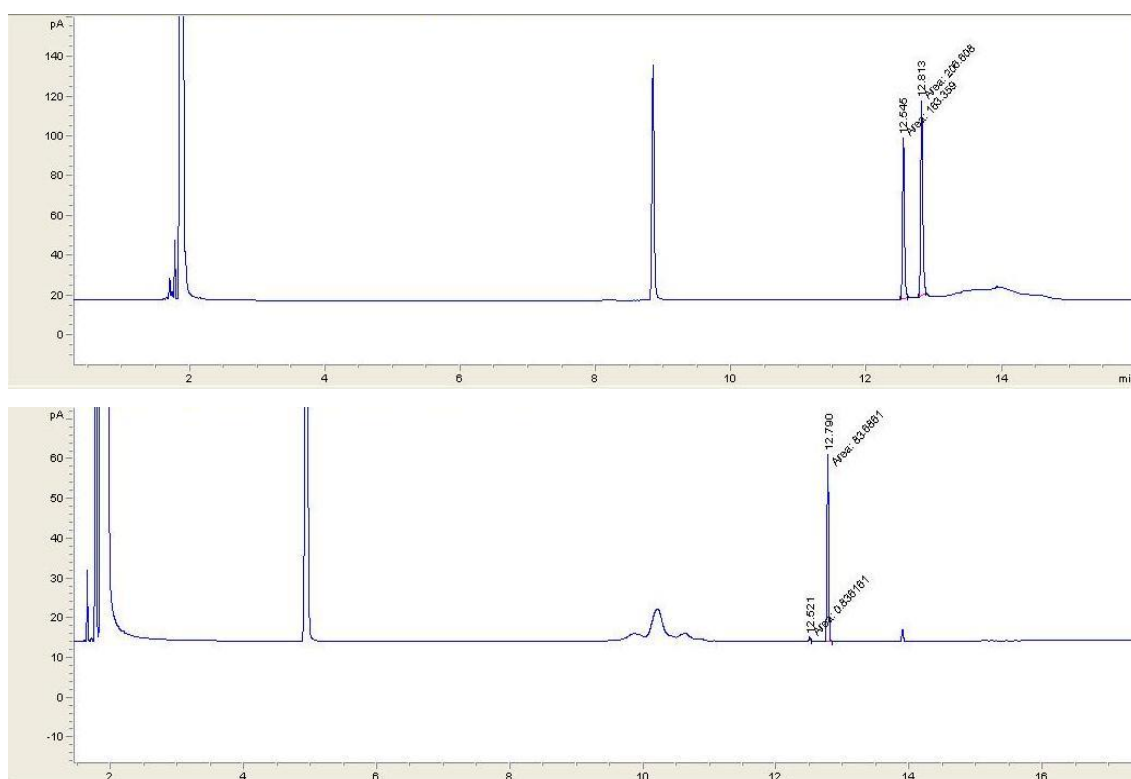
Figure 57: DNA sequence *Ochrobactrum antropi* transaminase Oa TA1.

8.5 Analytical traces

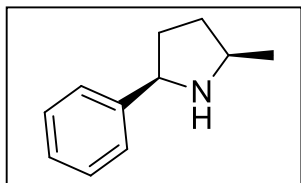
8.5.1 (2*S*,5*R*)-2-Methyl-5-phenylpyrrolidine.



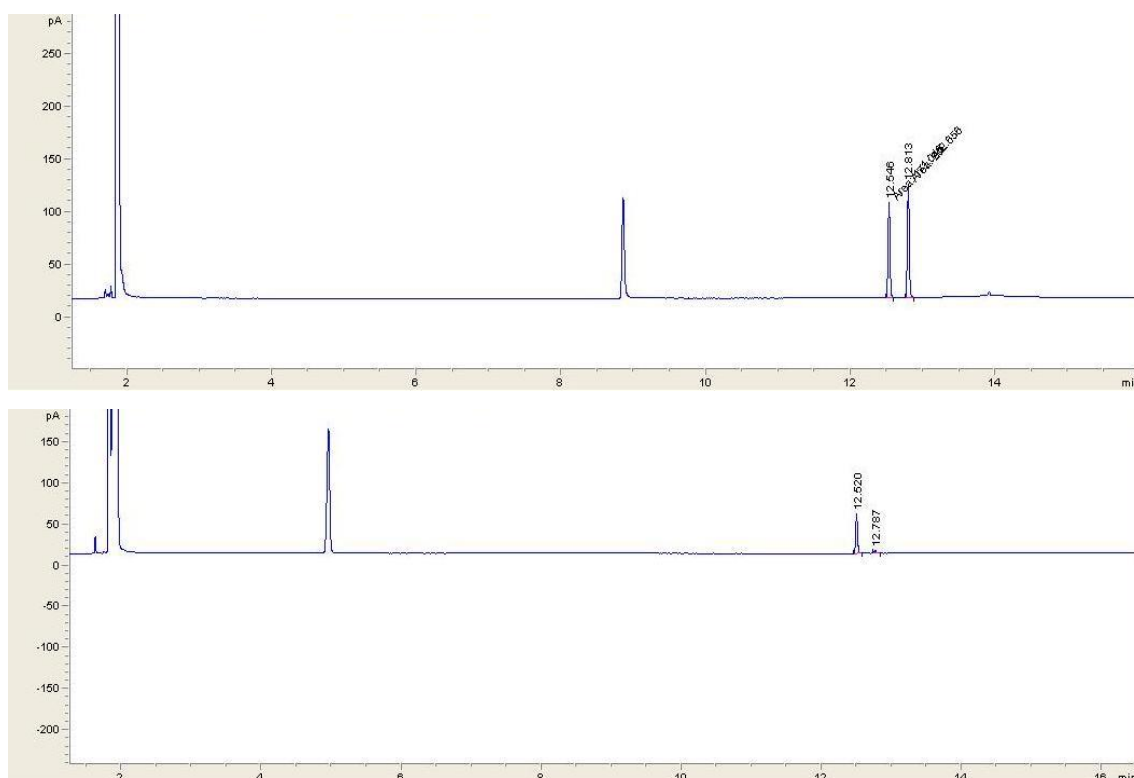
The reaction was set up as described in the general procedure using MAO-N D9 as biocatalyst. After 24 hours GC analysis showed 98% *de*.



GC conditions: CAM Column. Retention time amines 12.5, 12.7 and imine 14.2 minutes

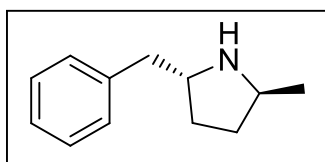
8.5.2 (2*R*,5*R*)-2-Methyl-5-phenylpyrrolidine.

The reaction was set up as described in the general procedure using MAO-N D11 as biocatalyst. After 48 hours GC analysis showed 90% *de*.

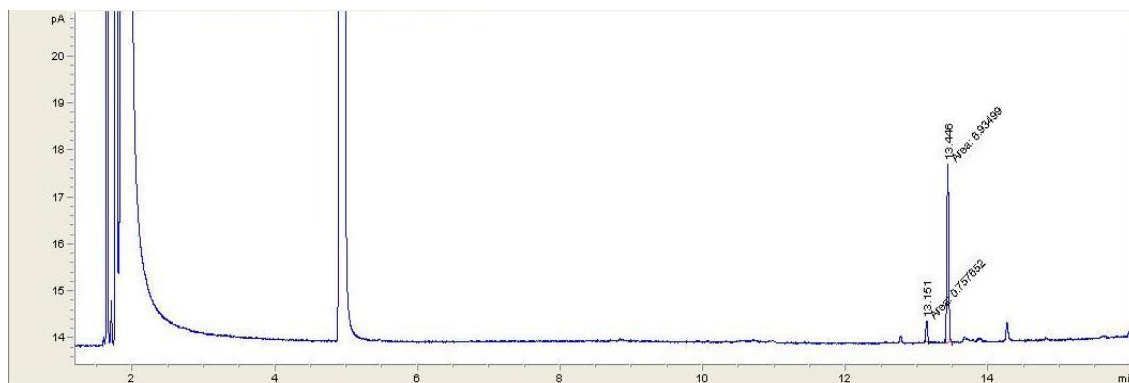


GC conditions: CAM Column. Retention time 12.5 and 12.8 minutes

8.5.3 (2S,5R)-2-Methyl-5-benzylpyrrolidine.

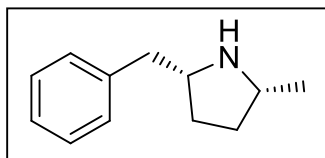


The reaction was set up as described in the general procedure using MAO-N D9 as biocatalyst. After 6 hours GC analysis showed 80% *de*.

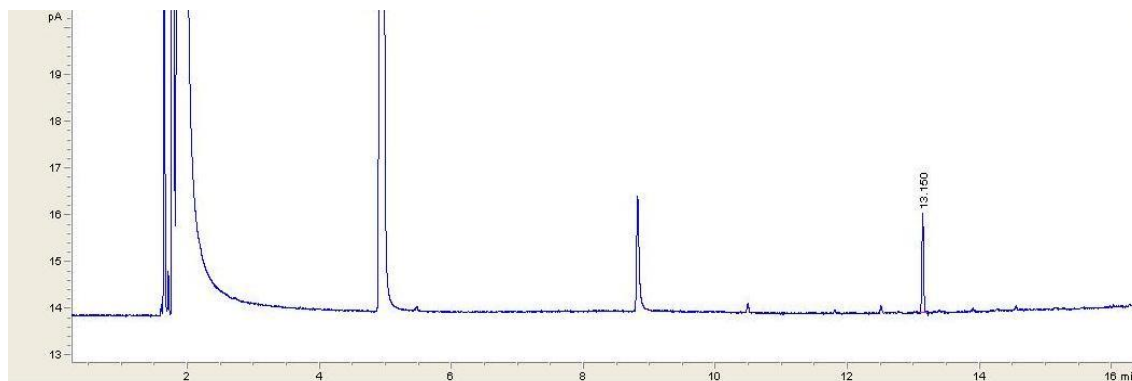


GC conditions: CAM Column. Retention time 13.2 and 13.4 minutes

8.5.4 (2R,5R)-2-Methyl-5-benzylpyrrolidine.

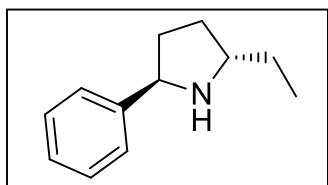


The reaction was set up as described in the general procedure using MAO-N D9 as biocatalyst. After 3 hours GC analysis showed 99% *de*.

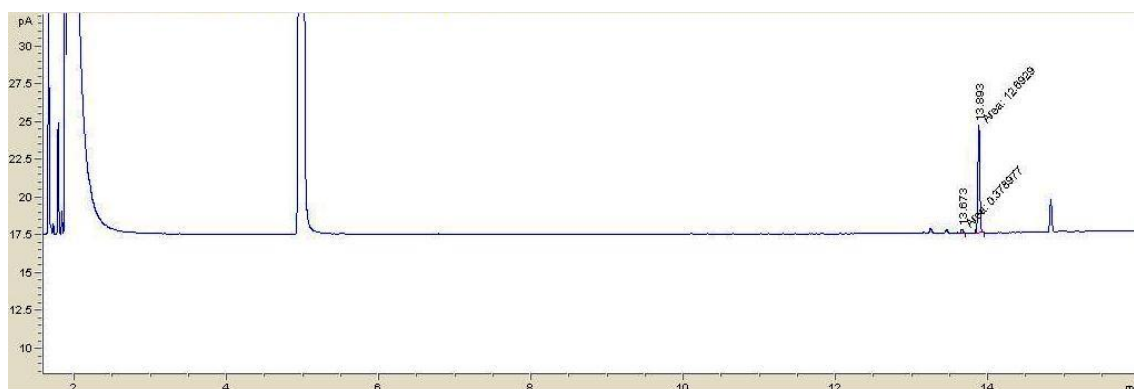
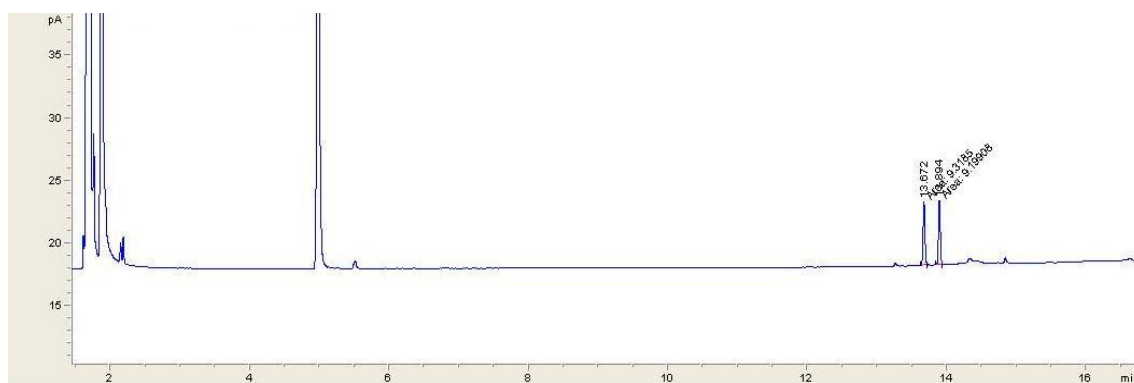


GC conditions: CAM Column. Retention time 13.2 minutes

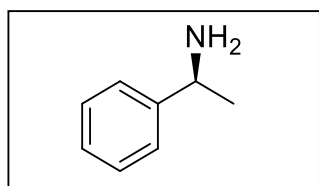
8.5.5 (2S,5R)-2-Ethyl-5-phenylpyrrolidine.



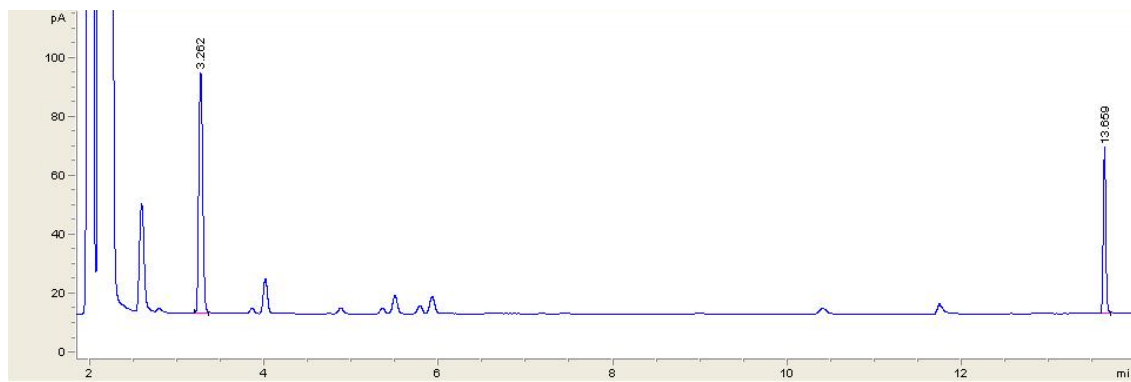
The reaction was set up as described in the general procedure using MAO-N D9 as biocatalyst. After 24 hours GC analysis showed 94% *de*.



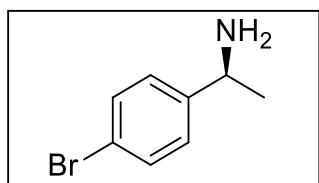
GC conditions: CAM Column. Retention time 13.7 and 13.9 minutes

8.5.6 (*S*)-1-Phenylethylamine

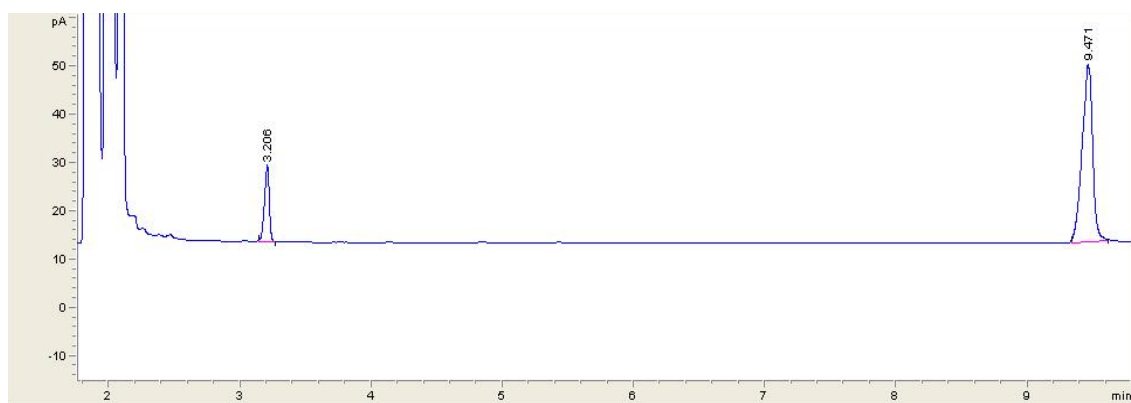
The reaction was set up as described in the general procedure using Cv TA2 as biocatalyst. After 24 hours GC analysis showed > 99% *ee*.



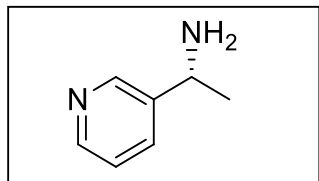
GC column Chirasil-DEX CB: (*S*)-1-phenylethylamine 13.7 min, ketone 3.3 min.

8.5.7 (*S*)-4-Bromo-1-phenylethylamine

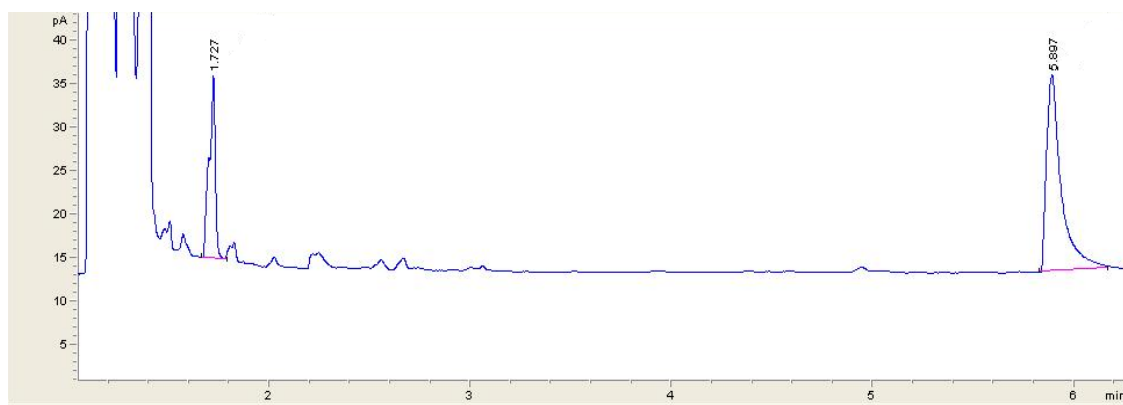
The reaction was set up as described in the general procedure using Cv TA2 as biocatalyst. After 24 hours GC analysis showed > 99% *ee*.



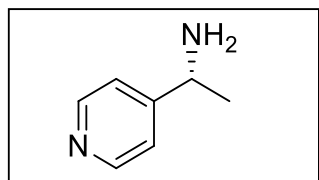
GC column Chirasil-DEX CB: (*S*)-4-bromo-1-phenylethylamine 9.5 min, ketone 3.2 min.

8.5.8 (*R*)-1-(pyridin-3-yl)ethanamine

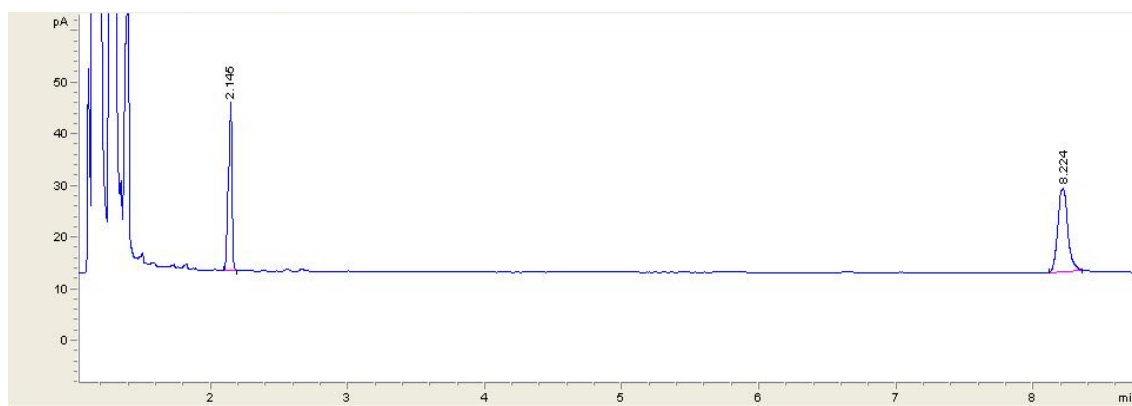
The reaction was set up as described in the general procedure using ATA-117 as biocatalyst. After 24 hours GC analysis showed > 99% *ee*.



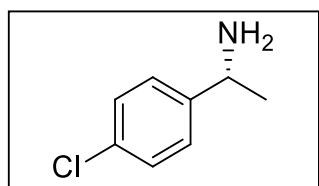
GC column Chirasil-DEX CB: (*R*)-amine 5.9 min, ketone 1.7 min.

8.5.9 (*R*)-1-(pyridin-4-yl)ethanamine

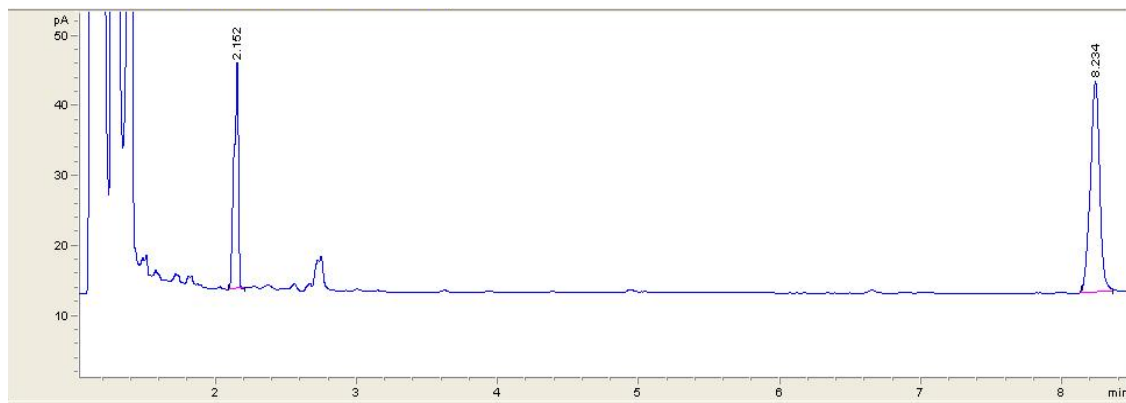
The reaction was set up as described in the general procedure using ATA-117 as biocatalyst. After 24 hours GC analysis showed > 99% *ee*.



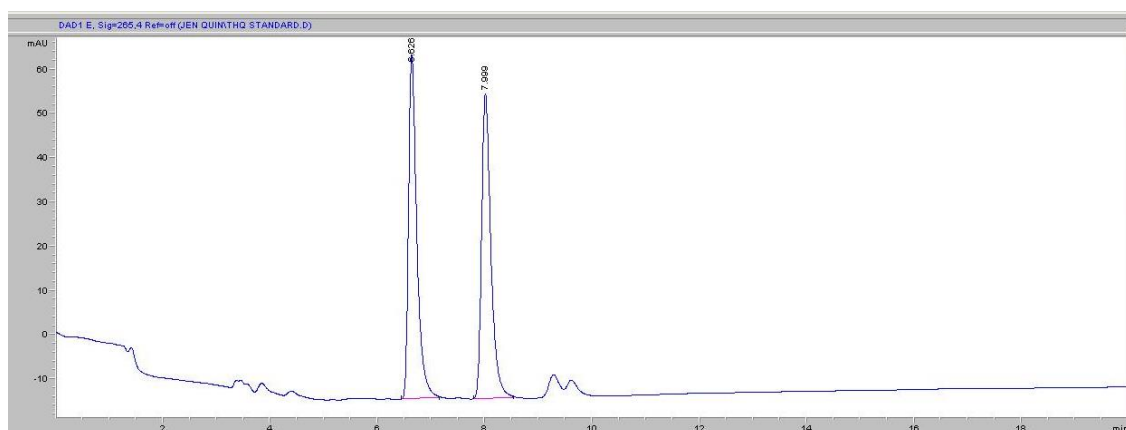
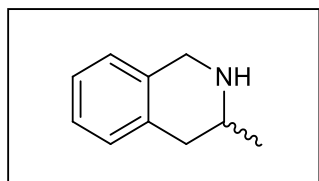
GC column Chirasil-DEX CB: (*R*)-amine 8.2 min, ketone 2.1 min.

8.5.10 (*S*)-4-Bromo-1-phenylethylamine

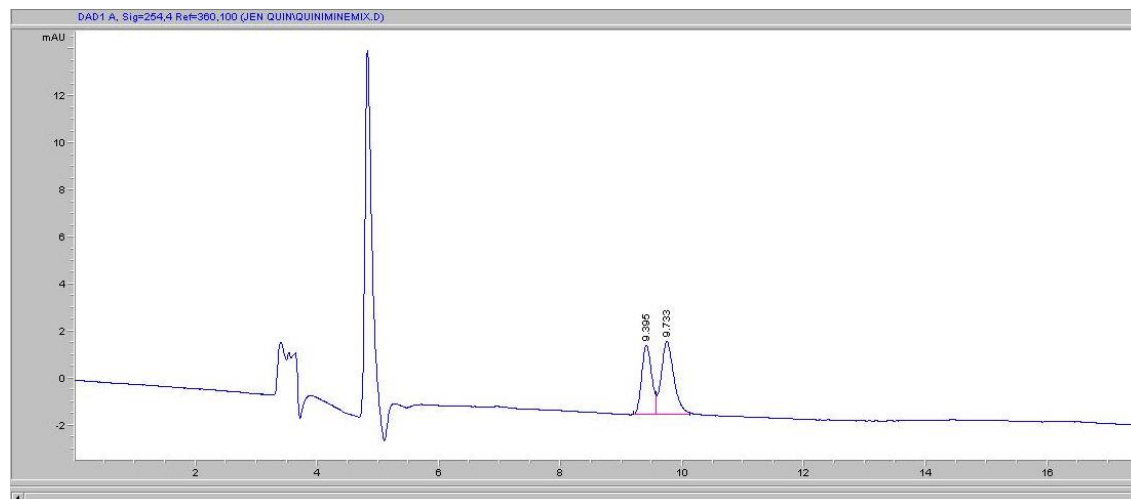
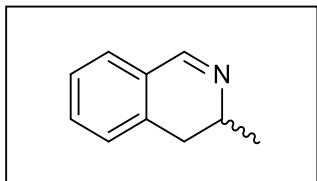
The reaction was set up as described in the general procedure using ATA-117 as biocatalyst. After 24 hours GC analysis showed > 99% *ee*.



GC column Chirasil-DEX CB: (*R*)-4-chloro-1-phenylethylamine 8.2 min, ketone 2.2 min.

8.5.11 (*Rac*)- 3-Methyl-1,2,3,4-tetrahydroisoquinoline

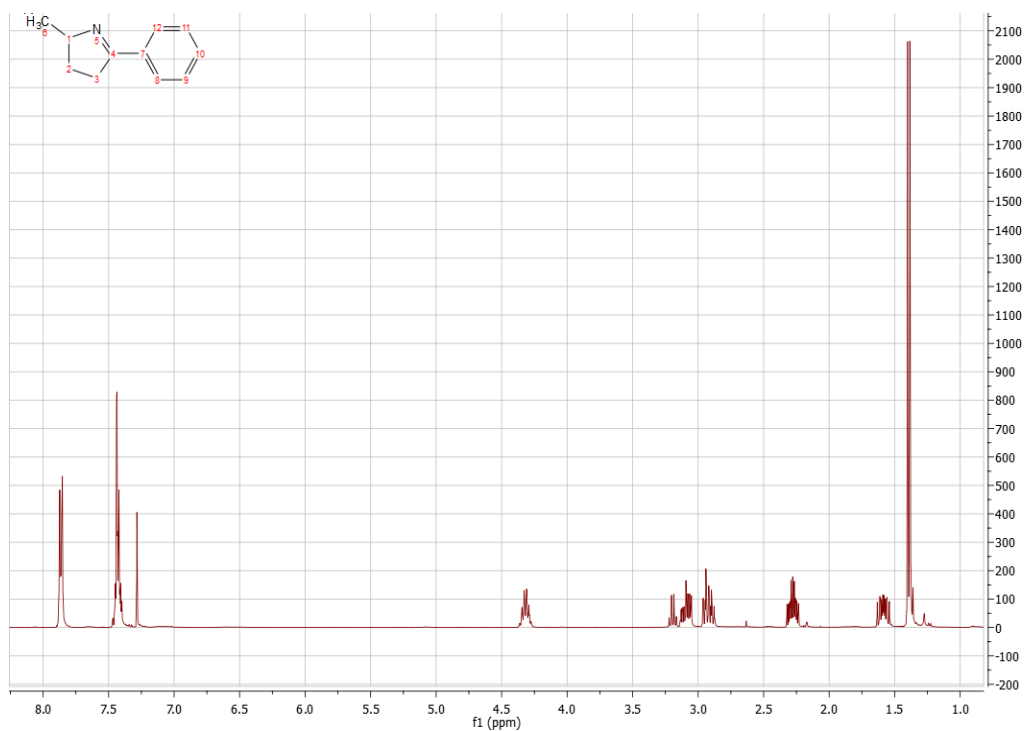
HPLC, Chiralpack IC 6.4 mm x 250 mm x 5 μ m, 90:10 (hexane/propan-2-ol) 1 mL/min: racemic amine 6.63 min and 8.0 min.

8.5.12 (*Rac*)- 3-Methyl-3,4-dihydroisoquinoline

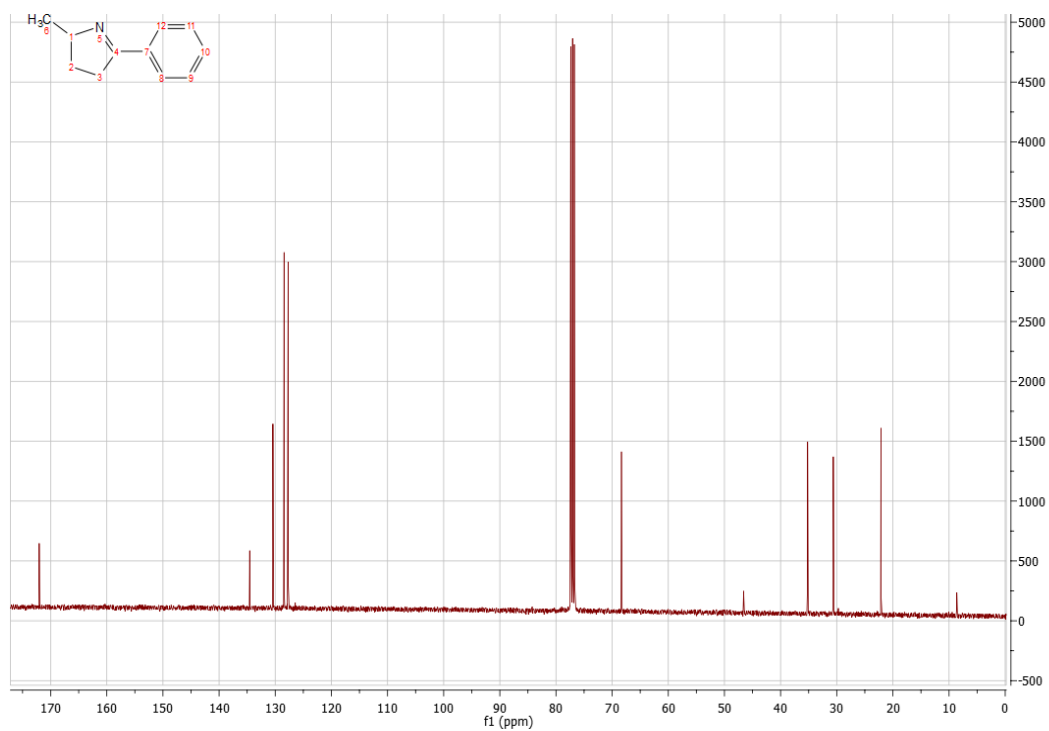
HPLC, Chiralpack IC 6.4 mm x 250 mm x 5 μ m, 90:10 (hexane/propan-2-ol) 1 mL/min: racemic amine
9.4 min and 9.73 min.

8.6 NMR data

8.6.1 2-Methyl-5-phenyl-3,4-dihydro-2H-pyrrole

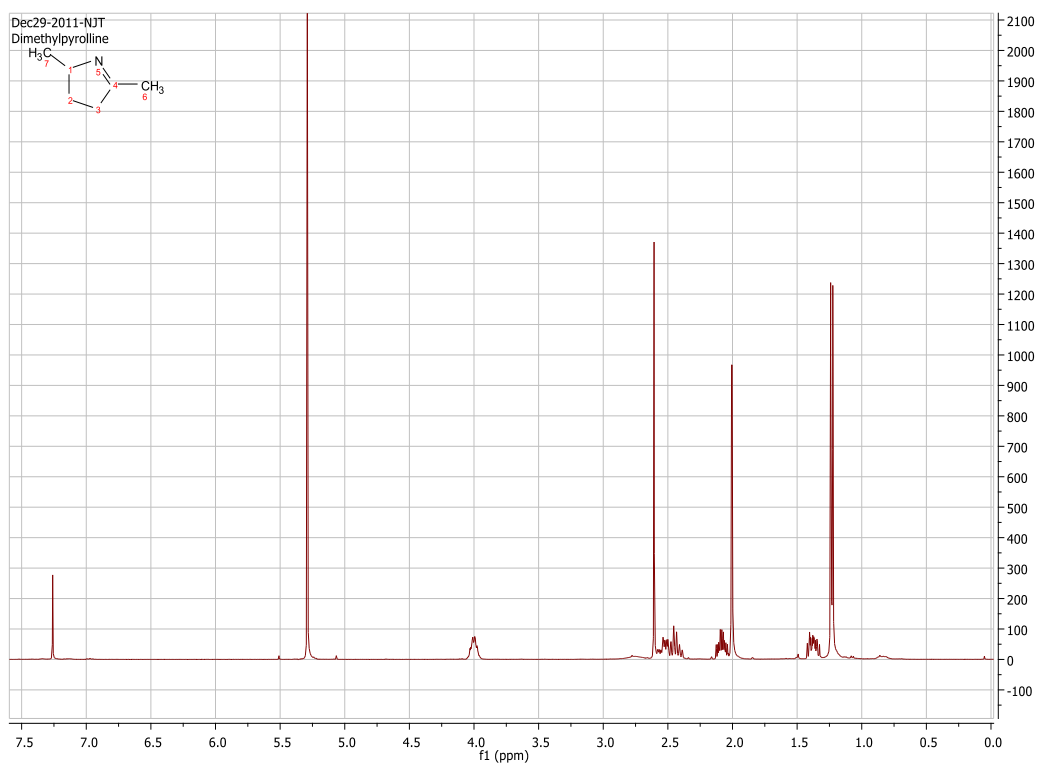


¹H NMR (400 MHz, CDCl₃): 7.89-7.84 (m, 2H), 7.48-7.39 (m, 3H), 4.48-4.26 (m, 1H), 3.09 (m, 1H), 2.92 (m, 1H), 2.28 (m, 1H), 1.59 (m, 1H), 1.39 (d, $J = 7.2$ Hz, 3H).



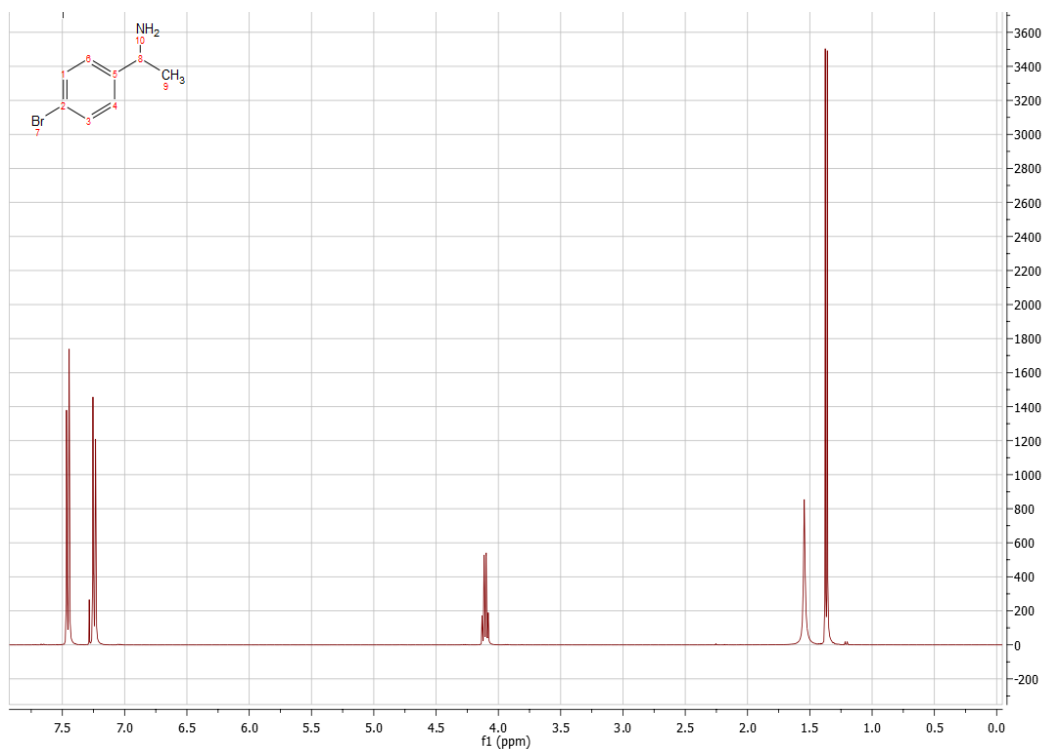
¹³C NMR (100 MHz, CDCl₃): δ 172.0, 134.5, 130.4, 128.4, 127.7, 68.3, 35.2, 29.5, 22.1.

8.6.2 2,5-Dimethyl-3,4-dihydro-2H-pyrrole

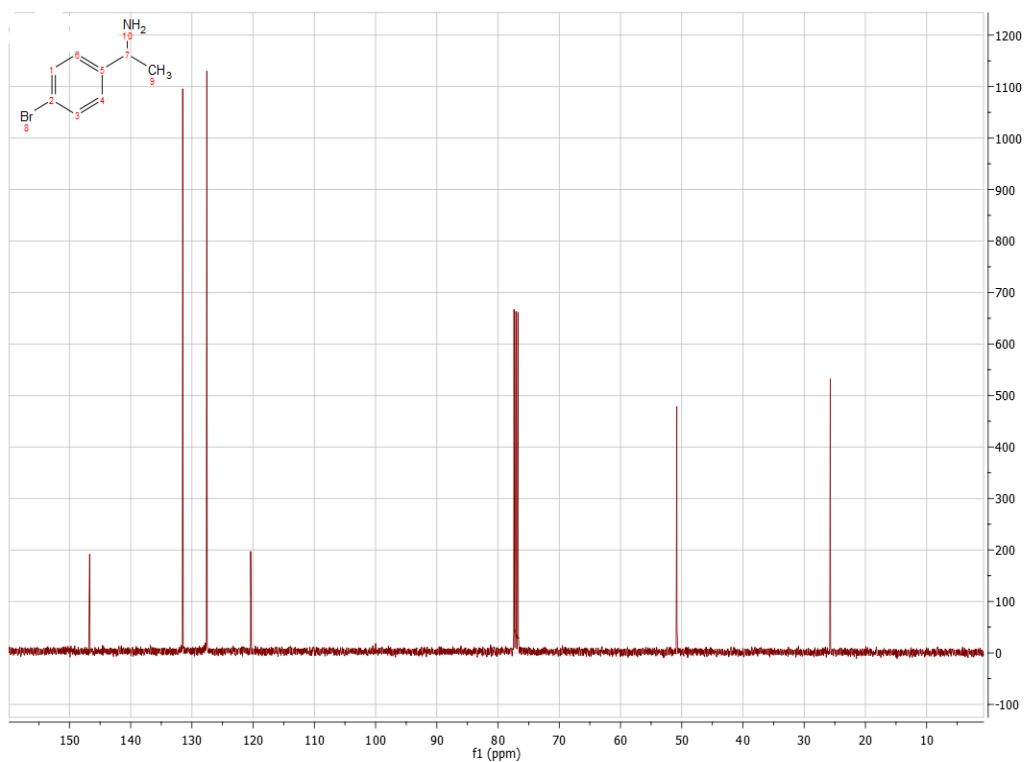


^1H NMR (400 MHz, CDCl_3): δ 4.06-3.92 (m, CH), 2.58-2.37 (m, CH_2), 2.14-2.03 (m, CH), 2.00 (s, CH_3), 1.37 (m, CH), 1.23 (d, $J = 6.8$ Hz, CH_3).

8.6.3 4-Bromo-1-phenylethanamine

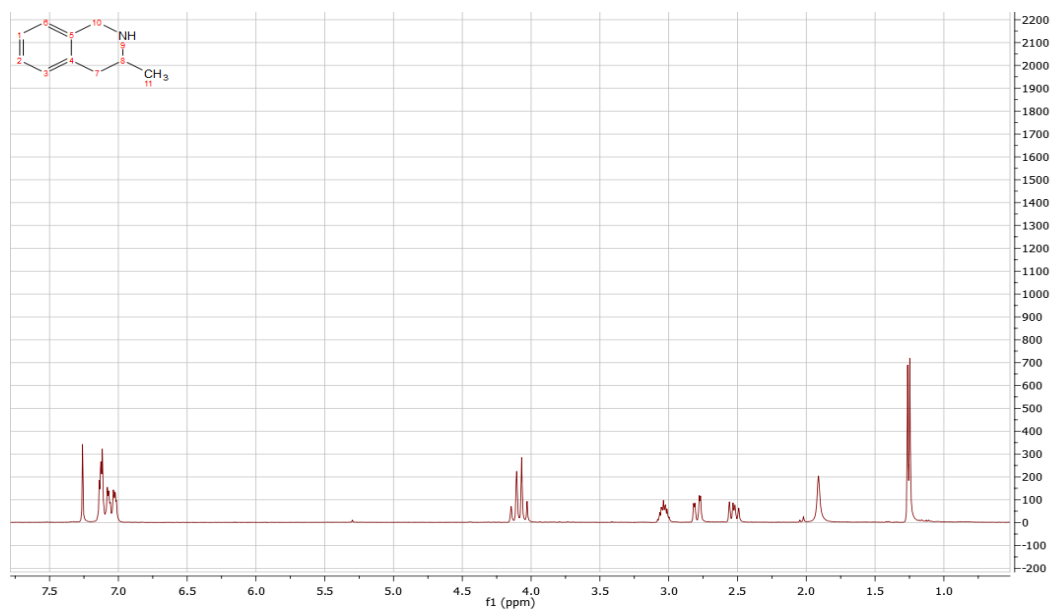


¹H NMR (400 MHz, CDCl₃): δ 7.48 – 7.43 (m, 2H), 7.26 – 7.22 (m, 2H), 4.11 (q, *J* = 6.6 Hz, 1H), 1.51 (s, 2H), 1.34 (d, *J* = 6.6 Hz, 3H).

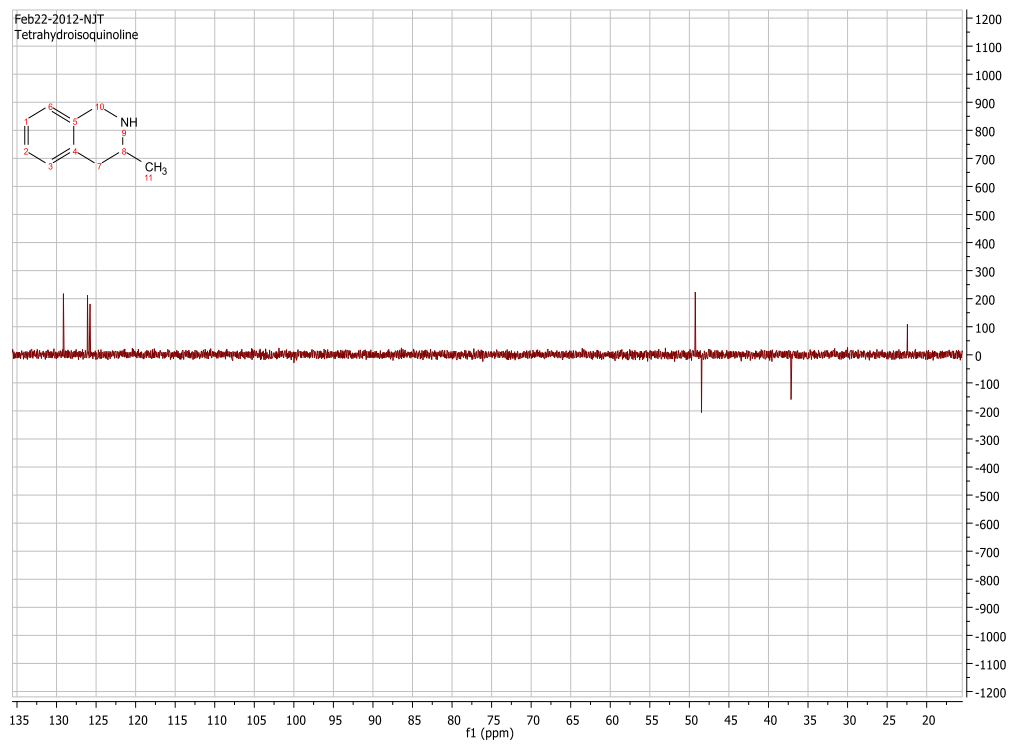
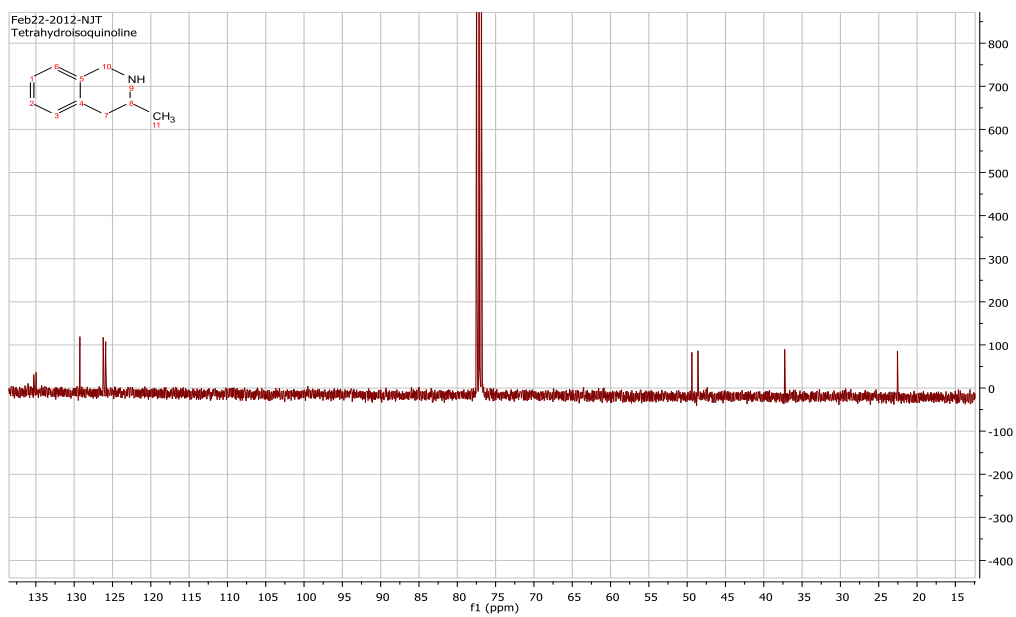


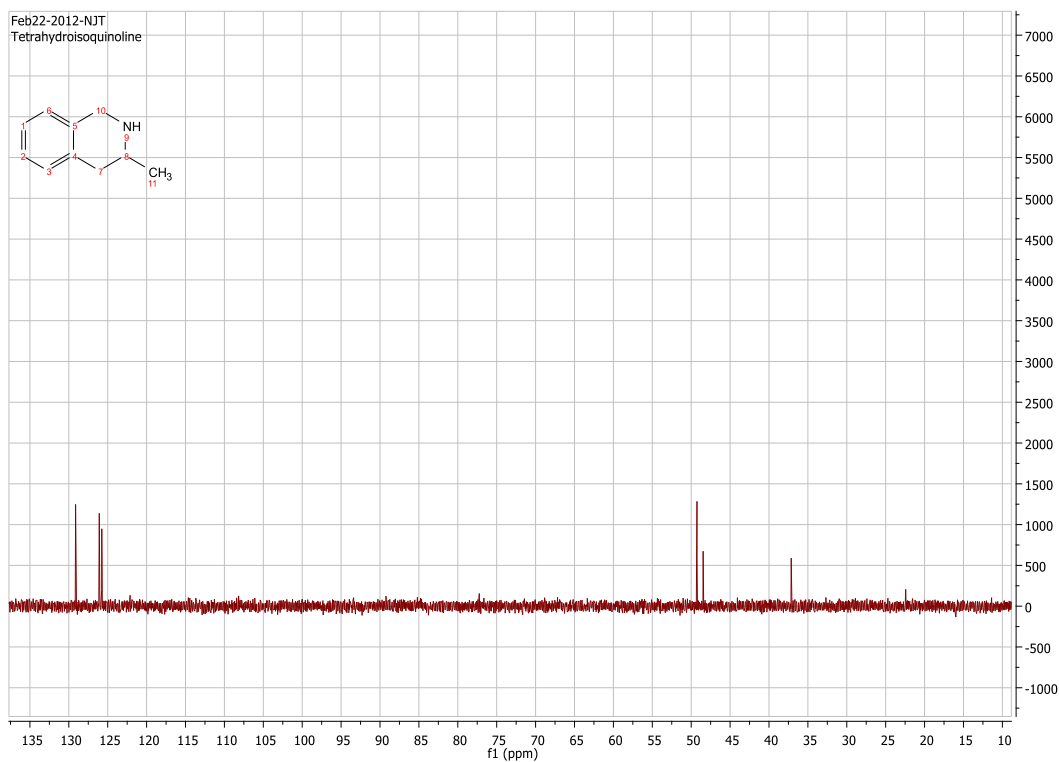
¹³C NMR (100 MHz, CDCl₃): δ 146.7, 131.5, 127.6, 120.4, 50.8, 25.8.

8.6.4 3-Methyl-1,2,3,4-tetrahydroisoquinoline



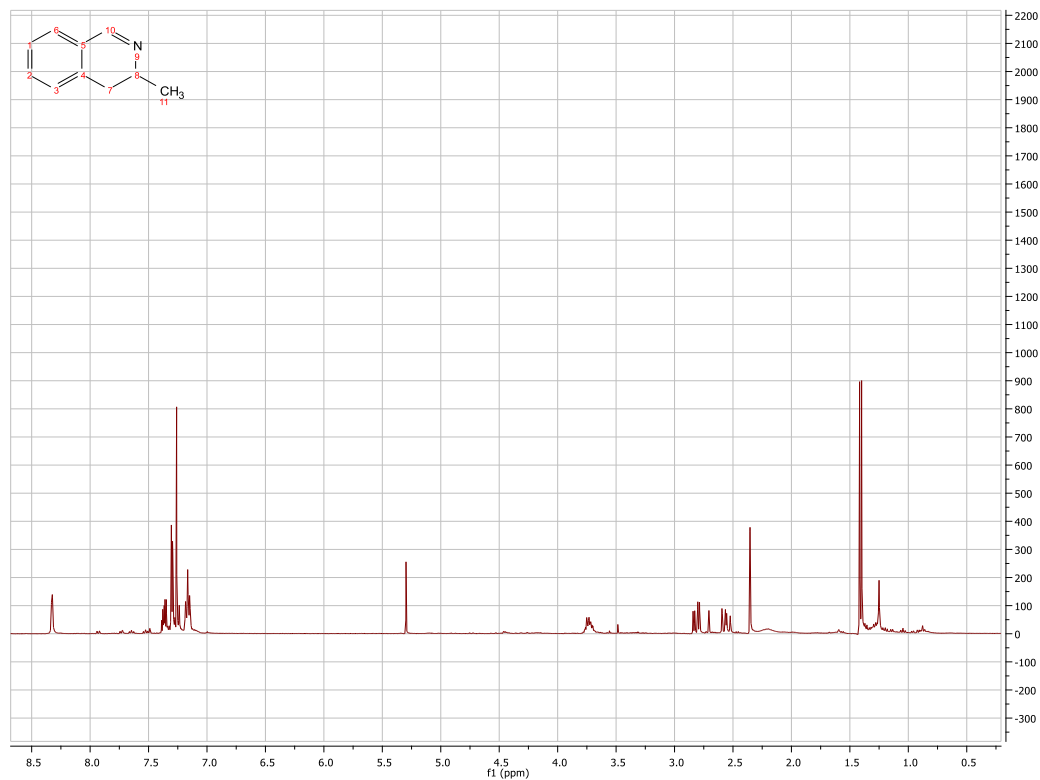
^1H NMR (400 MHz, CDCl_3): δ 7.07 (m, 6H, Ar), 4.09 (q, $J = 1.9$ Hz, CH_2), 3.10 – 2.96 (m, 1H, CH), 2.79 (dd, $J = 16.4, 3.6$ Hz, CH), 2.53 (dd, $J = 16.3, 10.7$ Hz, CH), 1.91 (broad s, NH), 1.26 (d, $J = 6.3$ Hz, CH_3).



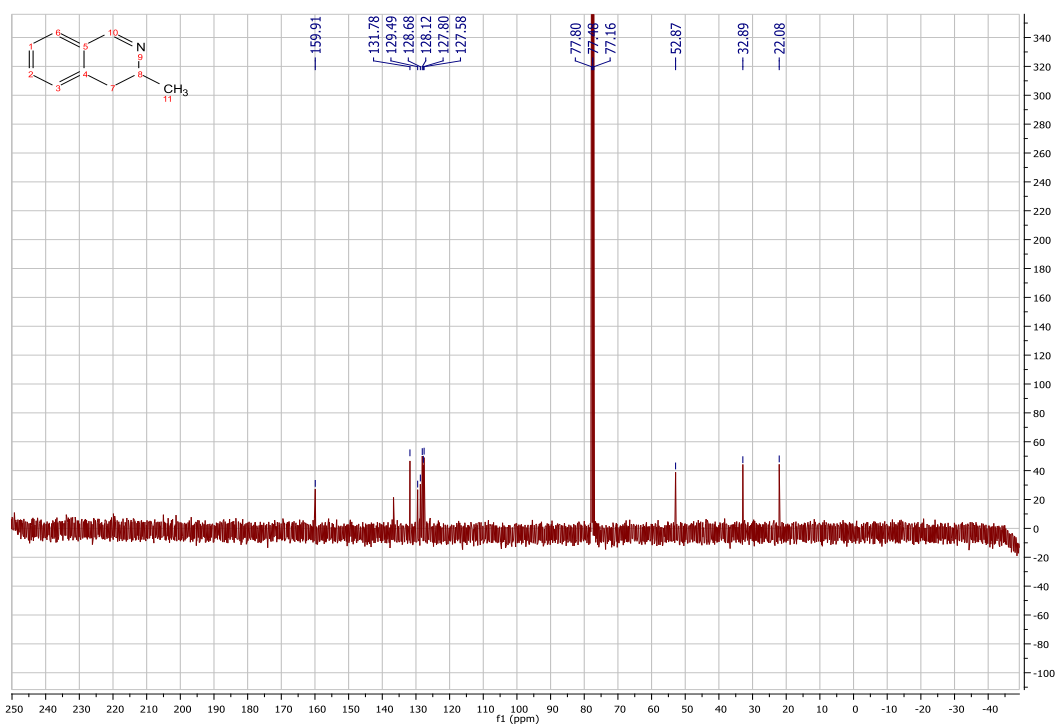


¹³C NMR (100 MHz, CDCl₃): δ 135.3, 134.9, 129.2, 126.2, 126.2, 125.9, 49.4, 48.6, 37.3, 22.6.

8.6.5 3-Methyl-3,4-dihydroisoquinoline

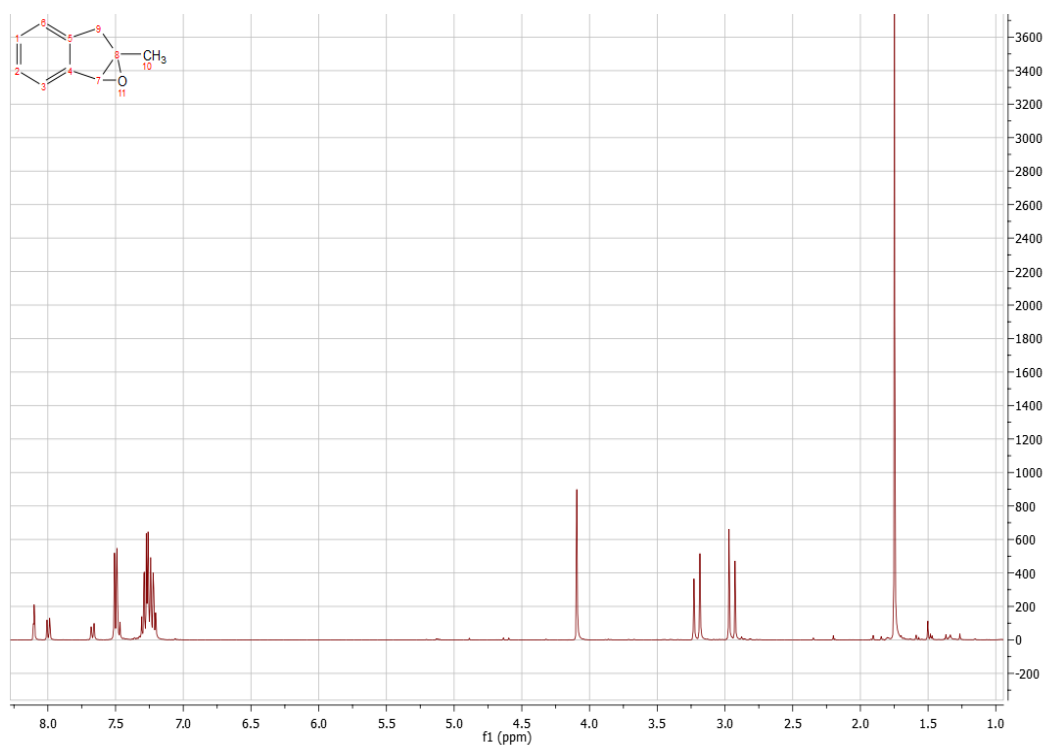


¹H NMR (400MHz, CDCl₃): δ 8.33 (s, 1H, CH), 7.40-7.32 (m, 1H, Ar), 7.29 (m, 1H, Ar), 7.20-7.12 (m, 2H, Ar), 3.81-3.63 (m, CH), 2.81 (dd, $J = 16.3$ Hz, CH), 2.62-2.49 (m, CH), 1.41 (d, $J = 20$ Hz, CH₃).



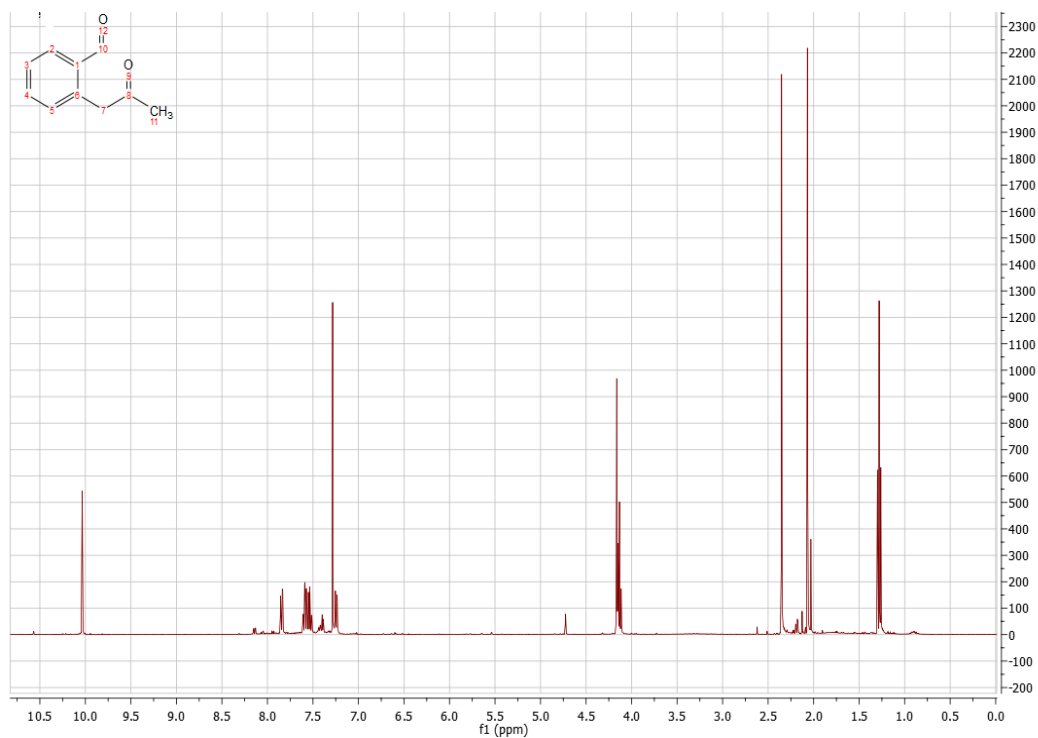
¹³C NMR (100 MHz, CDCl₃): δ 160.0, 136.7, 131.8, 129.5, 128.7, 128.1, 127.8, 127.6, 52.9, 32.9, 22.1.

8.6.6 2-Methylindene oxide



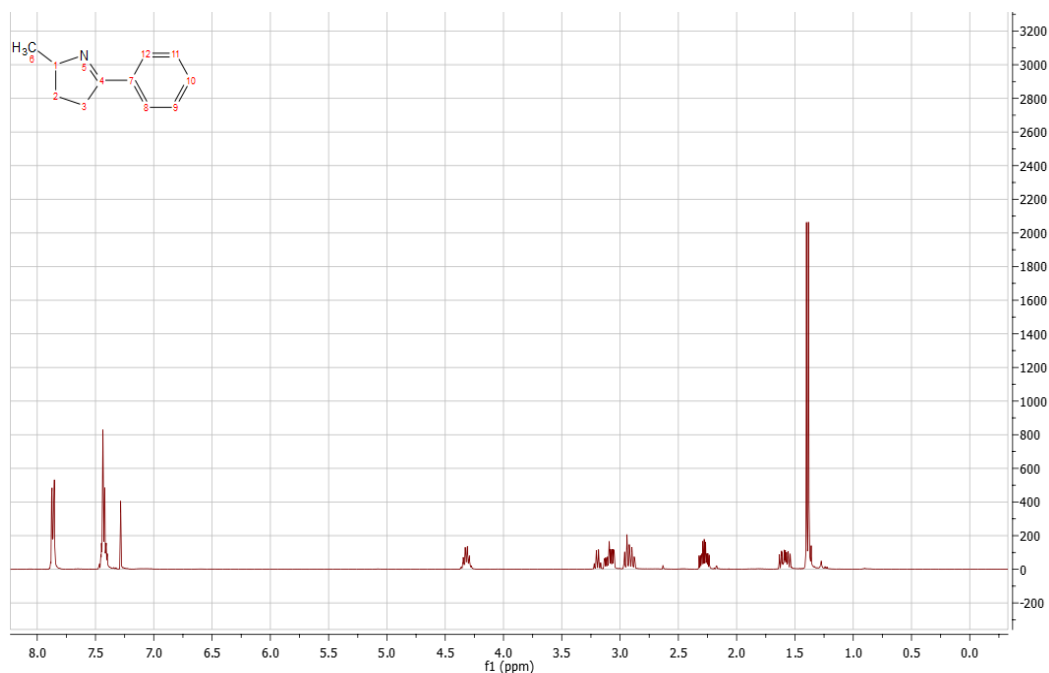
^1H NMR (400 MHz, CDCl_3): δ 7.54 (d, $J = 7.2$, 1H, Ar), 7.32-7.19 (m, 3H, Ar), 4.09 (s, 1H, CH), 3.21 (d, $J = 17.7$ Hz, CH), 2.95 (d, $J = 17.7$ Hz, CH), 1.75 (s, CH_3).

8.6.7 2-(2-Oxo-propyl)benzaldehyde

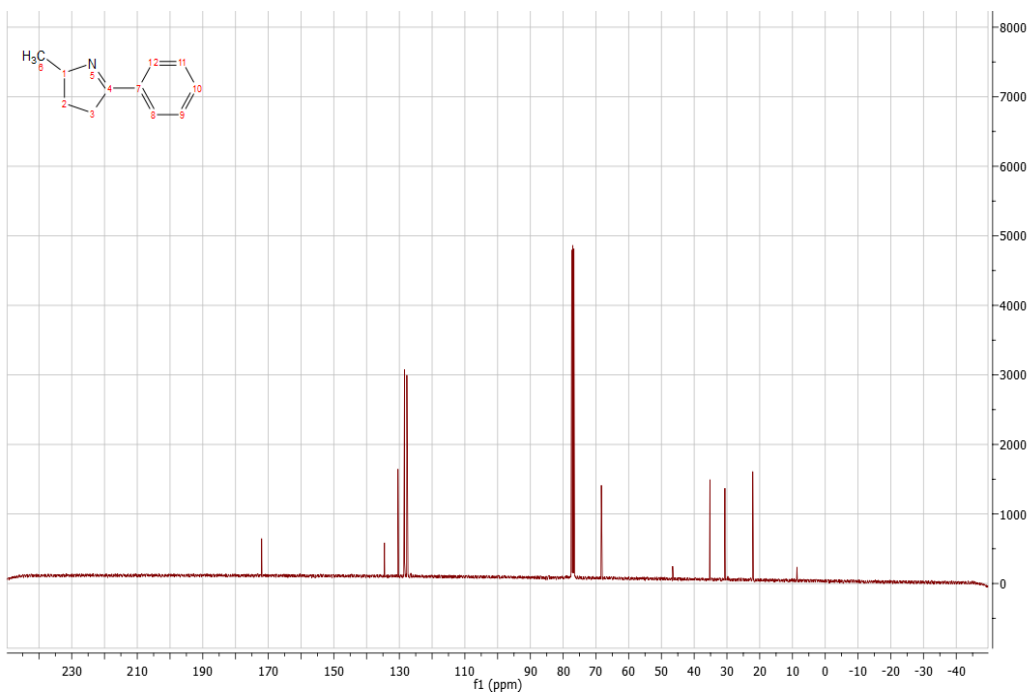


¹H NMR (400 MHz, CDCl₃): δ 10.01 (s, CH), 7.82 (dd, $J = 7.4, 1.6$ Hz, 1H, Ar), 7.60-7.47 (m, 2H, Ar), 7.22 (m, br, 1H, Ar), 4.13 (s, CH₂), 2.33 (s, CH₃).

8.6.8 2-Methyl-5-phenyl-3,4-dihydro-2H-pyrrole

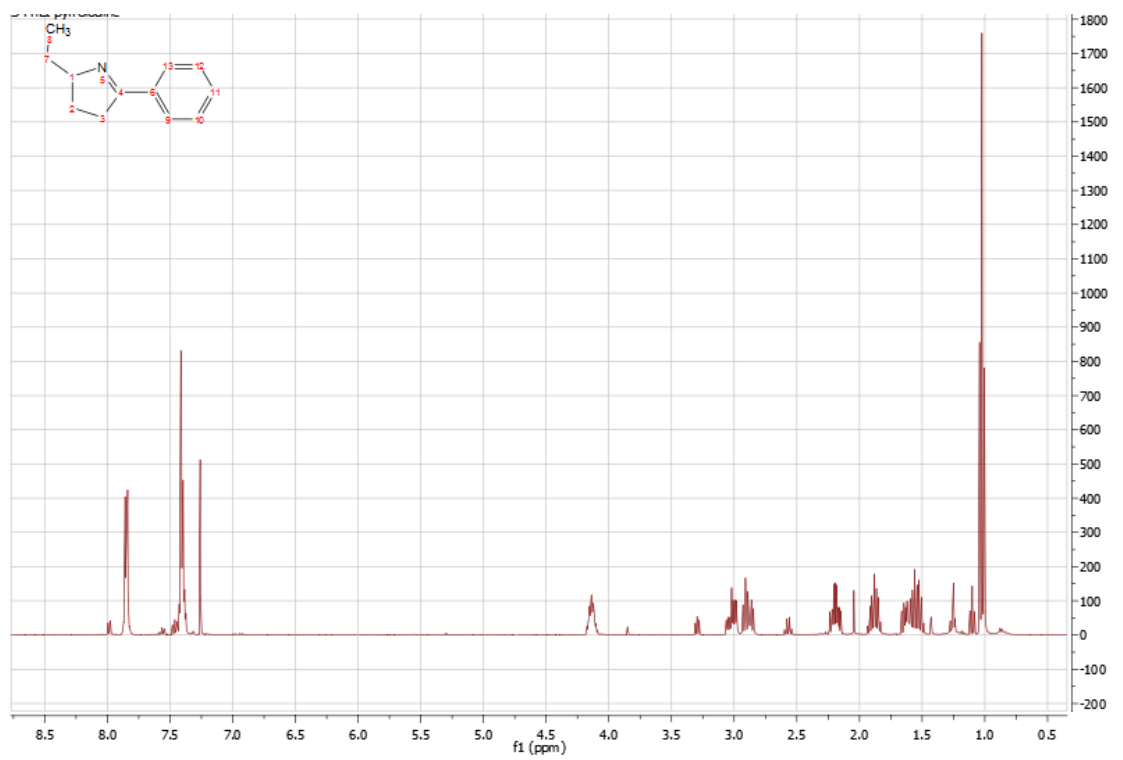


^1H NMR (400 MHz, CDCl_3): δ 7.89-7.84 (m, 2H, Ar), 7.48-7.39 (m, 3H, Ar), 4.48-4.26 (m, CH), 3.09 (m, CH), 2.92 (m, CH), 2.28 (m, CH), 1.59 (m, CH), 1.39 (d, $J = 7.2$ Hz, CH_3).

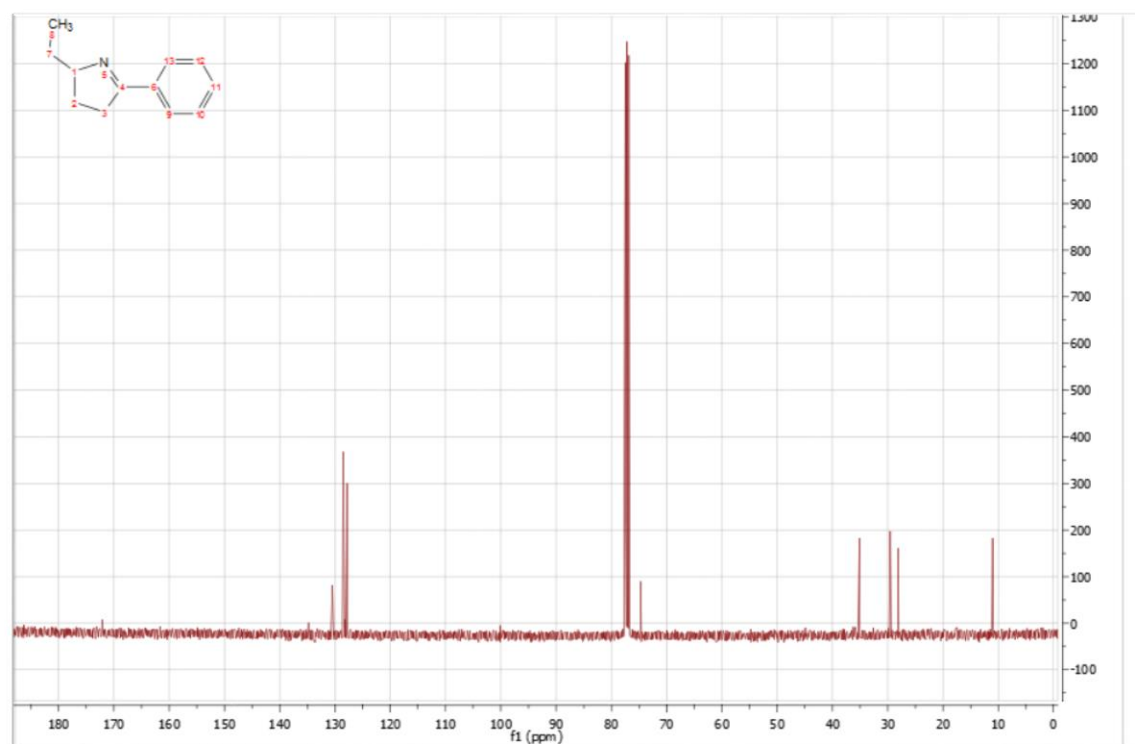


^{13}C NMR (100 MHz, CDCl_3): δ 172.0, 134.5, 130.4, 128.4, 127.7, 68.3, 35.2, 29.5, 22.1.

8.6.9 5-Phenyl-2-ethyl-3,4-dihydro-2H-pyrrole.



¹H NMR (400 MHz, CDCl₃): δ 7.87-7.83 (m, 2H, Ar), 7.43-7.37 (m, 3H, Ar), 4.18-4.09 (m, CH), 3.07-2.97 (m, CH), 2.94-2.84 (m, CH), 2.24-2.15 (m, CH), 1.93-1.83 (m, CH), 1.67-1.50 (m, CH₂), 1.04-1.00 (t, $J = 8$ Hz, CH₃).



¹³C NMR (100 MHz, CDCl₃): δ 1712.0, 134.4, 130.9, 129.0, 128.1, 74.51, 35.0, 29.9, 28.3, 11.4.

8.7 Publications

A fast and sensitive assay for measuring the activity and enantioselectivity of transaminases, Hopwood *et al.*, *Chem. Commun.*, 2011, **47**, 773-775.

A Fast, Sensitive Assay and Scale-Up of ω -Transaminase Catalysed Reactions, *Practical Methods for Biocatalysis and Biotransformations 2*, Hopwood *et al.*, Wiley, Page 74.

Structures of a gamma-aminobutyrate (GABA) transaminase from the *s*-triazine-degrading organism *Arthrobacteraurescens* sp. TC1 in complex both with PLP, and its external aldimine PLP-GABA adduct, Bruce *et al.*, *Acta Crystallographica*. Submitted.